NASA Contractor Report 4600

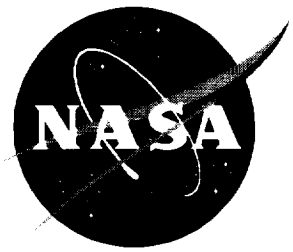

Experimental Uncertainty and Drag Measurements in the National Transonic Facility

Stephen M. Batill
University of Notre Dame • Notre Dame, Indiana

National Aeronautics and Space Administration
Langley Research Center • Hampton, Virginia 23681-0001

Prepared for Langley Research Center
under Cooperative Agreement NCC1-177

June 1994

Table of Contents

List of Figures

List of Tables

List of Symbols

a	Y intercept for linear function (Eq. 4.2.3)
A	Y intercept for linear function (Eq. 4.3.3)
Az	Single axis AOA roll orientation of misalignment (deg)
B_a	Bias limit for y intercept (Eq. 4.2.7)
B_A	Bias limit for data reduction parameter (Eq. 4.3.9)
$B_{A_{curve\ fit}}$	Bias limit due to curve fit (Eq. 4.3.5)
$B_{A_{other}}$	Bias limit due to other sources
$B_{A_{WS}}$	Bias limit due to working standard
B_m	Bias limit for slope of straight line (Eq. 4.2.8)
B_M	Bias limit for data reduction parameter (Eq. 4.3.10)
$B_{M_{curve\ fit}}$	Bias limit due to curve fit (Eq. 4.3.6)
$B_{M_{other}}$	Bias limit due to other sources
B_P	Bias limit for parameter P
B_{P_i}	Bias limit for the i th parameter P
$B_{P\ ij}$	j th bias source for the i th classification for parameter P
B_r	Bias limit for the result
B_V	Bias limit for measured voltage
B_{XM}	Bias limit for the measured parameter XM (Eq. 4.3.12)
C	Confidence level
C_D	Drag Coefficient
C_L	Lift Coefficient
N	Number of data points in a sample
m	Slope (Eq. 4.2.2)
M	Mach number or slope (Eq. 4.3.4)
Omax	Single axis AOA misalignment angle
P	Individual parameter
P_i	i th individual parameter
$PL_{\bar{P}_i}$	Precision limit for the mean of the i th parameter (Eq. 5.5.2)
P_{TRUE}	True value for parameter P
P_x	Precision limit for the parameter X
r	Computed result
r_k	k th result in a sample of N results
$\bar{r}$	Mean value for a sample of N results
S_a	Precision index due to curve fit for intercept (Eq. 4.2.5)
S_m	Precision index due to curve fit for slope (Eq. 4.2.6)

S_{P_i}	Precision index for the i th parameter P
$S_{\bar{P}_i}$	Precision index for the mean value of the i th parameter P
S_r	Precision index for the result
S_x	Precision index for the parameter X
S_{x_i}	Precision index for the i th value of the abscissa
S_{Y_i}	Precision index for the i th value of the ordinate
$S_{\bar{X}}$	Precision index for the mean of the parameter X
t	Scale factor for small samples (Student t)
$U_{r_{ADD}}$	Uncertainty in the result r, additive combination (Eq. 2.7.9)
$U_{r_{RSS}}$	Uncertainty in the result r, quadrature combination (Eq. 2.7.10)
U_X	Uncertainty in parameter X
X	Independent parameter
X_{BF}	Bias factor for parameter X (Eq. 5.4.1)
X_{PF}	Precision factor for parameter X (Eq. 5.5.4)
X_i	i th value in a sample of the parameter X
$\bar{X}$	Mean value of a sample of N parameters
XM	Measured parameter in engineering units (Eq. 4.3.2)
Y	Ordinate for linear curve fit
Y_i	i th value of the ordinate Y

Greek Symbols:

α	Callender-Van-Dusen PRT sensor calibration constant
β	Callender-Van-Dusen PRT sensor calibration constant
δ_{ik}	Kronecker delta (= 1 if i = k, and = 0 if $i \neq k$)
Δ	Finite difference in a parameter
λ	Callender-Van-Dusen PRT sensor calibration constant
μ	Mean value of the parent population (Eq. 2.5.1)
σ	Standard deviation of the parent population (Eq. 2.5.2)
σ_{est}	Unbiased estimate of the standard deviation of the dependent variable in linear regression (Eq. 4.2.4)
θ_i	Sensitivity of the result with respect to the i th parameter (Eq. 2.7.3)
θ_i'	Relative sensitivity of the result with respect to the i th parameter (Eq. 2.7.7)
ρ_{Bik}	Correlation coefficient between the biases B_{P_i} and B_{P_k}

Acronyms and Computer Variables:

A/D	Analog to Digital
AGARD	Advisory Group for Aerospace Research and Development
ANSI	American National Standard Institute
AOA	Angle of Attack Sensor
AOAS	Single axis AOA sensitivity constant
AOAB	Single axis AOA bias constant
AOAZ	Single axis AOA roll orientation of misalignment
AOAM	Single axis AOA misalignment angle
ASME	American Society of Mechanical Engineers
AXFRAW	Output from the axial force bridge of the balance
BALPOW	Excitation voltage for force balance
DAS	Data Acquisition System
DAU	Data Acquisition Unit
ELEVA	Output from single axis AOA
EU	Engineering Unit
IDV	Integrating Digital Voltmeter
MPA	Model Preparation Area
NTF	National Transonic Facility
NF1RAW	Output from the normal force bridge of the balance
NF2RAW	Output from the normal force bridge of the balance
PS50V	Output from Ruska static pressure sensor (50 psia range)
PT100V	Output from Ruska total pressure sensor (100 psia range)
RLMRAW	Output from the rolling moment bridge of the balance
R0	PRT resistance at 0° C
SEE	Standard Error of Estimate
SF1RAW	Output from the side force bridge of the balance
SF2RAW	Output from the side force bridge of the balance
PRT	Platinum-resistance temperature
S1 - S6	Force balance primary sensitivity constants
WNF1	Weight tare from normal force components
WAF1	Weight tare from axial force component

Preface

This work was conducted under research grant NASA-NCC1-177 with the NASA Langley Research Center, Hampton, Viginia. The study was performed at the National Transonic Facility at NASA Langley between August and December 1993 by the Principal Investigator, Stephen Batill. The NASA Project Engineer was Richard Wahls. The author wishes to acknowledge the assistance of Richard Wahls, Jean Foster and Jerry Adcock of NASA Langley and John Ertel and Bill Spengler of the Calspan Corporation. Their assistance and the insight they provided into the operation of the National Transonic Facility proved invaluable in performing this study. He would also like to recognize Elwood Putnam and Blair Gloss for their support and recognition of the importance of quality in wind tunnel measurements.

Summary

This report documents the results of a study which was conducted in order to establish a framework for the quantitative description of the uncertainty in measurements conducted in the National Transonic Facility (NTF). The importance of uncertainty analysis in both experiment planning and reporting results has grown significantly in the past few years. Various methodologies have been proposed and the engineering community appears to be "converging" on certain accepted practices. The practical application of these methods to the complex wind tunnel testing environment at the NASA Langley Research Center was based upon terminology and methods established in ANSI and ASME standards. The report overviews this methodology.

Computers have established a dominate role in experimental data acquisition and processing in wind tunnels. This study focused on the influence of computer based data acquisition in both the calibration process and the actual measurement.

Since many of the instruments used in the NTF are calibrated on a regular basis, the uncertainty associated with these calibration experiments was also considered. This assessment is complicated by the fact that most of these calibration experiments are performed in an environment which is quite different from that which the instrument is exposed to in the wind tunnel. The role of the calibration experiments and the uncertainty in their results is also discussed in this report.

Preliminary estimates of both bias and precision errors were performed using data collected at the NTF. This required a detailed description of the measurement process as performed at the NTF and this description is included in the report. These preliminary uncertainty estimates were developed to demonstrate the methodology for a complete system uncertainty analysis and were not intended to provide a comprehensive assessment of the system uncertainty. This preliminary study did highlight the importance of certain instruments and role of the calibration experiments performed prior to actual measurements in the NTF.

Section 1. Introduction

In recent years there has been an increased awareness of the importance of "quality" in every phase of engineering activity. One indication of quality in an experimental measurement is the uncertainty or "error" associated with the "result" of the experiment. Quantifying the "error" and the associated "level of confidence" in a particular result is the purpose of an "experimental uncertainty analysis."

1.1 Background

Probably the most difficult aspect of performing an "uncertainty analysis" for an engineer is that there is no single, well defined methodology which is universally accepted. One of the earliest cited references to a systematic methodology for performing an uncertainty analysis was developed by Kline and McClintock[1†] This early work appeared to provide a "standard" for the propagation of error into an experimental result and has been cited in numerous textbooks on experimental methods during the past forty years. In the sixties a couple of books appeared which provided a brief background in the appropriate methods of statistical analysis as applied to the interpretation and presentation of experimental data[2,3] and suggested a number of statistical concepts which could be applied to the analysis of experimental data.

As computers began to play a larger part in experimental data processing about three decades after the original work of Kline and McClintock, there appeared to be increased interest in the issues related to uncertainty analysis as indicated in References 4-7. These changes have also lead to a number of more recent or revised books specifically dedicated to the subject.[8-12] These works introduced additional concepts and in particular a growing distinction between systematic or bias "errors" and random or "precision" errors and the role that each plays in an experimental uncertainty assessment.

There has also been considerable effort expended, particularly by the metrology community, in the application of statistical methods to defining the uncertainty in measurement standards for use in instrument calibration and that

---

† (All references cited in the text are indicated with superscript numerals and are given in Section 7. The cited references are not intended to be an all inclusive list of related publications but were those that the author found useful in this study).

work has continued to the present.[11-15] These efforts appeared to have provided a strong foundation for the current statistical methods used in uncertainty analysis and in particular issues related to "curve fitting."

As each of these efforts added to the body of knowledge in this area, there still was no consensus as to notation or even interpretation of the results of an uncertainty analysis. This lack of consensus was eased somewhat by the development of an engineering standard in 1985.[16] This standard provided a basic framework for the application of uncertainty analysis methods to experimental measurements. It also appears to have provided the motivation for a very useful textbook[17] which provides additional insight into various terms and concepts developed in the Reference 16 and emphasizes the utility of performing an uncertainty analysis at various stages of experiment planning, debugging and during the presentation of results.

Where each of the references cited above were "generic" in nature and were intended for a wide variety of scientific and engineering applications, the aerospace community has also been involved with the development of methods and standards with very specific applications in mind. Much of this effort appeared to be focused in the gas turbine engine community and a sampling of this relatively extensive work is included in References 18 - 20.

The importance of uncertainty analysis in experiment planning and presentation of results has not been lost on the wind tunnel testing community and AGARD is currently involved in the development of a rather comprehensive document related to uncertainty analysis for wind tunnel applications (This work has not yet been published but a draft was available to the author and will be referred to as the "AGARD Draft" in this report). There have also been efforts to consider individual aspects of the problem of uncertainty analysis for wind tunnel applications,[21] but to date this author has not identified a published, compete system uncertainty assessment for a wind tunnel.

A review of the selected references cited above will illustrate the diversity in terminology and various concepts that have been applied to this topic called uncertainty analysis. Though "standards" have been developed in recent years, there still appears to be considerable discussion as to the appropriate methods and interpretation of results. This is most likely due to the fundamental character of uncertainty analysis which has its basis in the 'inexact" sciences of probability, statistics, experience and professional judgment. This is to say that the methods used in uncertainty analysis would not be classified as "deterministic" in

character and they are often susceptible to considerable confusion; much of the confusion is based in semantics. Though the mathematics can be relatively straightforward, the semantics can be a problem and the assumptions are critical. The best solution to this problem therefore appears to require one to apply those techniques which appear to be most appropriate for the particular experiment at hand and then to carefully explain how the results have been achieved and how they should be interpreted. That has been the approach taken in the current effort.

1.2 Project Goals

The purpose of the project described in this report was to build upon recent developments as related to uncertainty analysis and to apply them to the problem of wind tunnel drag coefficient measurements. Considering the limitations imposed by time and resources for this effort, its primary purpose was to provide guidelines and a framework within which more detailed evaluation of specific wind tunnel test measurements could be conducted in the future.

The project goal was to initiate the development of a complete, end-to-end system accuracy assessment for data obtained in a "production" wind tunnel environment. Due to the complexity of the test facility and the cost of its operation, this type of wind tunnel is usually highly automated and both the tunnel process control and data acquisition are computer-based. It is the interaction between the tunnel and its simulation of the "aerodynamic environment", the instruments and the data acquisition system which complicate the uncertainty analysis for the complete system. Though "accuracy" information is often available for individual instruments, this information is often the result of calibration experiments which are conducted using methods and in environments much different from the conditions encountered in the wind tunnel. Developing an understanding of how the individual instruments are integrated into a complete system and how this integration influences the overall system accuracy was one of the primary goals of this study.

Though methods which are applicable to a variety of wind tunnel facilities were evaluated and developed as part of this study, the initial application was to the problem of drag measurements conducted in the National Transonic Facility (NTF) at the NASA Langley Research Center. The purpose was to provide

substantiation for a statement of the results for a given test point that the measured drag coefficient was:

$$C_D = X \pm U_X \qquad \text{(with stated confidence level)}$$

where the uncertainty in the measured value X was quantified as U_X. The estimation of U_X and the confidence level was to be based upon currently accepted methods in uncertainty analysis. The ANSI/ASME standard [16] was used a guideline for most of the methodology and terminology (though not symbology) as applied in this study. The specific application did require the use of alternative approaches in certain cases and these exceptions to this standard are discussed in the report.

Section 2 of this report includes a very brief overview of selected topics related to the uncertainty analysis presented in this report. It is not the intention of this document to provide a general "tutorial" on uncertainty analysis but to highlight those issues which have direct bearing on the problem at hand. A more comprehensive background in uncertainty analysis can be developed from a number of the cited references.

Section 3 presents a rather detailed description of the "measurement process" as it is performed at the NTF. This includes a description of the various "calibration" experiments and the "flow" of information from the fundamental measurements to the computed results.

One characteristic of the experiments conducted in the wind tunnels at the NASA Langley Research Center is the extensive use of specialized instruments and the subsequent requirement for calibration of these instruments. An approach for dealing with instrument calibration and the influence of experimental uncertainty in the calibration experiment on the final measured result is presented in Section 4.

In order to demonstrate the techniques presented in this report a brief example is provided using data from a test in the NTF and this is presented in Section 5. Most of the discussion is related to two test points for a subsonic transport configuration operating at relatively low angles of attack. The data reduction procedures used in the NTF were employed to provide much of the information required to make the uncertainty estimates. Both bias and precision estimates are made for these test points and combined to provide an estimate of the experimental uncertainty. The methods used to estimate each contribution to

the uncertainty are presented for this example. Due to limitations on time and expertise, only a limited number of potential contributions to the system uncertainty could be considered during this preliminary study. Issues such as modeling of the wind tunnel gas, wind tunnel corrections and model dynamics have not been included in the uncertainty estimates. It should be emphasized that these preliminary estimates were developed in order to establish a framework for more comprehensive uncertainty analyses to be performed in the future.

The final section, Section 6, provides a summary of some of the observations and conclusions as well as issues to be considered as this preliminary uncertainty assessment is extended and applied to future wind tunnel tests.

One final note of introduction to this study. Much of the methodology associated with uncertainty analysis is "uncertain." The reader should be cautioned that in order to estimate the uncertainty in an experimental result, there are many assumptions which must be made and considerable engineering judgment exercised - an aspect that is upsetting to some more "scientifically" oriented engineers. Though there is some mathematics involved which appears to provide a "quantitative" foundation for the estimates, the success of the analysis will depend upon sound understanding of the measurement process, as well as experience and one's ability to make good "guesses". The approximate nature of the results should always be considered and one should avoid getting overwhelmed by minute details as they proceed toward the overall goal.

Section 2. Overview of Experimental Uncertainty Methodology

The previous Section cited a series of references which describe various concepts and methods associated with experimental uncertainty analysis. The following discussion is not intended as a comprehensive review of uncertainty analysis but as a brief overview of various issues of interest in this study. Many of the concepts and much of the terminology has been adapted from References 16 and the "AGARD Draft".

2.1 Basic Concepts

Measurement uncertainty analysis can be used to plan an experiment, identify corrective action in order to achieve test objectives, or to qualify the results of an experiment. Depending upon the purpose of the analysis different information will be available and different procedures may be followed[17]. In the reporting phase of the project, and that is the phase that this study is concerned with, the purpose of the uncertainty analysis is to determine numerical estimates to provide upper limits to,

1. random precision errors and,
2. systematic or fixed bias errors.

These two components of the total measurement error are then combined to provide an estimate of the uncertainty in the results of the measurement. These two components will be described in more detail in the following section but it should be emphasized that radically different approaches are taken to determine each component. The precision error estimate is usually based on a statistical evaluation of the results of numerous experiments and is in some respects a measure of the repeatability of the measurement process and inherent unsteadiness in the phenomena being studied. The bias error estimate is truly an "estimate" and has its basis in experience and engineering judgment - which can create problems for an engineer who wants to be "certain about the uncertainty."

The final issue that must be addressed is the amount of information available on the measurement process in order to perform the uncertainty analysis. For the current study it was assumed that the measurement process was completely defined and the methodology established. In the case of the NTF, the procedures for data acquisition and processing have evolved during the past 10 years and there are well established testing techniques. In the process of acquiring and processing the information necessary to develop the "result" of the

measurement all known errors have been eliminated and all known calibration corrections have been applied. Since the measurements that will be evaluated have already been performed, some insight is available from previous tests as well as the experiences of instrumentation and wind-tunnel test engineers. All of the equipment and instruments used in the measurement have either been calibrated or the manufacturer's specifications are available.

2.2 Terminology

Various terms are used to describe the accuracy, uncertainty, precision, quality... etc. of the results of an experiment or a "measurement". Often each term carries with it numerous concepts and the use of a particular term may be confusing if it is not carefully defined. It was the author's experience that establishing a common framework for the discussion was often the most crucial step in arriving at a useful result from an uncertainty analysis and conveying that result to others. This is due to the fact that certain aspects of the process called "uncertainty analysis" are still evolving. Many of the references cited in the previous Section are primarily devoted to establishing a "semantic" framework for discussing measurement uncertainty and should be studied in detail by anyone who wishes to become conversant in this language. It is the responsibility of the engineer who attempts to quantify the uncertainty associated with a stated result to carefully define the approach taken and the terms used.

The following is very brief collection of a limited number of terms or concepts which are used in this report. These definitions are not meant to be all inclusive but are intended to help the discussion in this report.

measurement or measured parameter- a useful, quantified parameter, this may be bits (i.e. digital representation of an analog voltage) , volts, temperature, force, etc.. This "number" is often used in subsequent calculations to determine a "result".

result - a quantity determined from the numerical manipulation of individual measurements and other numerical quantities such as handbook values, data from tables, etc..

measurement error - difference between an "estimated" value (be it a measurement of a single parameter or a result) of a quantity and the "true value" of the quantity.

true value - the actual value of the parameter being measured (at the instant of the measurement) . It is important to realize that the true value is always an "unknown" and its definition depends upon how the measurement will be used in a "conceptual" sense. There are numerous variations on the concept of "true value" and each may have an appropriate place in a given experiment.

fixed bias error - systematic error which is "constant" for some known period of time (e.g. the error in a calibration constant for a particular instrument which is fixed between calibrations).

random precision error - probabilistic component of the error which is due to variations, often temporal, in the measurement system characteristics or the process being measured (e.g. the variations in local flow angle due to wind tunnel turbulence).

precision limit- an estimate, with statistical support, of the "limits" on the precision error with a statement of confidence.

bias limit - an estimate of the "limits" on the true bias error with an assumed or inferred statement of confidence.

confidence level - a quantifiable expression indicating the probability that the true value is within the stated limit of the estimated value of a quantity.

measurement uncertainty - a combination of the precision and bias errors and its associated confidence level.

2.3 Measurement Error Sources

All experimental measurements (not to be confused with counting experiments) have some error associated with them. Often this error does not influence the utility of the measurement but in some cases quantifying the error and understanding its origin can add considerably to the value of the result. In the

wind tunnel experiments considered during this study there were various sources of measurement error. Classifying the sources of these errors, as suggested by many of the practitioners of uncertainty analysis[16-17], allows for a systematic assessment of their influence on the measurements. A useful, though not unique, classification of errors includes calibration errors, data acquisition errors and data reduction errors.

One important aspect of the NASA wind tunnel test environment is the role of calibration experiments. All of the instruments and sensors used to monitor the tunnel and to measure the model orientation and aerodynamic forces are calibrated on a regular basis. These calibration experiments are used to monitor the condition of the instruments and sensors and to provide "calibration" constants to characterize the performance of the instruments. The calibration experiments also have uncertainty associated with their results. The uncertainty associated with the results of these calibration experiments influences the results achieved in the wind tunnel tests since the calibration data is used to process measurements made with the same instruments and sensors in the wind tunnel. The calibration errors can include the errors associated with the working standards used as part of the calibration, the manner in which the calibration experiment is conducted and the data processing or "curve fitting" which used to provide the parameters which characterize the instrument's performance. It should be emphasized that "between calibrations" many of the errors associated with the calibration process are fixed since the calibration parameters do not change. Since this calibration information is "fixed or frozen" between instrument calibrations these errors contribute to the systematic or bias errors in the result. Early in the development of the methods of uncertainty analysis it was often stated that calibration '"removed" systematic errors and though calibration may serve to reduce systematic errors, it cannot completely eliminate them. The importance of the calibration experiments and their associated uncertainty is discussed in more detail in Section 4 of this report.

The data acquisition process is also a source of measurement error. In the modern wind tunnel environment the data acquisition process is composed of two basic steps. The first is the conversion of a physical property (i.e. temperature, pressure, force, etc.) to a proportional analog equivalent in the form of a "voltage" using an electronic transducer. The second step is the measurement of voltage by a computer-based, electronic analog to digital (A/D) conversion processor. Thus the basic "measurement" is the conversion of analog voltages to "bits".

All of those factors which influence the generation of the voltage signal which originates at the transducer or sensor, the relationship between the desired physical quantity and the voltage and everything that influences the voltage before the A/D conversion may be classified as data acquisition errors. This would include instrumentation error sources (i.e. voltage supplies, filters, amplifiers, ..), environmental effects (i.e. temperature, humidity,..), sensor and probe errors, spatial errors and others particular to a given system. These data acquisition errors can contribute to both the bias and precision components of the uncertainty. Only through a complete understanding of the measurement system and the phenomena being studied can these error sources be effectively identified. It appears to this author that the most important step in a uncertainty analysis is developing a complete understanding of the measurement process. Without this the uncertainty analysis will be of limited value.

The third classification of error sources are related to data reduction. Once the results of the calibration experiments have been "frozen" as calibration constants and the voltages converted to "bits" the remaining processes to be performed in order to achieve the result of an experiment are the selection of appropriate "physical constants" and numerical calculations. Often the data reduction process is similar to that used in the calibration experiments to provide the parameters for subsequent measurements with the instruments. Computational resolution, interpolation, iterations, curve fitting and other numerical procedures can be the sources of data reduction errors.

As will be discussed in the following sections, the "error" in a measurement, be it either bias or precision, will be the result of various error sources. The ability to identify the appropriate error sources and quantify their contributions represents the basis of an uncertainty analysis. In the current study only limited time and experience was available to the author in the attempt to identify potential error sources. One of the most important outstanding issues remaining at the completion of this preliminary uncertainty analysis is to perform a more comprehensive assessment of the error sources particular to the NTF.

2.4 Uncertainty Analysis Methodology

As indicated earlier, the methodology outlined in Reference 17, with some exceptions, was adapted for the current study. The following six steps serve as an outline for the procedure followed in this study.

1. Define the measurement process
2. Identify and quantify the elemental bias error sources
3. Calculate bias errors for each measured parameter
4. Propagate bias errors through the data reduction process to the result
5. Estimate the precision limit of the result from multiple measurements
6. Calculate "uncertainty" of the result

These steps can be illustrated schematically as shown in Figure 1. This figure, which was adapted from similar "flowcharts" in Reference 17, illustrates the "flow" of error sources from the individual measurement systems and individual measured parameters to the result. Actually two different approaches for quantifying the precision error are considered in this report. If appropriate data is available estimates of the precision error from multiple measurements of the result is preferred, although not always possible.

Since the purpose for the study was to evaluate the uncertainty in the drag measurements in the NTF one of the first steps was selecting a set of data associated with an already completed test program which could be used to evaluate the methods which were developed. Fortunately data existed which could be used to quantify the uncertainty using either single sample or multiple measurement approaches. Using the terminology of References 16 and 17, the preferred procedure, outlined in Figure 1, would be based on "more that one" test or be referred to as an Nth order uncertainty analysis with an end-to-end assessment of the precision error. The following sections provide some insight into the details for each of these steps and the preliminary test case is presented later in the report.

2.5 Precision Error

The precision error (or often referred to as the repeatability) estimate has its basis in probability and statistics. The "scatter" in data observed when multiple measurements are recorded at nominally the same test conditions provides a qualitative assessment of the precision of the measurement process as well as an indication of the variations occurring in the process being measured. Extracting useful quantitative insight from these multiple measurements can be accomplished through statistical analysis of the information. References 22 and 23 provide a good background in many of the concepts which are used to define the precision error in an estimate. They should be referred to for additional details

and the following is included to provide as only a brief overview of certain issues central to the current application to uncertainty analysis.

Consider a single number, X_1, which represents an individual measurement or realization of a parameter, X. If that measurement is repeated and yields X_2, one might expect a different result from the original measurement. This can be done many (N) times. The most complete representation of the statistical character of the variable X would be if N was allowed to go to infinity. Two parameters that define the "characteristics" of an infinite population of random numbers are the mean, μ, and standard deviation, σ.

$$\mu = \lim_{N \to \infty} \frac{1}{N} \sum_{i=1}^{N} X_i \qquad \text{Eq. 2.5.1}$$

$$\sigma = \lim_{N \to \infty} \left[\frac{1}{N} \sum_{i=1}^{N} (X_i - \mu)^2 \right]^{\frac{1}{2}} \qquad \text{Eq. 2.5.2}$$

In the case of experimental data, the mean can be interpreted as a "best estimate" of the parameter and the standard deviation is an indication of the "scatter" in the data. The utility of these statistics often depends upon the probability distribution of the data and the following discussion assumes that the random variables of interest have a normal or Gaussian probability distribution.

Unfortunately one must work with a "finite" number of samples which often only represent a small subset of the "parent" population. One attempts to generalize to the manner in which the random numbers are "distributed" in the parent population from the limited sample. The size of the sample influences the ability to extrapolate to the parent population. The finite sample size requires the definition of finite sums (the infinite sums indicated above would be very difficult to evaluate since it may take a long time to get that much data!) The mean of a sample of a population is written as,

$$\bar{X} = \frac{1}{N} \sum_{k=1}^{N} X_i \qquad \text{Eq. 2.5.3}$$

This is an estimate of the mean of the parent population and it depends upon the sample size, N, and the statistical characteristics of the data. An "estimate" of the standard deviation of the population is referred to as the precision index of the sample, S_x .

$$S_x = \left[\frac{1}{N-1} \sum_{k=1}^{N} (X_k - \bar{X})^2 \right]^{\frac{1}{2}} \qquad \text{Eq 2.5.4}$$

With one additional piece of information the two estimated parameters, $\bar{X}$ and S_x, can then be used to make "probabilistic" statements about the mean value and "future" measurements.

For a normally distributed random variable one can make certain statements about the probability that a single "new" realization of the random variable will lie within some prescribed interval about the mean. For relatively large sample sizes (and thirty is large enough in most cases) it can be shown that approximately 68% of the time a "new" random number will fall within a range of $\pm S_x$ of $\bar{X}$. It is also true that 95% of the time this "new" value will be a range of $\pm 2S_x$ of $\bar{X}$. This provides very useful information particularly if you recall that the goal of the uncertainty analysis is to identify "intervals" in which true values of the measurements lie. This information not only provides the size of the interval but also allows one to state the "confidence or coverage" placed on these interval as indicated by the percentage of times that a random variable would fall in the interval.

Recall that the approximation to the population standard deviation depends upon the size of the sample. As the sample size increases, the approximation is improved. For sample sizes less than thirty, the value of S_x can be scaled by a "t" parameter to allow for similar statements to those made above. The sample size is used to introduce one additional concept useful in statistics and that is the "degrees-of-freedom" which is related to the size of the sample and certain characteristics of the statistic derived from the sample. Though this term is used in many statistical inference techniques its use in the current application is limited as will be discussed below. Based upon the sample size it is

possible to select a scale factor "t" for a selected value of confidence level, C , so that one can make the statement for a single realization of the random variable X_i :

$$" \; X_i - t\,S_x < \mu < X_i + t\,S_x \quad C\% \text{ of the time } "$$

The values for "t" for a desired confidence level, C, and sample size, N, can be found in tabular form in most books on statistics or estimated using rather straightforward numerical techniques[24]. In this way one can make a statement about the mean of the population, often considered the true value for an unbiased parameter, in terms of a single measurement and the precision index of the sample. The interval width, $t\,S_x$, introduced above is referred to as the precision limit, P_x . In uncertainty analysis the precision limit is an estimate of the precision error for a given confidence level.

One additional concept which is useful ,when the mean value of multiple measurements is used to estimate the true mean value, is the precision index of the mean. Precision index of the mean or the sample standard deviation of the mean, $S_{\bar{X}}$,

$$S_{\bar{X}} = \frac{S_x}{\sqrt{N}} \qquad \text{Eq 2.5.5}$$

can be used in conjunction with the appropriate t factor to indicate the interval in which the population mean lies with respect to the sample mean. This allows one to make a similar statement as that above for the mean of the sample, $\bar{X}$,

$$" \; \bar{X} - t\,\frac{S_x}{\sqrt{N}} < \mu < \bar{X} + t\,\frac{S_x}{\sqrt{N}} \quad C\% \text{ of the time } "$$

Reference 16 goes to great lengths to discuss various alternative methods for estimating the precision index and its associated degrees-of-freedom for cases where there are multiple sets of measurements available or samples of various sizes. In the AGARD Draft, the recommendation is made that for most practical cases related to wind tunnel applications making the assumption of large sample sizes and assuming a t factor of 2 and a coverage of 95% will provide useful results and eliminate much the complexity associated with the

determination of the precision error. This is just an example of a lack of a universally accepted approach and one must just be careful to explain how the issue of sample size and coverage was treated in a particular uncertainty analysis.

One other issue that must be addressed when determining the precision index for a sample is that the information must be sampled over an 'appropriate' time interval to adequately represent the precision index. Consider the time history of the "data" shown in Figure 2. If the data is sampled during the time interval Δt shown in Figure 2a, an incorrect representation of the precision index will be determined. This becomes a problem in many of today's computer based data acquisition systems where large amount of data can be recorded in a very short period of time. This is an important issue when one wants to make multiple measurements and compute the mean value of a parameter so that the precision error estimate can be determined using the precision index of the mean. The implication being the larger the "N," the smaller the precision index, and this can lead to erroneously small values of the precision error.

In a similar manner the sample must include all of the sources of precision error in the experiment that one desires to consider in assessing the uncertainty in the experimental result. The concepts of precision and repeated measurements are directly related and the manner in which the experiment is repeated influences the contribution of each factor. In the case of wind tunnel tests one may wish to consider the influences of test condition unsteadiness, the ability to duplicate test conditions or model positions, the influence of model assembly and disassembly and dynamic effects such as model vibration. Thus simply making multiple sequential measurements at a single "test point" may not allow one to adequately characterize the precision in a given experiment.

The discussion above implied that the calculations were being performed in order to determine the precision in a desired "result" by conducting multiple experiments to yield that result. That would be referred to as an end-to-end precision error estimate and if that information is available it should be the preferred method for making an estimate of the precision error. As indicated in many of the previously cited references, it is also possible to determine the precision index for each of the measurements that are used to determine a result. If this is done then the precision error of the result can be determined using the propagation of errors approach identical to that to be discussed in the next

section on bias errors. The selection of the appropriate approach is usually based upon the availability of appropriate data.

2.6 Bias Error

Unlike the previous discussion of precision error where it was recommended that the precision error be determined on an "end-to-end" basis and was "statistical" in nature, the bias error estimates must be done at the level of the individual parameter measurements and is based more upon judgment than arithmetic. The fundamental character of bias errors is that they are "fixed" and do not vary as additional measurements are made as one attempts to repeat the experiment. They represent the difference between the true mean of the population of all possible measurements and the true value of the desired parameter. Since neither the true mean nor the true value are known, estimating the bias error is often quite difficult.

Figure 1 schematically illustrates the manner in which the bias errors are estimated. Individual bias contributions are identified and quantified for each parameter used in the determination of the result. These bias errors are combined to provide a bias limit for each parameter. The bias limit is an estimate of the upper limit of the bias error and it is stated with a confidence level or "coverage" consistent with the desired overall uncertainty. This coverage should be consistent with that used to describe the precision limit. As before one wishes to make an estimate of the bias limit, B_P , for a given parameter P such that ,

$$" \; P - B_P < P_{TRUE} < P + B_P \quad C \,\% \text{ of the time } "$$

The bias limits are not influenced by "repeated" measurements.

The procedure for estimating the bias limits first requires the identification of each parameter which is used to "compute" the result. Some of these parameters are measurements conducted as part of the given experiment, others are the results of earlier experiments or calibration experiments and still others are taken from handbooks, plots, etc.. Once each parameter is "fixed" as a "number" with a finite number of significant figures the bias error in each will contribute to the bias error in the final result.

In order to identify and subsequently quantify the bias error contributions to each parameter it is often helpful to separate them into various classes of error

sources. The same classification discussed above can be used to help identify potential bias error sources.

1. Calibration errors - depends upon the details of the calibration process
2. Data Acquisition / Installation errors
3. Data Reduction errors

The value of each of these bias contributions may depend upon the value of the parameter so the bias limit can vary with test conditions. Once all of the potential contributions to the bias limit for the parameter P have been identified and quantified they are combined by addition in "quadrature". The expression , $B_{P\,ij}$, represents the j^{th} bias source in the i^{th} error classification. Then the total bias limit in the parameter P due to each elemental bias contribution is estimated as,

$$B_P = \left[\sum_{j=1}^{m} \sum_{i=1}^{K} B_{P\,ij}^{2} \right]^{\frac{1}{2}} \qquad \text{Eq 2.6.1}$$

This implies that all of the contributions would not be expected to occur simultaneously and, characteristic of quadrature addition, the final bias limit is dominated by the most significant terms.

It should be noted that bias errors need not be symmetric. They can be can be asymmetric (i.e. $B_{i\,j}\,(+) \neq B_{i\,j}\,(-)$) and then each "side" of the bias limit must be determined independently. This was not an issue in this study and the reader is referred to Reference 17 for a more detailed development of asymmetric bias limits.

It was this author's experience that the most difficult task in performing the uncertainty analysis for the NTF was estimating the bias limits for the parameters considered in this study. A number of approaches were taken and they are discussed in the Sections of this report related to calibration and results. The usefulness of the final results obviously depends upon one's ability to identify those critical components of the bias error and to establish reasonable values for each.

2.7 Uncertainty in a Result

The result of an experiment is often a function of a number of independently measured parameters and "constants" which were the results of earlier experiments (often calibration experiments) or analysis. The result can often be expressed as an analytic function "r" of several variables, P_i , and thus can be written as a closed-form expression for the result,

$$r = r(P_1, P_2, \ldots, P_j) \qquad \text{Eq 2.7.1}$$

In some cases the result may be developed using a computer based numerical algorithm which cannot be written as a simple analytic expression. The uncertainty in the result computed by either an analytic expression or a numerical algorithm will be the result of the uncertainty in each of the parameters used to determine the result and any "errors" associated with the numerical or analytic procedures used to compute the result.

The method used to estimate the error in the final result, referred to as the propagation of errors, is based upon a first order Taylor series expansion of the result in the region near the nominal value of the result. A somewhat detailed development of the basic expression for the propagation of errors in presented in an appendix of Reference 17 and in a number of the other previously cited references. It is again important to emphasize that when one determines the uncertainty in a result that it is an approximation. The value of the uncertainty in the result in most cases is only valid for the nominal values of the parameter P_i which were used to compute the result. Implying that a value of uncertainty determined for a single test point is valid throughout the operating range of an experiment can lead to erroneous conclusions.

As indicated in the earlier discussion, in the reporting phase of an experiment the best estimates for the precision limit of the results would be determined using a statistical assessment of multiple measurements under appropriately controlled, "repeated" conditions. That was the approach taken for the preliminary results developed as part of this study. Therefore the emphasis in this section is related to the propagation of bias errors into the computation of the results of an experiment.

The expression for determining the bias limit for a result r is determined using a relation in the form,

$$B_r = \left[\sum_{i=1}^{j} (\theta_i B_{P_i})^2 \right]^{\frac{1}{2}} \qquad \text{Eq. 2.7.2}$$

where θ_i are the "sensitivities" of the result to variations in each parameter P_i: The sensitivities are first partial derivatives, or approximations thereof, of the result with respect to each parameter. If the analytic expression for r can be formulated in a reasonable fashion then,

$$\theta_i = \frac{\partial r}{\partial P_i} \qquad \text{Eq. 2.7.3}$$

This expression would then be evaluated at the appropriate nominal values of the parameters, P_i. If the expression for r is not readily available or performing the differentiation is not straightforward, as is the case in many computer-based data reduction procedures, a difference numerical approximation can be developed for the partial derivative,

$$\theta_i \approx \frac{\Delta r}{\Delta P_i} =$$

$$\frac{r(P_1, P_2, P_i + \Delta P_i \ldots, P_j) - r(P_1, P_2, P_i \ldots, P_j)}{\Delta P_i} \qquad \text{Eq. 2.7.4}$$

Equations 2.7.3 and/or 2.7.4 can be used in conjunction with Equation 2.7.2 to estimate the bias limit for the result r. An alternative set of expressions which may also be used provides the "relative" bias in the result based upon relative bias limits for each of the contributing parameters and relative sensitivities. One advantage in dealing with the relative formulation is that it can help avoid some problems with "units". The expression for the relative bias limit is,

$$\frac{B_r}{r} = \left[\sum_{i=1}^{j} (\theta_i' \frac{B_{P_i}}{P_i})^2 \right]^{\frac{1}{2}} \qquad \text{Eq. 2.7.5}$$

Where the relative sensitivities, θ_i' , are defined as,

$$\theta_i' = \frac{\partial r / r}{\partial P_i / P_i} = \frac{P_i}{r} \frac{\partial r}{\partial P_i} \qquad \text{Eq. 2.7.6}$$

for cases where the analytic derivatives can be determined, or

$$\theta_i' = \frac{\Delta r / r}{\Delta P_i / P_i} \qquad \text{Eq. 2.7.7}$$

for the numerical approximation. Again each sensitivity is computed at "nominal" values of individual parameters, P_i .

The expressions given above are for those cases in which the bias in each of the parameters P_i are independent, that is they are uncorrelated. For example consider a case where two pressure transducers are calibrated using the same working standard. The contribution to the bias limit for each individual pressure sensor due to the working standard would be "perfectly" correlated for each measurement. If the bias limits for some of the parameters used in computing the result are correlated then additional terms are needed in the expression for the bias limit of the result. It takes the form,

$$B_r = \left[\sum_{i=1}^{j} [(\theta_i B_{P_i})^2 + \sum_{k=1}^{j} \theta_i \theta_k \rho_{Bik} B_{P_i} B_{P_k} (1 - \delta_{ik})] \right]^{\frac{1}{2}} \qquad \text{Eq.2.7.8}$$

where δ_{ik} is the Kronecker delta (= 1 if i = k and =0 if $i \neq k$) and ρ_{Bik} is the correlation coefficient between the biases B_{P_i} and B_{P_k}. The issue of correlated bias limits is addressed in more detail in Reference 17. Appendices A and B have

been included in this report to provide additional insight into the problems which can be encountered when determining the bias limit in a result.

Once both the bias limit, B_r, and the precision index, S_r, and associated "t" factor for the result have been determined for a particular test point or set of test conditions, there are two options for stating the uncertainty in the result depending upon the manner in which the bias and precision errors are combined. The two options influence the "coverage" or level of confidence of the resulting uncertainty. Note that finally after using the terminology "error" up to this point in the development, the term "uncertainty" is now applied to the final combined result. If the bias limit and precision limit are simply added or "superimposed" then one can write,

$$U_{r\,ADD} = (B_r + t S_r). \qquad \text{Eq. 2.7.9}$$

If the bias limit was comparable in coverage to the precision limit , and the precision limit was based upon a 95% coverage, then Eq. 2.7.9 (i.e. simply adding the two components) provides an uncertainty in the result with 99% coverage or the "odds" are 99 in 100 that the true value of the result with lie within this interval of the computed result.

It appears as if the preferred approach for combining the bias and precision errors is addition in quadrature, much like that used to combine the bias limits. This takes the form,

$$U_{r\,RSS} = \left[B_r^2 + (t S_r)^2 \right]^{\frac{1}{2}} \qquad \text{Eq. 2.7.10}$$

and if the "t" factor is selected for a 95% coverage, the uncertainty in the result is also then determined for 95% coverage. In this report Eq. 2.7.10 is used to compute the uncertainty in the result. This the allow a statement for the result in a form,

$$r \pm U_r \quad \text{(95\% confidence level)} \qquad \text{Eq. 2.7.11}$$

Once the uncertainty in the result has been established it is possible to more effectively evaluate how the result can be interpreted and used in future

calculations. Some sources indicate that it would be preferred to state the uncertainty as well as the bias limit, precision index and associated degrees of freedom so that when this result is used in other computations one can establish their uncertainty. The specific form in which the uncertainty is stated may not be as important as providing an associated description of how it was determined, the assumptions made, etc.. Until a truly accepted standard for uncertainty analysis is established, it is up to the individual to make sure that they have adequately supported and documented the approach taken.

Section 3. Measurement Process in the NTF

The National Transonic Facility is a unique national resource capable of high-Reynolds-number, wind-tunnel testing. References 25-27 provide details on the NTF, its operation and data systems. Test planning, model development and tunnel operation in this facility are complicated since it is a cryogenic wind tunnel and testing is normally conducted at very high total and dynamic pressures as well as very low total temperatures. The complexity of the system and its associated costs have provided the motivation for the facility to be continuously aware of the importance of data quality and system productivity.

3.1 Overview of the Data Acquisition System for the NTF

The facility uses a state-of-the-art computer based, automated data acquisition (DAS) and data reduction systems. There are multiple computers and various procedures which can be used by the NTF in conducting a wind tunnel test. The current report is limited to a simple example in which the test objectives would be to measure the lift and drag coefficients, corresponding angle of attack, Mach number and Reynolds number for a single configuration. The data for a single test condition was recorded and analyzed after the test using "off-line" data reduction procedures.

As indicated in Section 2.4 the first step in an uncertainty analysis is to "describe the measurement process" and that is the purpose of this section. In order to determine the drag coefficient for a single configuration at a single test condition a number of "experiments" must be performed and information from each of these experiments is used to compute the final result, the drag coefficient. To provide some perspective for the complexity of this task, there are approximately 11 "experiments" performed prior to the actual tunnel-on measurement and a conservative estimate indicated that there are more than 250,000 pieces of information which are acquired and processed to make a single C_D calculation.

The following attempts to outline in a very general manner the "measurement process" for drag measurements in the NTF. Only limited details are provided for each aspect of the process and the goal of the section is to identify the primary flow of information and its eventual impact on the system wide data uncertainty. More details on the current data acquisition system and data reduction procedures should be available by contacting the NTF.

A very crude "abstraction" of the NTF measurement system is shown in Figure 3. The primary components in the system are the wind tunnel, the "aircraft" model, the pressure and temperature sensing systems which monitor the tunnel conditions and the force balance and model orientation instruments which monitor the model. The information from each of the main instrumentation systems is acquired by the data acquisition system (DAU) and converted into digital information for subsequent processing by the data reduction software.

A more detailed representation of the system was prepared and is shown in Figure 4. The figure is "inverted" and the information in the system "flows" from the bottom to the top. There are a series of sensors used to monitor the tunnel conditions and their output is used to compute the desired "results" such as Mach number, Reynolds number, dynamic pressure, etc.. The wind tunnel model's interaction with the fluid results in pressures acting on the model and a temperature distribution within the model. The model is supported by a six-component, strain gage balance. The electrical, analog output from the various temperature, pressure, orientation and strain sensors is passed through a signal conditioning system which independently filters and amplifies each signal. These analog signals are then multiplexed, sampled and converted to digital representation. All of the sensor input, except the orientation or AOA sensors, are digitized by a single A-to-D unit. This information is then combined with a significant amount of other "data" as part of the data reduction process.

A wide variety of results are available each having their own respective uncertainty and each additional calculation has the potential for adding to the uncertainty. In the case of aerodynamic coefficients, various "corrections" are often required in order to transform a non-dimensional "force" measured in the wind tunnel to an estimate of the actual aerodynamic characteristic that the full-scale aircraft would encounter in flight. The study documented in this report did not address many of the issues of data processing but focused on the process up through the point indicated by the box labeled "Uncorrected Coefficients". Once one has determined the uncertainty associated with the uncorrected coefficients it can influence the selection and assessment of the various corrections which can be applied to the results.

A series of pressure transducers are used to sense the total pressure in the tunnel plenum and the static pressure in the test section. Currently Ruska transducers are used and they are connected via a series of manifolds so that the specific transducer which is being monitored by the data acquisition system

depends upon the pressure level being sensed. This pressure measuring system and the transducers are referred to as "Ruskas" through the remainder of this report. The temperature measurement system which is used to sense the total temperature in the tunnel uses a platinum-resistance temperature probe. This probe and the temperature measurement system are referred to as the PRT in this report. Additional details on these systems are provided in Reference 27.

The two central features of the type of measurement system used in the NTF are the sensors which convert the physical properties into electrical voltages and the process of conversion of the analog information to digital information. Many of the issues related to the sensors are far beyond the scope of this limited study. Since many of the sensors are "calibrated" the performance of the sensor is not directly considered in the uncertainty analysis. Issues related to "is the sensor actually sensing what is desired" are central to the uncertainty estimates. From the perspective of the test engineer, the process of converting the analog signals to digital information is central to the measurement process. One might consider that this is where the actual "measurement" takes place. Once this has occurred, the information is "frozen" (neglecting certain issues relate to computational round-off, truncation, etc.,.) and in the modern computing environment, things become quite precise.

Figure 5 presents a more detailed schematic representation of this part of the data acquisition process. Each analog channel, of the three represented in the figure, is amplified and filtered before it is introduced to the programmable gain amplifier, PGA, which is part of the analog to digital converter. The manner in which the analog voltage signal is processed is important to the uncertainty analyst since it is the voltage level of the signal, which varies from test point to test point, that will influence the relative uncertainty in the digitized result. Also each of these components modify the "signal" produced by the sensor. As indicated on this schematic each of these channels can be independently "calibrated". The calibration of each of these channels, done on a daily basis, also influences the uncertainty in the final result. Figure 6 illustrates a more detailed view of a single channel of the analog input to the DAU. It is used to illustrate the various configurations that this system can assume. The input amplifier gain can be varied from 1 to 500. Each channel is filtered at either 1 or 10 Hz and this has a marked effect on the sampling rates, data averaging and the ability of the system to rapidly move from test point to test point. Additional amplification can occur after multiplexing and the analog data is converted to its

digital representation at rates from 10 to 50 samples per second per channel. For the test cases used in this report each channel of analog data was sampled at 10 Hz.

3.2 Basic Measurement Systems

The measurement system described above, also known as the NTF, is not only used to collect information on the wind tunnel model of interest, but also to conduct a number of "calibration" experiments. It is actually only one of a number of "facilities" used to develop the information that is necessary to interpret the information collected during aerodynamic testing in the NTF. The following discussion overviews the individual experimental "set-ups" for the experiments required to collect all of the information necessary to measure the drag coefficient on a wind tunnel model. It highlights the information collected as a result of each experiment. Each of these "set-ups" were used to define each of the steps in the measurement process and to highlight for the author those points in the process where data was "collected" and information processed.

3.2.1 DAU System

One of the fundamental systems is the DAU. It is used to acquire a majority of the data collected at the NTF. Therefore one of the basic experiments which is required is the calibration of the DAU. Figure 7 illustrates the DAU and the process used for calibration. This type of schematic will be used to represent each of the basic systems. The "source" of the information is usually presented in a box in the upper left hand corner of the figure. Information "flows" from the source in an analog form (solid lines) or in digital format (dashed lines). The output from the process is on the lower right-hand side of the figure in the "bold" oval. The "units" associated with the information are often indicated at appropriate locations on the figures. Some of the elements in the figures represent pieces of equipment such as filters, amplifiers or A/D converters, others represent data reduction processes like curve fitting. These figures are a useful way of understanding how information progresses from analog to digital form and to differentiate between data collection and data processing activities. This is an important distinction in understanding the measurement process from an uncertainty analysis perspective.

For the DAU calibration a precision voltage source is used as the working standard. The voltage source is "commanded" to produce a certain voltage level

which, upon closure of the calibration relay contact, introduces that voltage to a given channel of the DAU. For a preselected and commanded voltage level the output from the analog to digital converter in bits is recorded. This voltage and "bits" information are processed by a linear curve fit to provide a slope and offset or bias (not to be confused with a bias limit or error) for each channel of the DAU. This slope and bias information is then stored and used to convert bits to digital "voltage" information in future measurements. Additional details on the DAU calibration process are included in Reference 28.

As with each of the systems or experiments discussed in the following sections, anytime an experiment generates a result that result has an uncertainty associated with it. In the case of the DAU the slope and bias for each channel are the results of this experiment and in order to eventually perform an uncertainty analysis for the complete system it is necessary to define the uncertainty in each of these results. Though both bias errors, such as those associated with the working standard , and precision errors, such as those associated with variations in the calibration experimental process, are present in these results, the result itself is very precise and it doesn't vary until the next calibration. If a result of the calibration experiment is in error, this error will be propagated as a bias error whenever the result is used in future calculations.

3.2.2 Pressure Measurement System

There are three separate "experiments" associated with the pressure measurement system. Recall that at any one test point there are at least two pressure measurements being taken, one static pressure and one total pressure. There are a number of possible transducers that could be used depending on the pressure level but for each transducer there is a calibration experiment in a calibration lab, a "two-point" calibration in the wind tunnel and then the actual measurement conducted at the test point. Figures 8-10 .

The Ruska is calibrated in a calibration laboratory using a dead weight tester as a working standard. The output from the Ruska is digitized using an integrating digital voltmeter (IDV). The working standard pressure (psi) and the IDV output (volts) are then used to provide calibration slope information. A bias is also computed but this is only used as "check" and the actual calibration curve offset or bias is determined using the experiment discussed below.

This highlights a point made earlier, that many of the instruments used in the NTF are calibrated in an environment and with procedures much different

than those used in the actual measurement process. Therefore the uncertainty of the instrument from the calibration experiment may not be the same as the level of uncertainty achieved in the actual measurement.

Figure 9 illustrates a second calibration experiment performed for the Ruska. In this case the Ruska is tested when installed in the wind tunnel and its output is processed through the DAU. Two "working standards" provide the test points. One is near vacuum and the other is the current atmospheric pressure which is actually sensed by another Ruska. In this experiment the "bits" output from the DAU are first processed using the calibration data developed for the appropriate channel. This information along with the values from the working standards is then used to determine the bias for a linear representation of the relationship between output voltage from the Ruska and pressure in engineering units. As one can see these experimental results will carry along the errors associated with the working standards, the DAU operation, the DAU calibration information and the curve fitting process.

The final experiment is the actual in-tunnel, test point measurement as presented in Figure 10. In this case the voltage output from the Ruska, digitized using the DAU system, is converted to voltage using the DAU calibration data and then converted to pressure using the earlier developed pressure system calibration data. These pressures may be considered as results or, as in most cases, they are used with other information as part of the data processing to achieve the information desired from the test. These measured pressures have associated with them precision errors which could be quantified by making multiple measurements at a "fixed" test point as well as bias errors which are due to errors in standards, calibration constants, installation errors, and other factors.

3.2.3 Temperature Measurement System

There are two experiments performed with the temperature measurement system, as illustrated in Figures 11 and 12. One is a calibration performed in the calibration laboratory and the other is the actual temperature measurement performed in the tunnel at the test point. The PRT calibrations use constant temperature baths for the working standards. Though only limited details are indicated for the calibration laboratory process the results of the calibration are the Callender-Van Dusen constants, α, β, and λ which are then stored for future use. The working standard "baths" are monitored using another PRT sensor.

The in-tunnel total temperature measurement actually involves measuring two voltages. One voltage is associated with the PRT sensor located in the tunnel and the other is the voltage across a "precision calibration" resistance. Both voltages are digitized using independent DAU channels, and then the "bits" measured by the DAU are converted to digital "voltages" using the DAU calibration constants. The digital voltages, the value of the calibration resistor and the Callender-Van Dusen constants are then used in the data reduction program to determine the total temperature. As indicated earlier in the discussion on the pressure measurements, the error in total temperature will have both bias and precision components. The bias errors will be due to the calibration and installation of the PRT as well as bias associated with the DAU channel calibrations.

3.2.4 Model Orientation Measurement System

Though there are various means for determining the angle of attack of a wind tunnel model in the NTF, the system discussed in this report uses a single axis, servo-accelerometer located on the wind tunnel model to sense the relative orientation between the accelerometer and the local gravity vector. This sensor is referred to as an "AOA" in this report. The information acquired from this sensor is processed along with other information concerning flow direction and position of the sensor in the model in order to measure the angle between the free-stream flow direction and an appropriate reference axis on the model.

In this case there are again three experiments associated with the orientation measurement, as illustrated in Figures 13-15. In the calibration laboratory, the working standard is provided by a precision indexing head which can be used to orient the AOA package to a variety of positions relative to the local gravity vector. Output from the instrument is digitized using an integrating digital voltmeter and the voltage and orientation information is "curve fit" in order to determine four parameters. These are the basic sensitivity, bias and two other parameters referred to as Omax and Az which are related to "misalignment" of the instrument relative to its mounting. Only the value for the sensitivity as determined in the calibration lab is actually used during data reduction and the other parameters are for reference purposes only.

Once the AOA package is mounted in the model and the model mounted in the wind tunnel, an additional calibration experiment is performed, see Figure 14. Using the model positioning system in the wind tunnel, the model is placed in

three different roll orientations, 0°, 90° and 180°. Using output from the sensor at these three measurement orientations and the instrument sensitivity from the calibration lab experiment, new values for bias, Omax and Az are determined. These values replace the reference values from the calibration laboratory experiment. (This may imply that the sensitivity and bias for the AOA are not independent parameters, since one is determined using the other. This could imply that bias errors in each are not uncorrelated - though this fact is not pursued in the current study. See Appendix B.)

The in-tunnel measurement system for the model orientation at the test point is shown in Figure 15. The output voltage from the IDV is combined with the calibration information from the two calibration experiments to provide the orientation of the sensor relative to the gravity vector. This information is then combined with other information on the tunnel and model to determine the angle of attack as part of the data reduction process.

As mentioned above the voltage output from the AOA is digitized using an integrating digital voltmeters for the calibration experiments and the tests conducted in the NTF. This is the only instrument of those considered in this report that does not use the DAU at the NTF for analog to digital conversion. As suggested by the dashed line in Figure 4, that capability does exist and has been used on some tests. It is obvious that one should be aware of the details of each aspect of the complete measurement system in order to be able to effectively assess the uncertainty. Changes in how the data is acquired or specified components of the system will influence the uncertainty estimates for the results.

3.2.5 Force Measurement System

As one might expect the balance is central to the aerodynamic force measurement system. The force balances are precision instruments, which in the case of the NTF, are exposed to an extremely hostile environment. The balances are approximately 2 inches in diameter and 15 inches long. They must support wind tunnel models that weigh hundreds of pounds and are subjected to aerodynamic loads that may be two orders of magnitude greater than the model weight.

The calibration of the multi-component wind tunnel balance is in its own right a very complex experiment. The procedure is illustrated in Figure 16 and discussed in some detail in Reference 29. Loads are applied to the balance through a complex mechanical system using precision weights. The balances

can be calibrated at room temperatures (as is done for most of the calibration information) or at cryogenic temperatures. During calibration the voltage applied to the balance bridges is measured as well as the voltage output from each of the six bridges. (The X6 symbol on the Figure is an indication that there are six strain gage bridge channels on each balance.) This is done for a wide variety of loading conditions and that data is process to provide a set of information referred to as the "balance deck". This includes the primary balance sensitivities, first and second order interaction coefficients, sensitivity shifts and zero shifts. As with any experiment each of these parameters which are the result of the calibration experiment has their own uncertainty. There is an ongoing effort to determine the uncertainty of each of these parameters and due to the complexity of this issue it is not discussed in detail in this report.

The balance is then installed in the model and another calibration is conducted in the Model Preparation Area (MPA) at the NTF. This calibration takes place in a cryogenic chamber and uses the DAU system for analog to digital conversion. There are nine channels of balance information which are required, the six strain gages bridges and the voltage from three thermocouples mounted on the balance. The balance output is effected by the temperature of the balance and temperature gradients within the balance. This information is used to provide updated zero shifts for the balance as installed in the model.

The balance measurement system in the tunnel is illustrated in Figure 18. The measured parameters consist of the voltage source, the six strain gage bridge imbalance voltages and the three thermocouple voltages. This data is combined with the calibration information to determine the forces transmitted from the model, through the balance and to the model support system. The NTF balance beams are configured to measure two normal forces, two side forces, an axial force and a rolling moment. These results are then converted into the three force components (axial, normal and side) and three moment components (pitch, yaw and roll) in the body axis system.

It should be noted that though the data acquisition system used in the MPA is the same as that used in the tunnel that there are important differences in the systems. There are different "wires" which carry the very low voltage bridge output signals from the MPA to the patch panel, and thus the DAU, than from those that carry the signal from the tunnel to the patch panel. Though there are probably many other subtle issues not mentioned in this brief overview, it is this type of difference that can become important in an uncertainty analysis. A very

thorough understanding of the measurement system is required in order to perform an effective uncertainty analysis. This is particularly the case when the system being evaluated is as complex as the NTF. Most of the references cited earlier in the report suggest the use of caution concerning the calibration of sensors and instruments in environments outside of the nominal test environment. But as one can see, this is done in almost every measurement system used in the NTF and this must be accounted for in the uncertainty analysis.

3.3 Basic Measurement Summary

The previous section outlined the certain aspects of the various calibration and in-tunnel experiments. The following is a brief outline which provides an overview of a "typical" sequence of tests and their associated results. Each of these tests are required to provide the information needed to determine the drag coefficient at a single test point. For the calibration experiments (a - k) a "standard" is indicated as well as the quantity/s measured and the result of each experiment. For the actual "measurements" conducted at a test point (l - p), the information recorded is indicated. This information is then combined with other data, often from the calibration experiments, to compute basic measurements (i.e. pressures, temperatures, forces, etc.) which in turn are used to determine results (i.e. Mach number, Reynolds number, angle of attack and C_D). Defining the measurement process and sequence in this manner proved useful in attempting to establish the source of bias errors for the information used in the final off-line data reduction process.

a. Ruska Calibrations
   standard - dead weight source
   measurement - voltages (IDV)
   result - "slope" constant
b. PRT Probe Calibration
   standard - constant temperature baths
   measurement - voltages (source unknown)
   result - Callender-Van Dusen constants

c. Single axis AOA Calibration

standard - mechanical positioning system

measurement - voltages (IDV)

result - "sensitivity" constant

d. 6-component Balance Calibration - Ambient temperature

standard - precision weights and mechanism

measurement - voltages (IDV)

result - "Balance deck"

e. 6-component Balance Calibration - Cryogenic temperatures

standard - precision weights and mechanism

measurement - voltages (IDV)

result - sensitivity shift correction parameters

f. 6-component Balance/Model - MPA- Cryogenic temperatures

standard - MPA temperature sensors

measurement - binary numbers, 0 to $\pm 2^{14}$ for nine channels

result - zero shift temperature correction parameters

g. Data Acquisition Unit Calibration - per channel

standard - precision voltage source

measurement - binary numbers, 0 to $\pm 2^{14}$

result - slope and bias constants for each channel

h. Ruska Two-point Calibration

standard - vacuum and Ruska

measurement - binary numbers, 0 to $\pm 2^{14}$

result - zero shift voltage

i. Single axis AOA In-tunnel Calibration - $T_{ambient}$

standard - reference block and tunnel model positioning system

measurement - binary numbers, voltage from IDV

result - bias and misalignment corrections

j. Model Weight Tare Measurements- $T_{ambient}$

standard - model positioning system

recorded data -binary numbers, 0 to $\pm 2^{14}$, balance output

result - weight tare corrections

k. Wind-off Zero Measurements - Cryogenic test point temperature
standard - model positioned at reference condition
measurement - binary numbers, balance output
result - wind off zero shift voltages

l. Ruska Total Pressure Measurement - Test point conditions
recorded data -sensor output voltage converted to binary number, 0 to $\pm 2^{14}$

m. Ruska Static Pressure Measurement - Test point conditions
recorded data -sensor output voltage converted to binary number, 0 to $\pm 2^{14}$

n. PRT Probe Measurement - Test point conditions
recorded data - sensor output voltage converted to binary number, 0 to $\pm 2^{14}$

o. Model Attitude Measurement - Test point conditions
recorded data - digital representation of sensor output in volts from IDV

p. 6-Component Balance Measurement - Test point conditions
recorded data - balance output voltage converted to binary numbers, 0 to $\pm 2^{14}$, for nine channels

3.4 Off-line Data Reduction

The NTF data system allows for both on-line and off-line data processing. The on-line systems provides near-real-time process parameters and "results". Not all corrections are applied to the on-line results and therefore they are often considered to be "approximate". This on-line capability provides "snapshots" of time-averaged information and provides the test directors and test engineers with information used to make decisions during the testing in the form of listings and data plots.

A majority of the data processing is conducted after the completion of the test and allows for more detailed analysis and re-analysis of the recorded information. This report is concerned with the uncertainty in the results developed using the off-line data processing. The primary "components" of the data reduction system are the computer and primary data processing software, the "DAS" tape and the setup "deck".

The basic software is developed from FORTRAN code and can be executed on a variety of computers. It is a rather extensive computer program but allows the user significant flexibility and numerous options for data processing.

The program also contains certain specific information such as "gas" constants and tunnel calibration information which cannot be altered by the user. The "DAS" tape is the primary source of recorded information and data. It contains the digital representation of the analog measurements from the DAU, the DAU calibration results and Ruska calibration constants. Most of this information is considered to be "raw" and the data has undergone very little processing.

The "setup" deck provides the user with a direct interface with the data reduction process. It contains the force balance, AOA and PRT calibration constants. It identifies the appropriate DAU output channels for data reduction and any special instructions or calculations requested by the user. When the study documented in this report was conducted, alteration of the "setup" deck was the only means available to evaluate the data reduction process. Therefore the parameters which were considered in the sensitivity analysis and subsequent error calculations were limited to those which could be accessed through the "setup" deck. This was due to the limited time available for the current effort and not an inherent characteristic of the data reduction process.

There were five parameters which were considered as the "results" in this preliminary study. These were,

Mach Number
Reynolds Number
Angle of Attack
Drag Coefficient, C_D
Lift Coefficient, C_L

These represent only a very limited subset of the literally hundreds of process or model parameters which can be computed as part of the data reduction process. Each are determined by a number of constants and measured data. Additional details on the methods used for data reduction can be found in Reference 29.

The uncertainty in each of these results will be influenced by the methods used to calculate the results. Certain issues such as computer precision and approximate numerical methods or approximate analytic models can influence the uncertainty estimates. These issues have not been addressed in this study and though it is not apparent that they will have a significant influence on the uncertainty estimates for the NTF, their effect should be considered as this uncertainty analysis moves from its preliminary to the application stage.

As related to data reduction, the most critical aspect which can influence the uncertainty in the result is a sound understanding of the "physics" which

influence the result. If improper models or assumptions are applied to the "measured" results, the "errors" can be significant even if all of the computations and numerical calculations are "exact". An inappropriate equation of state, erroneous gas constant, or an assumption that the pressure at point "a" is equal to that a point "b" can result in an uncertainty which exceeds all of those estimated for the actual measurement process. As is the case with the measurement process, a thorough understanding of the "physics" is a prerequisite for an effective uncertainty analysis.

Section 4. Calibration and Uncertainty

Computer-based, automated data acquisition and processing systems have provided significant improvements in the manner in which experiments are performed but they have also provided some additional challenges. They can allow for the acquisition of large amounts of information and on occasion may encourage the user to consider a result to be "correct" because the computer processed the data with great precision. In determining the result of an experiment, the computer usually manipulates two types of information; data acquired as part of the actual measurement and "constants", some of which are the results of other experiments often referred to as calibrations. This section addresses a number of issues related to the data developed in calibration experiments and subsequently used in the primary measurement process.

Calibration is the method used to exchange "large" bias errors in an instrument for the "smaller" bias errors of the standard used for the calibration and the precision errors in the calibration process. In the case of the NTF, all of the instruments used in the wind tunnel tests are calibrated, some on a daily basis. Most of the publications related to uncertainty analysis strongly recommend that instrument calibrations be performed under the same conditions as the actual measurement process. As indicated in Section 3, in the case of the NTF some of the calibrations are conducted in the tunnel itself but often the calibration is performed in a specialized calibration laboratory. Since these calibration experiments provide a majority of the "data" used in the calculation of the results of a wind tunnel test, the information developed during calibration and its uncertainty are an important contributor to the overall uncertainty of the result.

4.1 The Calibration Experiment

Quantifying the influence of the uncertainty in the "instrument" as it will be used in the actual measurement process is complicated when the calibration of the instrument is conducted in an environment and with data acquisition systems which are different than those used with the instrument in the wind tunnel. When this occurs one may wish to consider that the calibration process is actually a separate "experiment" from which specific information is determined and used in the subsequent application of the instrument. In this case it is important to realize what information is actually provided by the calibration process and to establish the required "uncertainty" for that information.

There are a number of assumptions upon which the approach for dealing with calibration uncertainty as presented in this report are based. They are:

1. "Calibration " is simply an experiment whose results are specific "numbers" which will be used in other experiments which are referred to as measurements. Uncertainty associated with the results of the calibration are "fixed" or "frozen" when used in the subsequent calculations and contribute to the bias errors in the actual measurement.
2. Automated, computer-based data acquisitions systems are used to "measure" voltages and only voltages. Actually the data acquisition systems produce finite precision, binary numbers which are hopefully proportional to voltage over a specified range. The voltage is the result of data reduction using the binary representation of the input signal and other "calibration" information.
3. The signal conditioning and analog-to-digital (A/D) systems used in the "calibration" experiment and the "measurement" system are/may not the same systems.
4. The "environment" in which the calibration takes place may not be the same as that for the measurement.

Consider the simple schematic shown in Figure 19. It represents two distinctly different experiments although some of the hardware is common to both. In the first experiment, referred to as "calibration", some type of sensor/transducer is exposed to an environment which results in a response from the transducer. This response is typically processed by a collection of electronic devices which make-up the "instrument". The instrument provides a voltage differential which is in some way related to the response of the sensor to the input provided by the "calibration" environment. This voltage is then introduced as input to a signal conditioning circuit, SP1, where it may be filtered or amplified or both. This modified voltage difference is then provided to an analog-to-digital (A/D1) converter which generates a "number of bits". This "number of bits" information, now in the form of digital information, is usually converted to a number with a finite number of significant digits which represents the voltage resulting from the sensor's response to the environment . It should be emphasized that each element in this process can be influenced by its environment and operating conditions and each of these influences can add to the uncertainty in the information developed.

In a parallel fashion, additional information is provided by a "working standard" and the results are digital information which contain a finite number of significant figures. It is expressed in the units of the physical quantity being measured, often a physical quantity expressed in engineering units, EU. Therefore the basic information recorded during the calibration experiment are digital data pairs (volts, EU) and each of these quantities has an associated "uncertainty" or "error". The EU error is due to the uncertainty in the working standard and the voltage errors are due to the processing and recording of the instrument output. One should note that for some instruments the data pairs are actually pairs of vectors of information. This is the case for the six-component wind tunnel balances used in the NTF. Though much of the following discussion is conceptually consistent with this more complex instrument, many of the practical issues are far beyond the scope of this report.

One needs to determine the uncertainty in the "results" of the calibration experiment which are typically calibration "constants" which are then used to process the information provided by the instrument in the wind tunnel. Before considering how to estimate the uncertainty in the calibration experiment, again refer to Figure 19 and the actual "measurement" experiment. In this case the same instrument is now used but in a different manner. The transducer/sensor is exposed to the test environment and again the instrument produces a voltage differential. This voltage differential is applied to another (most often with different characteristics) signal conditioning system, SP2, and a different A/D system DAU2. The "bits" information from DAU2 are converted to "voltage" in digital form. That voltage has a certain "error" associated with it and it undergoes numerical processing (data reduction) in order to provide a measure of the physical parameter in engineering units. The numerical processing involves the calibration constants determined from the calibration experiment. Therefore the measurement, expressed in engineering units, carries with it uncertainty due to both the calibration and measurement process.

4.2 Curve Fitting

The calibration constants that are used to characterize a given instrument's performance are often determined from a linear regression analysis or "least-squares curve fit". Curve fitting is a data processing procedure in which the basic concepts of propagation of errors or statistical analysis can be applied in order to estimate the required uncertainty information. References 22 and 24

present detailed developments and associated numerical procedures for regression analysis so the following only highlights aspects that are directly related to the methods applied in this study.

Consider the results of the calibration experiment to be ordered pairs of data. Recall that each piece of digital information has associated with it an error. Most developments for least squares curve fitting are based upon the assumptions that there is no uncertainty in the independent variable and that the dependent variable satisfies certain statistical requirements. This assumption is quite reasonable in cases where the calibration process is "steady" and the uncertainty in the working standard is significantly less than the precision of the instrument. This assumption may not be correct in cases where the precision of the instrument and the working standard are comparable.

Assuming that these assumptions are satisfied then the sets of data are in the form, (X_i , Y_i) for i = 1,N. For the simple case considered in this report the least squares curve fit will be used to quantify a linear relationship between X and Y and provide the slope, m, and intercept, a, for the expression:

$$Y = m X + a \qquad \text{Eq. 4.2.1}$$

For the straight-line fit a rather simple expression can be written for the two "results" a and m explicitly in terms of the "measurements" X_i and Y_i for all N measurements.

$$m = \frac{N \sum_{i=1}^{N} X_i \; Y_i - \sum_{i=1}^{N} X_i \sum_{i=1}^{N} Y_i}{N \sum_{i=1}^{N} X_i^2 - \left(\sum_{i=1}^{N} X_i \right)^2} \qquad \text{Eq.4.2.2}$$

$$a = \frac{\sum_{i=1}^{N} X_i^2 \sum_{i=1}^{N} Y_i - \sum_{i=1}^{N} (X_i \; Y_i) \sum_{i=1}^{N} X_i}{N \sum_{i=1}^{N} X_i^2 - \left(\sum_{i=1}^{N} X_i \right)^2} \qquad \text{Eq. 4.2.3}$$

Since the parameters used to determine a and m had associated with them an uncertainty (at least the Y_i's did), then both a and m also have an uncertainty. Estimating this uncertainty is an important part of the regression analysis since it provides an indication of the utility of the resulting regression coefficients.

A number of approaches can be used to estimate the uncertainty in these parameters but considering the context of this report, an approach based upon error propagation was used. If one considers the determination of a and m as simply a data reduction process using numbers with their own uncertainties, then the uncertainty in a and m can be determined using the methods outlined in Section 2.7. This requires an estimate of the uncertainty in each measured parameter. If one assumes no uncertainty in the independent variable, then the precision index for x, which is S_{xi}, is zero. The precision index for the dependent variable can be based upon the unbiased estimate of the standard deviation associated with the dependent variable can be expressed as,

$$\sigma_{est} = SYi = \left\{ \frac{\sum_{i=1}^{N} [\, y_i - a - m\, x_i \,]^2}{N - 2} \right\}^{1/2} \qquad \text{Eq. 4.2.4}$$

This parameter is also referred to as the standard error of the estimate (SEE).[17] This estimate is then used with Eq. 2.7.2 as applied to the computed parameters "a and m" to yield estimates of the precision indices for a and m,

$$S_a = \left[\sum_{i=1}^{N} \left(\frac{\partial a}{\partial Y_i} S_{Y_i} \right)^2 \right]^{\frac{1}{2}} \qquad \text{Eq. 4.2.5}$$

$$S_m = \left[\sum_{i=1}^{N} \left(\frac{\partial m}{\partial Y_i} S_{Y_i} \right)^2 \right]^{\frac{1}{2}} \qquad \text{Eq. 4.2.6}$$

The precision limit can be determined from the precision index by scaling with the appropriate t factor for the desired level of confidence and appropriate degrees of freedom. The degrees of freedom for the estimate of the standard deviation is based upon the number of points in the "fit" and the number of coefficients. In this case it is N-2 where N is the number of points to which the straight line is fit.

Once the two estimates of the precision limits for the parameters a and m have been determined they become fixed as bias errors and are treated as such in the remaining calculations.

$$B_a = t\, S_a \qquad \text{Eq. 4.2.7}$$

$$B_m = t\, S_m \qquad \text{Eq. 4.2.8}$$

This is due to the fact that these parameters are "frozen" until the next time a curve fit is conducted.

4.3 Bias Errors in the Measurement Due to Calibration

In the case of a calibration experiment, the independent variable, X, is usually the value of the working standard and is often expressed as a quantity in engineering units. The dependent variable, Y, is the sensor output often expressed as volts. When the calibration experiment is complete, the curve fit performed and the uncertainties computed, the instrument is now used in a measurement. When this occurs the expression,

$$Y = a + m\,X \qquad \text{Eq. 4.3.1}$$

is then rearranged and "used" in the form,

$$XM = A + M\,Y \qquad \text{Eq. 4.3.2}$$

where XM is the measured parameter in engineering units corresponding to the voltage Y. The slope and intercept for this reciprocal relation are,

$$A = -\frac{a}{m} \qquad \text{Eq. 4.3.3}$$

$$M = \frac{1}{m} \qquad \text{Eq. 4.3.4}$$

Since A and M are the result of computations using 'a' and 'm', one can estimate the bias limits for A and M from the bias limits for 'a' and 'm' using propagation of errors, Eq. 2.7.2, and assuming that the bias limits in 'a' and 'm' are uncorrelated.

$$B_{A_{curve\ fit}} = \left[\left(\frac{\partial A}{\partial a} B_a \right)^2 + \left(\frac{\partial A}{\partial m} B_m \right)^2 \right]^{\frac{1}{2}} \qquad \text{Eq. 4.3.5}$$

$$B_{M_{curve\ fit}} = \left[\left(\frac{\partial M}{\partial a} B_a \right)^2 + \left(\frac{\partial M}{\partial m} B_m \right)^2 \right]^{\frac{1}{2}} \qquad \text{Eq. 4.3.6}$$

Evaluating these two expressions yields

$$B_{A_{curve\ fit}} = \left[\left(\frac{B_a}{m} \right)^2 + \left(\frac{a}{m^2} B_m \right)^2 \right]^{\frac{1}{2}} \qquad \text{Eq. 4.3.7}$$

and

$$B_{M_{curve\ fit}} = \frac{B_m}{m^2} \qquad \text{Eq. 4.3.8}$$

Then in the process of using the calibration constants to evaluate the "measured" parameter XM the bias due to the curve fit may be combined with other bias limits. These other bias limits can be attributed to the working standard or other sources as the particular application requires. Then the bias limits in A and M are computed by addition in quadrature.

$$B_A = \left[\left(B_{A_{\text{curve fit}}} \right)^2 + \left(B_{A_{WS}} \right)^2 + \left(B_{A_{\text{other}}} \right)^2 \right]^{\frac{1}{2}} \quad \text{Eq. 4.3.9}$$

$$B_M = \left[\left(B_{M_{\text{curve fit}}} \right)^2 + \left(B_{M_{\text{other}}} \right)^2 \right]^{\frac{1}{2}} \quad \text{Eq. 4.3.10}$$

This form is based upon the assumption that the biases in the curve-fitting and calibration process are uncorrelated. The bias limit for the "measured" parameter XM is then computed recalling Eq. 4.3.2 and Eq. 2.7.2 where the bias error in the two computed parameters A and M as well as the bias in the measured parameter Y are combined and propagated through the data reduction process to determine the bias in XM.

$$B_{XM} = \left[\left(\frac{\partial XM}{\partial A} B_A \right)^2 + \left(\frac{\partial XM}{\partial M} B_M \right)^2 + \left(\frac{\partial XM}{\partial Y} B_Y \right)^2 \right]^{\frac{1}{2}} \quad \text{Eq. 4.3.11}$$

Which results in the expression,

$$B_{XM} = \left[\left(B_A \right)^2 + \left(v\, B_M \right)^2 + \left(M\, B_v \right)^2 \right]^{\frac{1}{2}} \quad \text{Eq. 4.3.12}$$

This bias limit is expressed in engineering units in the measured result. It could be combined with other bias limits in XM due to estimated biases in the

measurement process or installation. If the parameter XM is a result, the bias limit could be combined with a measured precision limit in parameter XM (determined from multiple measurements) to yield an uncertainty in XM. Or as is the case for most of the measurements, it can be propagated into the calculation of other results to determine the bias limits of the computed results.

Section 5. Uncertainty Estimation - Preliminary Results

This section presents the results of a preliminary end-to-end system uncertainty analysis performed using information from the NTF. It should be emphasized from the beginning that this represents a "framework" for a more comprehensive uncertainty analysis and the "approach" associated with each step is of much greater concern than the "results." As with any uncertainty analysis, as the results of this preliminary study are evaluated, additional factors can be introduced and parameter estimates, particularly with regard to the bias estimates, can be improved. There are many results which are determined from a test in the NTF. In this study the primary results for which uncertainty estimates were made were the Mach and Reynolds numbers, angle of attack and the non-dimensional force coefficients in the wind-axis system C_L and C_D.

5.1 Nominal Test Point

Though one may be tempted to refer to a single "uncertainty" for an entire experiment or facility, in practice, each data point or measurement has associated with it its own unique uncertainty estimate. This is particularly important in those cases where the parameter sensitivities depend upon the nominal parameter values - a most common occurrence. For the study presented in this report, data for a series of tests on a subsonic commercial transport model were available. The basic test conditions are summarized as,

Mach No. = 0.80

Reynolds No. = 40.7×10^6

Total Temperature = -250° F

Dynamic pressure = 2660 psia

This represents a near full scale test simulation which is the purpose of the cryogenic capabilities of the NTF. The tests were conducted in nitrogen in order to achieve the cryogenic conditions and thus proper Reynolds number scaling.

The wind tunnel balance NTF113A was used for these tests. The "angle of attack" or AOA device was designated as 12-6. Each of the balances and orientation sensors used at the NTF have their own designation, calibration and calibration history. The detailed information available for each of these devices was invaluable in preparing the uncertainty estimates.

Most of the results presented in this study are for the two test points shown below. These represent only two test points in a large series of tests

conducted with this model. These test points were selected so that the same DAU calibration and wind-off-zero information was used for each test point. The two points represent a near "zero-lift" case and a near "cruise" case and will be referred to as Test Points A and B in this report.

Test Point	Angle of Attack	C_D	C_L
A	-0.92°	0.01517	0.034
B	2.18	0.02144	0.394

These two test points represent "single" measurements and therefore precision error estimates conducted using either would be based on "single point" measurement techniques. During the test on this particular aircraft model a series of measurements were also conducted which allowed for the use of multiple measurement techniques for the precision limit estimates. One of these tests was considered in some detail in the current study. In this case 10 sequential measurements were recorded. The model was positioned at the desired angle of attack and the tunnel conditions established. The computer was manually signaled to record a data point, the conditions were maintained and then after a delay of about 10 seconds another data point recorded. This process was repeated until the 10 data points had been measured. The average values for the model conditions are given below and the other test parameters were the same as those for test points A and B. These 10 measurements will be referred to as Test Points C through L in this report.

Test Point	Angle of Attack	C_D	C_L
C - L	1.64°	0.01935	0.357

These 10 test points were then considered in more detail as discussed in the following sections and were used to establish end-to-end precision limit estimates.

5.2 Sensitivity Calculations

In order to determine the uncertainty in the experimental results one must determine the "sensitivities" of the results to variations in the contributing measurements as discussed in Section 2.7. There are two options for

determining these derivatives. The first is by analytic evaluation of the partial derivatives as was done in Reference 23. Though in certain cases this is both very direct and provides additional useful information, it was not the approach taken during this study. Since the actual data reduction software which is used to process the measurements taken in the NTF was available, the sensitivities were determined from numerical estimates of the partial derivatives. This involved a systematic perturbation of the individual parameters about the nominal test conditions.

Due to the time constraints imposed upon this study the only parameters which were included in the uncertainty estimate were those which sensitivities could be determined directly from the data reduction software. This limited the analysis to include only those parameters which could be altered via the SETUP data for the off-line data processing. Certain measurements and constants which are stored on the DAS tape were not considered but it must be emphasized that this was not necessarily due to the fact that they were not important, only that they were "inaccessible" during this preliminary study.

Two types of parameters were considered during the sensitivity calculations. They were classified as "fixed" parameters and "measured" parameters. The fixed parameters were those developed during previous calibration experiments or tests. The measured parameters were unique to a given test point and are the average values of the 10 analog to digital conversions at a 10 Hz sample rate. The data processing program automatically applies the DAU calibration information to the "bit" information from the analog to digital converter so the that the measured parameters are in units of voltage.

The following list includes all of the parameters considered during this preliminary study. The notation used to identify each parameter is consistent with the data processing program and associated documentation[27].

1. Balance sensitivities: S1 - S6 [fixed]
   (note the primary sensitivities correspond to the following force components : S1 - AF, S2 - SF, S3 - NF, S4 - RM, S5 - PM, S6 - YM)
2. Balance input voltage: BALPOW [measured]
3. Balance bridge output voltages: NF1RAW, NF2RAW, SF1RAW, SF2RAW, AXFRAW, RLMRAW [measured]
4. AOA output voltage: ELEVA [measured]
5. AOA calibration constants: AOAS, AOAB, AOAZ, AOAM [fixed]

6. Weight Tare results: WNF1, WAF1 [fixed]
7. Ruska output voltages: PT100V, PS50V [measured]
8. PRT calibration constants: R0, alpha, beta, lambda [fixed]

The primary balance sensitivities were incremented by fixed values which ranged from approximately 0.1% to 1% of their magnitude. The remaining parameters were incremented by 1% of their magnitude. No consideration was taken at this time as to the accuracy of the estimate for the gradient. The nominal value of the result with the unperturbed parameter and the value resulting from the perturbed parameter were used with Eq. 2.7.4 to estimate the sensitivity and then Eq. 2.7.7 was used to determine the relative sensitivities for each test point.

The relative sensitivities were computed using a simple computer spreadsheet program and the results for test point A and B are given in Tables 1 and 2. The relative sensitivities were computed for the primary results which were considered as part of this study: Mach and Reynolds numbers, angle of attack, C_L and C_D. In the various columns in Table the symbol "P" refers to the individual parameter, thus for example, dRe/Re/dP/P in the row associated with the parameter PT100V, is the relative sensitivity in Reynolds number to variations in the output from the Ruska used to measure total pressure. Though these calculations were conducted in a very tedious, manual fashion for this study, one could consider the automation of this process through modification of the existing data process code or possibly with recent developments in automated differentiation software.

5.3 Bias Error Estimates

As indicated in the earlier discussion the bias error estimates are only as good as the "estimator's" judgment and experience. This is particularly true for a system as complex as the NTF where there are many different potential sources for bias errors. The approach used in this study was to make a "reasonable" but conservative estimate of the bias error. Then the contribution to the overall error in the result (C_D, Re, M, etc.) was determined. If the effect was an insignificant contribution no additional effort was made to improve the estimate. If the effect was significant, then consistent with the time and resources available, a somewhat less conservative estimate was established.

The first set of parameters considered were the fixed parameters. Since in each case these were the results of earlier calibration experiments, the experimental

uncertainty in the result from the calibration was "frozen" as a bias error in the actual measurement. The following briefly outlines the information source for the bias error estimates for the fixed parameters. Appendix C details the calculations for each.

1. Balance Primary Sensitivities

   There were two sources of information available for estimating the bias errors in these parameters. A number of the NTF balances have undergone repeated calibrations therefore there is a history of calibration results and two calibrations conducted within the past two years were available for balance NTF113A. These were used to make a very crude estimate of the precision index for the calibration process. Along with the calibration parameters there is also an estimate of the "accuracy" of each force or moment component as measure in the calibration experiment[31]. It was assumed that these percentage errors could be used as estimates of the percentage bias limits in the primary sensitivities. At the time this research was being conducted, the Instrumentation Research Division at the NASA Langley Research Center was working to develop techniques based upon statistical assessment of the large amount of data recorded during the calibration experiments to provided improved estimates of the uncertainty in all of the balance calibration constants. One would anticipate that this work will result in improved estimates for the bias errors in all of the fixed parameters associated with the balance.

2. AOA Constants

   The primary sensitivity is determined in a calibration laboratory experiment. Only two calibrations were available for the 12-6 AOA device but 5 were available for the comparable 12-4 instrument. An in-tunnel calibration experiment was performed to determine the three other AOA parameters, the bias, Az, Omax. Fortunately, data from three separate calibration experiments for this particular test were available and simple statistics were used to estimate the precision indices associates with these results. The resulting precision limits from the calibration experiments were then frozen as bias errors for the subsequent measurements.

3. PRT Constants

   The bias estimates for these constants were developed in the same manner as those for the AOA sensitivities. Three calibration results for a "typical" PRT system were available. An estimate of the precision limit due

to the calibration process was frozen as the bias limit for the instrument calibration constants.

4. Tare Weight

Since little data was available for this parameter, a simple estimate based upon the difference in the model weight estimate from the axial and normal force measurements in the tare weight test was used as the bias limit. This bias limit estimate was then applied to both parameters WNF1 and WAF1.

It must be emphasized that the calculations shown in Appendix C represent preliminary estimates for these bias limits and that continued evaluation of the results of the calibration experiments which determine these fixed parameters are required in order to provide more realistic estimates.

The bias errors in the measured parameters are due to uncertainties in the data acquisition process which include instrument installation , the analog-to-digital data conversion process, and data processing. For this preliminary estimate only a limited number of contribution factors were considered. These are briefly outlined below.

1. Analog input to DAU
   - Uncertainty in working standard - manufacturer
   - Data reduction, calibration curve fit (bits vs. volts)
   - Data processing (bits to volts)

2. Other analog to digital conversion processes, IDV
   - Manufactures specifications

As one evaluates these bias estimates it is important to recognize that factors related to the instrument installation have not been considered.

Appendix D contains the sample calculations used for one channel of the DAU. For this particular experiment it was Channel 18 which was used to provide the input voltage from the axial beam of the balance. Similar calculations were performed for each of the measured parameters.

Tables 3 and 4 summarize the bias error estimates for Test Points A and B. The Tables include the value of the parameter and its units. In the case of measured parameters the DAU channel and its range are also indicated. The various bias factors are added in quadrature (Eq. 2.6.1) and the bias error estimate listed. The Tables also

indicate the non-dimensional relative bias in percent of the nominal value of the parameter for that Test Point.

Since some of the bias estimates depend upon the value of the nominal value of the parameter, they differ between test points. Others are the same for each test point. The largest relative bias errors exist for the AOA parameters determined as part of the in-tunnel calibration and the "beta" coefficient in the Callender-Van Dusen equation used for the PRT probe.

5.4 Propagation of Bias Errors

Once the bias limit estimates and sensitivities have been developed for the appropriate fixed and measured parameters, it is possible to estimate the bias limit in the results. The biases in the results were computed using a computer based spreadsheet program and Eq. 2.7.5. The size of the spreadsheet preludes its presentation in this report and the results presented below are summarized from calculations performed using the spreadsheet. Due to the repetitive nature of the calculations and the "dynamic" nature of the uncertainty estimates, the spreadsheet appears to be an ideal vehicle for off-line, post processing of these results. If the sensitivities were computed as part of the data reduction process, it is feasible that the bias error estimates could be made as part of the actual data reduction software. This approach would require a significant modification to the current NTF software and was not considered as part of the current study.

The assumption was made that all of the parameters used in this study were independent and thus the problem of correlated bias errors was eliminated. In the case of the measured parameters this assumption appears quite valid since each measurement is performed with its own instrument. There may be reason to further examine this assumption for a number of the fixed parameters. These parameters have been determined based upon measurements performed in earlier calibration experiments and as illustrated in Appendix B, if the bias errors in these parameters are correlated they will influence the bias estimate in the computed result. This does seem somewhat unlikely based upon the bias estimates made in this report but as these estimates are refined, one should determine if the estimates are correlated.

The individual terms which are added in quadrature in Eq. 2.7.5 are referred to as the "relative bias factors" in this report. Thus the relative bias factor in result "X" from parameter "i" is defined as,

$$X_{BF} = \left(\theta_i \frac{B_{P_i}}{P_i}\right)^2 \qquad \text{Eq. 5.4.1}$$

By ranking these non-dimensional bias factors for each of the results computed as part of this study, one is able to establish the dominate error sources for each result. Tables 5-9 illustrate the bias factors for the primary results Mach and Reynolds numbers, angle of attack, and the non-dimensional force coefficients C_L and C_D for Test Point A. Similar results for Test Point B are provided in Tables 10-14. In each Table only those parameters which have contributions within a couple of orders of magnitude of the dominate factor are included and any others, though they may be non-zero, were ignored.

The bias limit estimates for each Test Point are summarized in Tables 15 and 16. The bias limit estimates are listed with a single significant figure (the 1 plus next digit for numbers starting with a 1) and the result is "rounded" to correspond with the magnitude of the bias error. The variation in error with test point is indicated for those results which vary between the test points as would be expected.

5.5 Precision Error Estimates

Unlike the case for the bias errors where both fixed and measured parameters were considered, the precision error estimates are only influenced by the measured parameters for these two test points. The fixed parameters do not vary between test points for the cases considered in this study. As indicated above the classification of "fixed" and "measured" parameters is influenced by the manner and sequence in which the tests are conducted. If AOA in-tunnel calibrations were repeated between the test points, then precision errors in the bias, Az and Omax parameters would add to the precision error estimates. With the data available for this study there were two approaches considered to estimate the precision limits in the results. In the first case a single result is computed based upon the mean value of multiple measurements of individual parameters. In the second case multiple results are computed (each based upon multiple measurements of individual parameters) and a statistical analysis of the multiple results provides an estimate of the precision limit in the result.

5.5.1 Single Result with Multiple Measurements

In Section 2.5 the concept of precision error was overviewed. At that point it was stated that the preferred approach to quantifying the precision error was to acquire multiple measurements of the same result and determine the precision index and thus the precision limit from those multiple results. In many wind tunnel applications this is possible though it can add to the time required for a test program and thus the cost.

When computer based data acquisition systems are used a single parameter measurement is often actually the average of multiple measurements sampled over a specified time increment so there is additional information available to help determine the contribution to uncertainty due to precision errors. For the case where a single result is computed and based upon the average of multiple individual measurements, an estimate of the precision index in the result can be determined by quantifying precision index of the individual parameter measurements. Then propagation of errors is used to estimate the precision index of the result and with the appropriate degree of freedom, one can determine the precision limit and associated coverage. Since this type of information was available for this preliminary study this approach was also used.

For the test program which provided the data from the NTF for the current report a single test point was computed by sampling 10 samples of each measured parameter during a 1 second interval. The 10 samples were averaged and the result was computed based upon the mean value of the parameters. By evaluating the statistical variation of each of these parameters during the sampling interval and using the propagation of errors, one can estimate the precision error in the result.

The precision index for "i th" parameter, P_i, can be determined using Eq. 2.3.4 to yield S_{P_i}. The estimate of the precision index for the mean value of P_i is,

$$S_{\bar{P}_i} = \frac{S_{P_i}}{\sqrt{N}} \qquad \text{Eq. 5.5.1}$$

and since the mean value of P_i is used in the calculation of the result, the precision index for the mean is used to determine the precision index of the result. There are a number of approaches that can be used when dealing with the sample size and its influence on these statistical estimates. The AGARD Draft recommends the use of the large sample size approximation for any case, i.e. always assume a "t" factor of 2 and a 95% coverage. Reference 16 provides a number of approaches for dealing with variable sample sizes and determining the degrees-of-freedom associated with the precision index of the result. Since for the data consider in this study the same number of samples were available for each parameter, the number of degrees-of-freedom associated with each estimate of the precision index are the same. This allows one to determine the precision limit for each parameter based upon the appropriate sample size. In this case, there were 10 points per sample, thus 9 degrees-of-freedom for each sample and a t factor of 2.26 for a coverage of 95%. The precision limit for the mean value of the "i th" parameter is written as,

$$PL_{\bar{P}_i} = t\, S_{\bar{P}_i} \qquad \text{Eq. 5.5.2}$$

The relative precision limit for the result is then determined from,

$$\frac{PL_r}{r} = \left[\sum_{i=1}^{j} \left(\theta_i' \frac{PL_{\bar{P}_i}}{\bar{P}_i} \right)^2 \right]^{\frac{1}{2}} \qquad \text{Eq. 5.5.3}$$

where $\bar{P}_i$ is the mean value of the "i th" parameter.

The precision limit of the mean for the measured parameters for Test Point A are given in Table 17. This information was then combined with the sensitivities for this test point and Eq. 5.5.3 was used to determine the estimate of the precision limit for the result. This was also performed using a computer spreadsheet program. As was done in the previous section a relative precision factor for result "X" was defined as,

$$X_{PF} = \left(\theta_i' \frac{PL_{\bar{P}_i}}{\bar{P}_i} \right)^2 \qquad \text{Eq. 5.5.4}$$

This allows for ranking of those factors which have the greatest influence on the precision limit of the result. Sample results are included in Tables 18 and 19 for Test Point A. For these two results at this test point the precision error is dominated by the fluctuations in the strain gage bridge output.

The precision limits estimated from Eq. 5.5.3 are shown in Tables 20 and 21 for Test Points A and B. The same type of rounding and truncation as applied to the bias limit estimates were used with these results. A brief discussion of these results in the light of a more detailed assessment of the measurements is included in Section 5.5.3.

5.5.2 Results from More Than One Test

As indicated above repeated test information was available in order to establish precision error estimates using multiple results and thus provide an end-to-end precision limit assessment. The precision index for a sample of N results computed using measurements taken at the "same" test conditions is,

$$S_r = \left[\frac{1}{N-1} \sum_{k=1}^{N} (r_k - \bar{r})^2 \right]^{\frac{1}{2}} \qquad \text{Eq. 5.5.5}$$

Results from a sequence of 10 test points which were collected in succession with approximately a 10 second interval between test points are given in Table 22. This Table also includes estimates of the precision index and precision limits (based upon 95% coverage) for each result. A comparison of these estimates with those obtained using the procedure described in the previous section indicate that these estimates are higher in almost every case. One should also recall that the both Test Points A and B were at a different angle of attack than the sequence of Test Points C - L. These results did indicate that one should consider in more detail the information used to develop the two estimates.

5.5.3 Qualitative Assessment of Precision Errors

As emphasized earlier, this study was intended to develop a framework for a system level uncertainty analysis for a facility like the NTF. Even though it was not intended to provide a comprehensive uncertainty assessment of the facility, the results of the previous two sections indicated that a somewhat closer examination might provide some insight into the differences in the precision error estimates.

Figures 20 - 22 present the 10 individual samples, measured in bits, for Test Point A for three of the measured parameters, AXFRAW, PTV100 AND ELEVA. The two parameters AXFRAW and PTV100 are output from the DAU and therefore the analog signal was passed through a 1 Hz low-pass filter before the conversion process. The ELEVA output was from the integrating digital voltmeter which has an output update rate of approximately 0.33 seconds. These figures imply that these relatively small samples are not normally distributed "random" numbers as was assumed in computing the precision index for each of these parameters. Considering the argument used in the

discussion for Figure 2, it appears that a 1 second sampling interval and a 10 Hz sample rate may not provide an adequate "sample" for the precision index estimates.

Figure 23 presents the value of the result, C_D, for Test Points C - L. Simple visual inspection of this Figure implies that this may be a more realistic "random" sample. One could perform a number of statistical tests on this sample to determine if it was representative of a normal distribution. An alternative presentation of this data is provided in Figure 24 which is a plot of C_D as a function of angle of attack. From this Figure it appears as if these results are rather well correlated indicating a systematic not random variation in both. Even though these were intended to be "identical" test points at a fixed angle of attack, there are other factors which do influence the measurements. During the data collection, the process control system is continually monitoring the Mach number, total pressure, total temperature, and angle of attack. Continuous closed-loop control of each of these parameters produces systematic variations in each which may be reflected in the experimental results. Extracting short term samples of any of these parameters may not yield appropriate statistics to characterize the true "random" character of the measurements.

Though one cannot draw any significant conclusions from this brief assessment of the measurements, it does imply that one should not rely on simple "statistics" in order to assess the precision errors. You must evaluate the results and the data that produced them. It also points out one of the useful aspects of performing an uncertainty assessment since the uncertainty analysis requires a careful evaluation of data sampling procedures and basic data characteristics.

5.6 System Uncertainty Estimates

The final step in the uncertainty analysis is the combination of precision and bias limit estimates to form the uncertainty estimate. Eq. 2.7.10 was used to estimate the uncertainty in each of the results considered in this study. The addition in quadrature provides a 95% coverage or confidence level which is consistent with the assumptions made throughout this study.

Tables 23 and 24 present the results of the uncertainty analysis for Test Points A and B using the single sample method. Recall from the beginning of this report it was suggested that a multiple sample, end-to-end assessment of the precision limit was the preferred approach. If this data is available, it is recommended that that approach be used. Since multiple samples for the results considered in this report for Test Points A and B were not available and the multiple samples for Test Points C-L were

demonstrated to contain a systematic variation which might be attributed to the tunnel control system, it was determined that the single sample precision limit estimates would provide the most reasonable precision limit estimates.

For these reasons, the single sample precision limits were used, even though earlier observations implied that the small (10 points) sample size and short sample duration (1 sec) may not be adequate. Since the uncertainty in each parameter is dominated by the bias error estimate, the selection of the technique to be used to estimate the precision limit is not critical for this particular case. The uncertainty in the tunnel parameters Mach and Reynolds numbers and angle of attack do not vary significantly between the two test points. The non-dimensional force coefficients do show considerable differences between the two points. This illustrates the fact that one cannot state a single uncertainty for all results over a complete range of parameters.

As a last comment, one must remember that the uncertainty estimates for the two test points were conducted in order to establish a procedure for performing an uncertainty assessment in a facility like the NTF. Significant additional effort is required before the bias estimates can be refined and the results presented above should not be considered as representative of all tests conducted in that facility.

Section 6. Conclusions

This study was conducted in order to establish a framework and identify methodology for an end-to-end uncertainty analysis for a wind tunnel system using computer based data acquisition and data processing. The methodology was based in part upon techniques presented in ANSI and ASME standards[16] Methods for establishing both bias and precision limit estimates were presented. The methods presented in this report were applied to a preliminary analysis of measurements of C_D and C_L at the NASA Langley Research Center National Transonic Facility. This preliminary analysis was useful in identifying important issues related to calibration experiments, bias limit estimates and data sampling procedures.

The unique characteristics of the type of experiment performed at the NTF are the complexity of the operating environment and the large number of calibration experiments which influence the uncertainty in the actual tunnel measurements. All of the instruments used at the NTF are calibrated on a very regular basis. The characteristics of the instrument as well as its uncertainty are parameterized by the calibration constants. These calibration constants themselves are the results of the calibration experiments and contain uncertainty due to the precision of the calibration experiment, uncertainty in the working standard used for the calibration and procedures used in the calibration experiment.

It should also be noted that the only "measurements", in the traditional sense of the term, which are conducted in the process of performing both the actual experiments and the calibration experiments are performed by an electronic circuit which converts "voltages" into an integer number which is proportional a voltage difference. The role of electronic sensors and the computer in wind tunnel testing has reduced the experimental process into a three step procedure. First, physical input to electronic sensors produce voltages which may be then subjected to other electronic "processing". Second, computer based data acquisition systems convert the voltages to integer, digital form with finite resolution. Third, the digital information is combined with the results of other experiments and numerical calculations are performed, usually by the computer, in order to determine "results." Therefore the uncertainty in the final result is intimately tied to the production, electronic processing, conversion, digital processing and interpretation of this electronic information.

Of particular concern in the experiments conducted at the NTF are the strain gage force balance and the angle of attack sensors. In this preliminary study these two instruments appear to have the greatest influence on the uncertainty in the lift and drag coefficients. The uncertainty is influenced by the uncertainty in the calibration constants which are used to process the digital representation of the electronic output from these sensors. In order to assess the uncertainty in the results determined using these calibration constants one needs to quantify the uncertainty in the calibration constants themselves. This is particularly important for this type of application where the calibration experiment takes place in an environment which is much different from that of the actual experiment. This is also influenced by the fact that the electronic data collection from these two instruments is quite different in the calibration experiment from that in the wind tunnel. Efforts currently underway to establish this type of uncertainty information from the calibration experiments will have a very positive effect on future detailed uncertainty analyses in this facility.

The preliminary results presented in this report should be considered as just that, preliminary. The uncertainty analysis includes both precision and bias limits and the preliminary assessment for the NTF was limited in its attention to each. The precision error estimates may be the "easier" of the two factors to establish with greater confidence since it can be accomplished by acquiring more wind tunnel data. A wider range of operating conditions and test points would have to be evaluated to begin to develop a more complete evaluation of the precision limit and its primary sources. Due to the cost of operation of the NTF this may have to be done as part of existing test programs but it can eventually provide insight into the "repeatability" of measurements within the facility.

Due to the complexity of the NTF system the bias error estimates may be more difficult to develop. Only limited bias influences were considered in the current study. There are still many issues which should be included in the bias error estimates. Some are related to the test environment and others to the instruments and techniques used in the measurement process. Some issues that still must be addressed are listed below with no special attention to priority.

- 'gas' modeling and constants
- flow angularity
- flow nonuniformity (spatial and temporal)
- balance temperature gradients
- loads carried across balance, (i.e. wires, tubes,..)

- temperature and pressure sensor installation errors
- base pressure measurements and corrections
- other tunnel corrections
- wind-off zero measurements
- model assembly and surface irregularities
- vibrations (model and support system)
- numerical procedures in data reduction

Each of these factors influence "numbers" which have a direct impact on the results (M, Re, $C_{L,}$, C_D, etc. ..) of a specific test and therefore they can influence the bias error estimates.

Improvements in the system uncertainty analysis can only be accomplished by continuing the process of understanding the "physics" of measurement environment and measurement techniques. Since most of the decisions made in estimating the uncertainty depend upon the judgment of the analyst, it is only through the improved understanding of the experiment that one can improve the uncertainty analysis. Uncertainty analysis is an ongoing process and must be considered as such to be an effective part of an experimental program.

Section 7. References

1. Kline, S.J., McClintock, F.A., "Describing Uncertainties in Single-Sample Experiments," Mechanical Engineering, Vol. 75, No. 1, pp. 3-9, Jan. 1953.

2. Statistical Treatment of Experimental Data, H.D. Young, McGraw-Hill, 1962.

3. Bevington, P.R. , Data Reduction and Error Analysis for the Physical Sciences, McGraw-Hill, New York, 1969.

4. Moffat, R.J., "Contributions to the Theory of Single-Sample Uncertainty Analysis," Journal of Fluids Engineering, Vol. 104, pp. 250-260, 1982.

5. Kline, S.J., "The Purposes of Uncertainty Analysis," Journal of Fluids Engineering, Vol. 107, pp. 153-160, 1985.

6. Moffat, R.J., "Using Uncertainty Analysis in the Planning of an Experiment," Journal of Fluids Engineering, Vol. 107, pp. 173-178, 1985.

7. Moffat, R.J., " Describing the Uncertainties in Experimental Results," Experimental Thermal and Fluid Science, 1:3-17, 1988.

8. An Introduction to Error Analysis, J.R. Taylor, University Science Books, 1982.

9. Taylor, J.L., Fundamentals of Measurement Error, Neff Instrument Corp., Monrovia, California, 1988.

10. Dieck, R.H., "Measurement Uncertainty Methods and Applications," Instrument Society of America Publisher, 1992.

11. Taylor, J.L., Computer Based Data Acquisition Systems - Design Techniques - Second Edition, Instrument Society of America, Research Triangle Park, NC, 1990.

12. Bevington, P.R. and Robinson, D.K., Data Reduction and Error Analysis for the Physical Sciences, McGraw-Hill, New York, 2nd Edition, 1992.

13. Ku, H.H. (editor), "Precision Measurement and Calibration - Selected Papers on Statistical Concepts and Procedures," National Bureau of Standards Special Publication 300, Vol. 1, Feb. 1969.

14. Natrella, M.G., "Experimental Statistics", National Bureau of Standards Handbook 91, Issued Aug. 1963, Reprinted with corrections Oct. 1966.

15. Taylor, B.N., Kuyatt, C.E., "Guidelines for Evaluating and Expressing the Uncertainty of NIST Measurement Results," National Institute of Standards and Technology Technical Note 1297, Jan. 1993.

16. "Measurement Uncertainty," ANSI/ASME PTC 19.1-1985, Part 1, Instruments and Apparatus, 1985. (revised version in preparation)

17. Coleman, H.W. and Steele, W. G. ,Jr., Experimentation and Uncertainty Analysis for Engineers, , John Wiley and Sons, Publ., 1989.

18. Abernathy, R.B. and Thompson, J.W., "Uncertainty in Gas Turbine Measurements," AEDC Handbook 73-5, February 1973.

19. Abernathy, R.B., and Ringhiser, B., "The History and Statistical Development of the New ASME-SAE-AIAA-ISO Measurement Uncertainty Methodology'" AIAA Paper 85-1403, 21st Joint Propulsion Conference, July 1985.

20. Covert, E.E. (editor), "Thrust and Drag: Its Prediction and Verification," Progress in Astronautics and Aeronautics, Vol 98, Chapter IV, pp. 281-330, 1985.

21. Rind, E., "Instrument Error Analysis as It Applies to Wind-Tunnel Testing," NASA TP 1572, December 1979.

22. Walpole, R.E., and Myers, R.H., "Probability and Statistics for Engineers and Scientists - 2nd edition," Chapter 8, Macmillan Publ., 1978.

23. Bendat, J.S., and Piersol, A.G., Random Data: Analysis and Measurement Procedures, Second Edition, John Wiley and Sons, Pub., New York, 1986.

24. Press, W.H., Flannery, B.P., et.al., "Numerical Recipes - The Art of Scientific Computing," Chapter 14, Cambridge University Press, 1986.

25. Bruce, W.E., and Gloss, B.B., "The U.S. National Transonic Facility, NTF", AGARD Report No. 774, Special Course on Advances in Cryogenic Wind Tunnel Technology, pp. 3.1-3.27, June 1989.

26. Fuller, D.E., "Guide for Users of the National Transonic Facility," NASA TM 83124, July 1981.

27. Foster, J.M. and Adcock, J.B, "User's Guide for the National Transonic Facility Data System," NASA TM 100511, December 1987.

28. Stewart, P.N., "Data Quality Analysis at the National Transonic Facility," NASA CR-4303, July 1990.

29. Ferris, A.T., "An Improved Method for Determining Force Balance Calibration Accuracy," Paper 93-092, Proceedings of the 39th International Instrumentation Symposium, Instrument Society of America, Albuquerque, New Mexico, pp. 321-336, May 1993

Appendix A: Correlated Bias Errors

When the bias in a result is determined using propagation of errors, it should be noted that if the various parameters used in determining the result have bias errors which are correlated, the resulting estimate of the bias in the result will be altered. There are various sources for correlated bias such as calibration against the same working standard. The expression given in Eq. 2.7.2 is altered if there are correlated bias terms. The bias error in the calculated result is determined using,

$$B_r = \left[\sum_{i=1}^{j} [(\theta_i B_{P_i})^2 + \sum_{k=1}^{j} \theta_i \ \theta_k \ \rho_{Bik} B_{P_i} \ B_{P_k} (1- \delta_{ik})] \right]^{\frac{1}{2}} \qquad \text{Eq. A.1}$$

where δ_{ik} is the Kronecker delta (= 1 if i = k and =0 if $i \neq k$)and ρ_{Bik} is the correlation coefficient between the biases B_{P_i} and B_{P_k}. Depending upon the "sign" of the correlation term, the bias can be larger or smaller than in the case of an uncorrelated bias.

The following two examples are included to illustrate the influence of a correlated bias error for a case where two parameters, x and y, are used to compute a result, r.

$$r = f (x , y) \qquad \text{Eq. A.2}$$

Then Eq. A.1 is reduced to,

$$B_r = \left[(\frac{\partial r}{\partial x} B_x)^2 + (\frac{\partial r}{\partial y} B_y)^2 + 2 \frac{\partial r}{\partial x} \frac{\partial r}{\partial y} \rho_{xy} B_x \ B_y \right]^{1/2} \qquad \text{Eq. A.3}$$

Since it is difficult to determine the bias in the parameters x and y, it would probably be even more difficult to quantify ρ_{xy}. Therefore in most practical applications it is recommended[18] that an effective approach is to rewrite the third term in the form,

$$\frac{\partial r}{\partial x}\frac{\partial r}{\partial y}\rho_{xy} B_x B_y = \frac{\partial r}{\partial x}\frac{\partial r}{\partial y} B_x' B_y' \qquad \text{Eq. A.4}$$

where B_x' and B_y' are computed using only those components of B_x and B_y that are from the same error source - i.e. they are perfectly correlated so that ρ_{xy} = 1. The following two cases illustrate the influence of correlated bias errors where the result r is either a sum or a difference between two parameters.

1) if $r = x + y$ and $B_x = B_y = B$, then,

$$B_r = \left[\left(\frac{\partial r}{\partial x} B_x\right)^2 + \left(\frac{\partial r}{\partial y} B_y\right)^2 + 2\frac{\partial r}{\partial x}\frac{\partial r}{\partial y}\rho_{xy} B_x B_y \right]^{1/2}$$

$$= \left[B^2 + B^2 + 2 B B \right]^{1/2} = 2 B$$

2) if $r = x - y$ and $B_x = B_y = B$, then

$$B_r = \left[\left(\frac{\partial r}{\partial x} B_x\right)^2 + \left(\frac{\partial r}{\partial y} B_y\right)^2 + 2\frac{\partial r}{\partial x}\cdot\frac{\partial r}{\partial y}\rho_{xy} B_x B_y \right]^{1/2}$$

$$= \left[B^2 + B^2 - 2 B B \right]^{1/2} = 0$$

This second example is often the source of potential confusion in conducting an uncertainty analysis. If the result is the difference between two measurements, as might occur in a drag increment test, it is often stated that all bias errors are eliminated. This is only true if the bias errors are perfectly correlated. Considering

all of the potential bias error sources, this is probably very rarely the case and therefore bias errors will be present, even in "incremental" testing. One should never discount the presence of bias errors without a comprehensive uncertainty analysis.

Appendix B. Bias Estimates Using Computed Results

In propagation of errors into the calculation of a result particular care must be taken to determine the "sensitivities" with respect to independent variables. This is illustrated by a detailed discussion in the AGARD Draft and the following is included in order to describe the cause of this problem.

Consider a simple experiment where a and b are independently "measured" parameters and there are three results which are computed as part of the data reduction process, Q, R and S. If

$R = f(a, b)$ - a "neat little" expression

$S = g(a, b)$ - another "neat little" expression

$Q = F(R, S)$ - one more "neat little" expression

but one could also write:

$Q = G(a, b)$ - a more complex expression due to forms of R and S.

If one wants to determine the bias error in Q, there are a number of approaches which might be considered.

One approach would be to determine the bias errors in the results S and R and then propagate those bias errors into the calculation of Q. This appears attractive since f, g and F are "easy" functions to work and determining analytic expressions for the sensitivities is often one of the more time consuming tasks in an uncertainty analysis. This would yield,

$$B_Q^2 = \left(\frac{\partial F}{\partial R} B_R\right)^2 + \left(\frac{\partial F}{\partial S} B_S\right)^2 \qquad \text{Eq. B.1}$$

where

$$B_R^2 = \left(\frac{\partial f}{\partial a} B_a\right)^2 + \left(\frac{\partial f}{\partial b} B_b\right)^2 \qquad \text{Eq. B.2}$$

$$B_S^2 = \left(\frac{\partial g}{\partial a} B_a\right)^2 + \left(\frac{\partial g}{\partial b} B_b\right)^2 \qquad \text{Eq. B.3}$$

substituting Eqs. B.2 and B.3 into Eq. B.1 yields,

$$B_Q^2 = \left[\left(\frac{\partial F}{\partial R}\right)^2 \left(\frac{\partial f}{\partial a}\right)^2 + \left(\frac{\partial F}{\partial S}\right)^2 \left(\frac{\partial g}{\partial a}\right)^2\right] B_a^2$$

$$+ \left[\left(\frac{\partial F}{\partial R}\right)^2 \left(\frac{\partial f}{\partial b}\right)^2 + \left(\frac{\partial F}{\partial S}\right)^2 \left(\frac{\partial g}{\partial b}\right)^2\right] B_b^2 \qquad \text{Eq. B.4}$$

An alternative approach would be to compute the bias in Q directly from,

$$B_Q^2 = \left(\frac{\partial G}{\partial a} B_a\right)^2 + \left(\frac{\partial G}{\partial b} B_b\right)^2 \qquad \text{Eq. B.5}$$

Now $\frac{\partial G}{\partial a}$ and $\frac{\partial G}{\partial b}$ could be computed by application of the "chain rule" and a little algebra yields an expression for the desired bias in terms of the more convenient expressions,

$$B_Q^2 = \left[\left(\frac{\partial F}{\partial R}\right)^2 \left(\frac{\partial f}{\partial a}\right)^2 + \left(\frac{\partial F}{\partial S}\right)^2 \left(\frac{\partial g}{\partial a}\right)^2 + 2 \frac{\partial F}{\partial R} \frac{\partial R}{\partial a} \frac{\partial F}{\partial S} \frac{\partial S}{\partial a}\right] B_a^2$$

$$+ \left[\left(\frac{\partial F}{\partial R}\right)^2 \left(\frac{\partial f}{\partial b}\right)^2 + \left(\frac{\partial F}{\partial S}\right)^2 \left(\frac{\partial g}{\partial b}\right)^2 + 2 \frac{\partial F}{\partial R} \frac{\partial R}{\partial b} \frac{\partial F}{\partial S} \frac{\partial S}{\partial b}\right] B_b^2 \qquad \text{Eq. B.6}$$

Comparing Eq. B.4 and Eq. B.6 show that there are "missing" terms in the expression for the bias in Q developed using the "interim" results and discounting the fact that the R and S are not "independent" parameters.

One of the purposes of an uncertainty analysis is to provide uncertainty assessments in the results of an experiment so that when the results are used in subsequent analyses one can estimate their uncertainty. The example shown above emphasizes that care must be taken when propagating bias errors or uncertainties to make sure that if the uncertainties are correlated, proper error propagation methods are used.

Appendix C: Bias Estimates: Fixed Parameters

The following briefly outlines the calculations used to establish the bias error estimates for a number of the fixed parameters. This data was collected from calibration reports and included to demonstrate the approach taken in this study. It should be considered in light of the limited time and data available for this effort. It is not a complete list of all the parameters considered.

1. Balance Primary Sensitivities: Balance NTF113A

Example: S1 - Axial Force (AF) Sensitivity

$$S1 = .37037 \text{ lbf} / \mu V / V$$

a. "Repeatability"

Consider the variation between the two available calibration experiments.

calibration date 1/2/92	S1 = .3703704 lbf / μV / V
calibration date 10/14/93	S1 = .370321 lbf / μV / V

If this as a sample with two data points and the precision index is based upon the difference between the two values, then,

$$| \Delta S1 | = 0.000049 \text{ lbf} / \mu V / V$$

The precision limit is estimated using the precision index and the "t" factor for one degree-of-freedom and a 95% confidence level (t = 12.7),

$$P_{S1} = 12.7 \times (0.000049 \text{ lbf} / \mu V / V)$$
$$= 0.000627 \text{ lbf} / \mu V / V$$

This is then "frozen" as a bias limit and is a measure of the "repeatability" in the calibration process.

$$B_{S1} = P_{S1} = 0.000627 \text{ lbf} / \mu V / V$$

b. Stated calibration accuracy:

The calibration report for this balance reported a full scale design load for the axial "beam" of 400 lb. It also stated a calibration "accuracy" for axial beam of 0.31% FS (full scale) with a 95% confidence level.[31]

Uncertainty in axial load = 400 lb x 0.0031 = 1.24 lbf

Actual axial force reading for Test Point A:

AF = 132 lbf

The relative "bias" limit at this value of the balance output would be estimated as:

$$B_{AF} / AF = 1.24 \text{ lbf} / 132 \text{ lbf} = 0.94 \%$$

Since the primary sensitivity S1 is linearly related to the balance output it was assumed that one could use the bias in AF as the basis for bias estimate in S1:

$$B_{S1} = 0.0094 \times .37037 \text{ lbf / mV / V}$$

$$= 0.00348 \text{ lbf / mV / V}$$

Then the two estimates were combined in "quadrature."

$$B_{S1} = \left[(0.000627)^2 + (0.00348)^2 \right]^{\frac{1}{2}}$$

$$= 0.00356 \text{ lbf / mV / V}$$

This produced a relative bias error estimate of 0.96 % for this calibration constant. This estimate is dominated by the contribution due to calibration "uncertainty" so that for this parameter the repeatability of calibrations was not a significant factor in the bias error estimate.

2. AOA Constants

a. Sensitivity - AOA1S (AOA 12-6)

The stated sensitivity used in the data reduction for the test points considered in this study was,

$$AOA1S = 0.270235 \text{ volts/g}$$

Date available on five successive calibrations of a "similar" AOA device (AOA 12-4).

calibration date 1/4/90	AOA1S = 0.268346 volts/g
calibration date 1/11/91	AOA1S = 0.268778 volts/g
calibration date 5/13/91	AOA1S = 0.268853 volts/g
calibration date 3/5/92	AOA1S = 0.268902 volts/g
calibration date 4/20/92	AOA1S = 0.268918 volts/g

Assuming the range (greatest difference between any two calibration points) was an estimate of the precision index and t factor of 2.78 (a 95% confidence level with four degrees-of-freedom), the precision limit for the calibration data can be determined.

$$P_{AOA1S} = 2.78 \times (0.000572 \text{ volts/g}) = 0.00159 \text{ volts/g}$$

This is then "frozen" and use as an estimate of the bias limit.

$$B_{AOA1S} = P_{AOA1S} = 0.00159 \text{ volts/g}$$

It should be noted that this estimate of the precision index does not account for the obvious "trend" in the calibration data. Since the sequential calibrations do not appear to yield "random" results, other sources should be considered in making the bias error estimates for the AOA sensitivity.

b. Bias, Az and Omax

The values used for these parameters in the data reduction for the test points considered in this study were,

AOA1B = 0.0002015 volts
AOA1Z = 47.2746 deg
AOA1M = 0.32108 deg

This data was derived from an in-tunnel calibration. Fortunately, three different "calibrations" were available for a very similar "test" using a comparable AOA sensor. These three calibrations provided additional data for developing a bias estimate for these parameters.

parameter	AOA1B	AOA1Z	AOA1S
#1	.0002015	47.27	.3211
#2	.0002135	48.33	.3172
#3	.0002405	46.61	.3141
Average	.0002185	47.40	.3175
Precision Index	.00002	0.867	.0035
t x Precision Index.	.000086	3.73	0.0151

The "t" factor (t = 4.3) was based upon a 95% confidence level and $\nu = 2$.

Appendix D: Bias Estimates: Measured Parameter

The following demonstrates the steps taken in order to estimate the bias error in one of the measured parameters. This represents the data reduction procedure used for one channel of the data acquisition unit and illustrates the process by which "voltage" is measured using the calibrated DAU.

Channel 18 - AXFRAW
Full Scale Voltage: 10.24 millivolt
Pre-amp gain: x500
PGA gain: x2

This channel was calibrated prior to the actual measurement. This was a "five-point" calibration in which a precision voltage source was used to apply a specified voltage to the input of the analog-to-digital converter. The average of fifty samples, rounded to a whole bit, were used to represent the A/D output.

Working Standard Voltage Source (millivolts)	A/D Converter Output (bits)
-7.680	-12262
-3.840	-6130
0.000	-1
3.840	6129
7.680	12261

The bias error in the channel output is due to uncertainty in the working standard, the curve fit used for the calibration and the data processing that converts the actual measurement to a digital "voltage".

a. Uncertainty in the Working Standard:

The bias in the working standard was determined from the manufacturer's standards for the precision voltage source and it depends upon the range and programmed value for the source.

B_{WS} = 3 μV

+ 0.002% programmed value (7.68 millivolt)
+ 0.0005% range (100 millivolt)
= 3 μV + .15 μV + 0.5 μV = 3.65 μV

b. Least Squares Curve Fit: bits vs. volts

A least squares curve fit was performed using the data listed in the table on the previous page. The procedures outlined in Section 4 were applied to this data. Recall that the computer measurement is in "bits" and this digital information must be converted to "voltage" units. This is done using the DAU calibration data for this particular channel. The DAU calibration is conducted on a very regular basis, at least once a day and often more frequently. This digital representation of voltage is eventually used with the instrument calibration information to convert the sensor output to actual "engineering units." Using the data from the table an estimate for m and a in the following expression was developed using Eqs. 4.2.2 and 4.2.3.

$$\text{bits} = m * \text{volts} + a$$

a = intercept = 0 bits
m = slope = 1596.5 bits/millivolt

Then computing an unbiased estimate of the standard deviation (SEE) associated with the dependent variable, using Eq. 4.2.4,

$$\sigma_{est} = S_{Yi} = 0.948 \text{ bits}$$

The precision limits for the intercept and slope can be computed using Eq. 4.2.5 and 4.2.6 and the appropriate t factor. Since there were five data points in the fit, a "t" factor based on a 95% confidence level and three degrees-of-freedom was used.

Precision index for intercept = $t\ S_a$ = 1.35 bits
Precision index for slope = $t\ S_m$ = 0.25 bits/μV

These precision limits are then "frozen" as the bias limits due to curve fitting.

c. Data "Reduction":

Once the curve fit is completed, the individual measurements are processed using the following formula.

$$VOLTS = M * BITS + A$$

where,

$$A = - a / m = 0 \text{ volts}$$
$$M = 1 / m = .62638 \ \mu V / bit$$

and "a" and "m" are the result of the least squares curve fit.

The bias limits for the parameters A and M were determined using Eqs. 4.3.7 and 4.3.8 and the bias limits for a and m determined from the curve fitting process,

$$B_A = \left[\left(\frac{B_a}{m} \right)^2 + \left(\frac{a}{m^2} B_m \right)^2 \right]^{\frac{1}{2}}$$

$$= 8.45 \times 10^{-7} \text{ volts}$$

and:

$$B_M = \frac{B_m}{m^2} = 9.73 \times 10^{-14} \text{ volts/bit}$$

Finally as an example, for channel 18 at Test Point A the DAU output was 1782 bits (i.e. BITS = 1782). This was the result of an average of 10 data points sampled during a 1 second interval and rounded to the nearest whole integer.

$$VOLTS (AXFRAW) = .62638 \ \mu V / bit \times (1782 \text{ bits}) + 0 \text{ volts} = 1.11619 \text{ millivolts}$$

This represents the basic measurement of the output of this instrument. This process is repeated for every data point "taken" using this channel.

d. Estimated Bias Components for Voltage Reading:

The bias estimated on the measured voltage will depend upon the voltage level, the uncertainty in the curve fit, and working standard.

1. Bias estimate on DAU output = 1 bit

   This is based upon the "least count" resolution of the A/D converter.

2. Bias estimate on WS = 3.65 μV

   This was determined from the manufacturer's specification as shown.

3. Bias estimate on the intercept (A)

   This is a statistical assessment of the curve fitting process.

$$B_A = \left[\left(B_{A_{\text{curve fit}}} \right)^2 + \left(B_{A_{WS}} \right)^2 \right]^{\frac{1}{2}}$$

$$= 3.75\ \mu V$$

4. Bias estimate on the slope (M)

   This is a statistical assessment of the curve fitting process.

$$B_M = \left[\left(B_{M_{\text{curve fit}}} \right)^2 \right]^{\frac{1}{2}}$$

$$= 9.73 \times 10^{-14} \text{ volts/bit}$$

e. Bias Estimate for Voltage Measurement:

These are combined to provide the voltage bias limit estimate

$$B_{VOLTS} = \left[\left(B_A \right)^2 + \left(BITS * B_M \right)^2 + \left(M * B_{BITS} \right)^2 \right]^{\frac{1}{2}}$$

$$= 3.8\ \mu V$$

Then for this data point, including bias errors only, the "measurement" can be interpreted as:

$$AXFRAW = 1.116 \pm .004 \text{ millivolts}$$

The bias limit is 0.34 % of the reading and it is dominated by the uncertainty in the working standard. This procedure was then repeated for each analog input channel.

Parameter	Nominal Value	units for P	dM/M/dP/P	dQ/Q/dP/P	dRe/Re/dP/P	dAl/Al/dP/P	dCD/CD/dP/P	dCL/CL/dP/P
S1 - AF	3.704 E-01	lbf/microv/volt	0.000	0.000	0.000	0.000	1.164	0.017
S2 - SF	2.020 E+00	lbf/microv/volt	0.000	0.000	0.000	0.000	0.000	0.000
S3 - NF	3.140 E+00	lbf/microv/volt	0.000	0.000	0.000	0.000	-0.188	2.949
S4 - RM	1.353 E+01	lbf/microv/volt	0.000	0.000	0.000	0.000	0.000	0.004
S5 - PM	9.099 E+00	lbf/microv/volt	0.000	0.000	0.000	0.000	-0.117	-0.067
S6 - YM	5.725 E+00	lbf/microv/volt	0.000	0.000	0.000	0.000	0.000	0.002
BALPOW	4.998 E+00	volts	0.000	0.000	0.000	0.000	-0.852	-2.869
NF1RAW	2.581 E+00	millivolts	0.000	0.000	0.000	0.000	-0.573	7.861
NF2RAW	-3.111 E+00	millivolts	0.000	0.000	0.000	0.000	0.269	-4.981
AXFRAW	1.116 E+00	millivolts	0.000	0.000	0.000	0.000	1.164	0.017
SF1RAW	-3.282 E-01	millivolts	0.000	0.000	0.000	0.000	0.000	0.001
SF2RAW	-7.665 E-01	millivolts	0.000	0.000	0.000	0.000	0.000	0.001
RLMRAW	1.622 E+00	millivolts	0.000	0.000	0.000	0.000	0.000	0.001
PT100V	6.322 E+00	volts	1.237	2.491	1.680	0.000	-2.442	-2.430
PS50V	8.248 E+00	volts	-1.249	-1.513	-0.698	0.000	1.559	1.536
ELEVA	3.431 E-03	volts	0.000	0.000	0.000	0.790	-0.046	0.006
AOA1S	2.702 E-01	volts/g	0.000	0.000	0.000	-0.736	0.043	-0.005
AOA1B	2.015 E-04	volts	0.000	0.000	0.000	-0.047	0.002	0.000
AOA1Z	4.727 E+01	deg	0.000	0.000	0.000	0.194	-0.021	0.001
AOA1M	3.211 E-01	deg	0.000	0.000	0.000	0.256	-0.027	0.002
WNF1	2.451 E+02	lb	0.000	0.000	0.000	0.000	0.077	-1.905
WAF1	2.450 E+02	lb	0.000	0.000	0.000	0.000	-0.035	0.000
RO	1.001 E+03	ohms	0.004	-0.013	1.071	0.000	0.010	0.013
alpha	3.920 E-03		-0.010	0.016	-1.880	0.000	-0.013	-0.016
beta	1.159 E-01		-0.002	-0.002	-0.015	0.000	0.002	0.003
lambda	1.496 E+00		-0.001	-0.001	-0.072	0.000	0.001	0.001

Table 1. Relative Sensitivities, Test Point A

Parameter	Nominal Value	Units for P	dM/M/dP/P	dQ/Q/dP/P	dRe/Re/dP/P	dAl/Al/dP/P	dCD/CD/dP/P	dCL/CL/dP/P
S1 - AF	3.704 E-01	lbf/microvolt/volt	0.000	0.000	0.000	0.000	0.377	0.000
S2 - SF	2.020 E+00	lbf/microvolt/volt	0.000	0.000	0.000	0.000	0.000	0.000
S3 - NF	3.140 E+00	lbf/microvolt/volt	0.000	0.000	0.000	0.000	0.743	1.169
S4 - RM	1.353 E+01	lbf/microvolt/volt	0.000	0.000	0.000	0.000	0.000	0.000
S5 - PM	9.099 E+00	lbf/microvolt/volt	0.000	0.000	0.000	0.000	-0.050	-0.002
S6 - YM	5.725 E+00	lbf/microvolt/volt	0.000	0.000	0.000	0.000	0.000	0.000
BALPOW	4.998 E+00	volts	0.000	0.000	0.000	0.000	-1.064	-1.154
NF1RAW	3.282 E+00	millivolts	0.000	0.000	0.000	0.000	0.458	0.837
NF2RAW	4.360 E-01	millivolts	0.000	0.000	0.000	0.000	0.238	0.329
AXFRAW	1.679 E-01	millivolts	0.000	0.000	0.000	0.000	0.378	0.000
SF1RAW	-3.495 E-01	millivolts	0.000	0.000	0.000	0.000	0.000	0.000
SF2RAW	-7.465 E-01	millivolts	0.000	0.000	0.000	0.000	0.000	0.000
RLMRAW	1.608 E+00	millivolts	0.000	0.000	0.000	0.000	0.000	0.000
PT100V	6.322 E+00	volts	1.246	2.510	1.690	0.000	-2.457	-2.448
PS50V	8.275 E+00	volts	-1.257	-1.530	-0.706	0.000	1.575	1.553
ELEVA	-1.121 E-02	volts/g	0.000	0.000	0.000	1.089	0.833	-0.002
AOA1S	2.702 E-01	volts	0.000	0.000	0.000	-1.098	-0.839	0.002
AOA1B	2.015 E-04	volts	0.000	0.000	0.000	0.019	0.014	0.000
AOA1Z	4.727 E+01	deg	0.000	0.000	0.000	-0.082	-0.067	0.000
AOA1M	3.211 E-01	deg	0.000	0.000	0.000	-0.108	-0.088	0.000
WNF1	2.451 E+02	lbf	0.000	0.000	0.000	0.000	-0.124	-0.166
WAF1	2.450 E+02	lbf	0.000	0.000	0.000	0.000	0.058	0.000
RO	1.001 E+03	ohms	0.005	-0.010	1.072	0.000	0.009	0.010
alpha	3.920 E-03		-0.009	0.018	-1.876	0.000	-0.015	-0.018
beta	1.159 E-01		0.000	0.001	-0.013	0.000	-0.001	-0.001
lambda	1.496 E+00		-0.001	0.000	-0.071	0.000	0.000	0.000

Table 2. Relative Sensitivities, Test Point B

Parameter	Nominal value	units	DAU channel	voltage range	BIAS - DAU calibration &DAU WS	BIAS - calibration	BIAS - other	BIAS - TOTAL (in parameter units)	Total BIAS in % of Parameter Value
S1 - AF	3.704 E-01	lbf/microv/volt				6.30 E-04	3.50 E-03	3.56 E-03	0.96 %
S2 - SF	2.020 E+00	lbf/microv/volt				1.98 E-02		1.98 E-02	0.98 %
S3 - NF	3.140 E+00	lbf/microv/volt				3.71 E-02	1.04 E-02	3.85 E-02	1.23 %
S4 - RM	1.353 E+01	lbf/microv/volt				1.65 E-03		1.65 E-03	0.01 %
S5 - PM	9.099 E+00	lbf/microv/volt				1.04 E-01	1.00 E-02	1.04 E-01	1.15 %
S6 - YM	5.725 E+00	lbf/microv/volt				3.56 E-03		3.56 E-03	0.06 %
BALPOW	4.998 E+00	volts	ACH97	5 v	8.97 E-04			8.97 E-04	0.02 %
NF1RAW	2.581 E+00	millivolts	ACH17	10 mv	3.72 E-03			3.72 E-03	0.14 %
NF2RAW	-3.111 E+00	millivolts	ACH19	10 mv	3.80 E-03			3.80 E-03	0.12 %
AXFRAW	1.116 E+00	millivolts	ACH18	10 mv	3.80 E-03			3.80 E-03	0.34 %
SF1RAW	-3.282 E-01	millivolts	ACH20	10 mv	3.84 E-03			3.84 E-03	1.17 %
SF2RAW	-7.665 E-01	millivolts	ACH21	10 mv	3.83 E-03			3.83 E-03	0.50 %
RUMRAW	1.622 E+00	millivolts	ACH13	5 mv	3.65 E-03			3.65 E-03	0.23 %
PT100V	6.322 E+00	volts	ACH179	10 v	1.39 E-03	1.30 E-03		1.90 E-03	0.03 %
PS50V	8.248 E+00	volts	ACH185	10 v	2.05 E-03	1.60 E-03		2.60 E-03	0.03 %
ELEVA	3.431 E-03	volts	DCH3				4.30 E-06	4.30 E-06	0.13 %
AOA1S	2.702 E-01	volts/g					1.59 E-03	1.59 E-03	0.59 %
AOA1B	2.015 E-04	volts					8.59 E-05	8.59 E-05	42.63 %
AOA1Z	4.727 E+01	deg					3.73 E+00	3.73 E+00	7.89 %
AOA1M	3.211 E-01	deg					1.51 E-02	1.51 E-02	4.70 %
WNF1	2.451 E+02	lb					1.00 E-01	1.00 E-01	0.04 %
WAF1	2.450 E+02	lb					1.00 E-01	1.00 E-01	0.04 %
RO	1.001 E+03	ohms				1.64 E-01		1.64 E-01	0.02 %
alpha	3.920 E-03					3.40 E-06		3.40 E-06	0.09 %
beta	1.159 E-01					1.90 E-02		1.90 E-02	16.39 %
lambda	1.496 E+00					3.62 E-02		3.62 E-02	2.42 %

Table 3. Parameter Bias Error Estimates - Test Point A

Parameter	Nominal value	units	DAU channel	voltage range	BIAS - DAU calibration &DAU WS	BIAS - calibration	BIAS - other	BIAS - TOTAL parameter units	Total BIAS in % of Parameter Value
S1 - AF	3.704 E-01	lbf/microv/volt				6.30 E-04	7.41 E-03	7.44 E-03	2.01 %
S2 - SF	2.020 E+00	lbf/microv/volt				1.98 E-02		1.98 E-02	0.98 %
S3 - NF	3.140 E+00	lbf/microv/volt				3.71 E-02	5.02 E-03	3.74 E-02	1.19 %
S4 - RM	1.353 E+01	lbf/microv/volt				1.65 E-03		1.65 E-03	0.01 %
S5 - PM	9.099 E+00	lbf/microv/volt				1.04 E-01	2.18 E-02	1.06 E-01	1.17 %
S6 - YM	5.725 E+00	lbf/microv/volt				3.56 E-03		3.56 E-03	0.06 %
BALPOW	4.998 E+00	volts	ACH97	5 v	8.97 E-04			8.97 E-04	0.02 %
NF1RAW	3.282 E+00	millivolts	ACH17	10 mv	3.72 E-03			3.72 E-03	0.11 %
NF2RAW	4.360 E-01	millivolts	ACH19	10 mv	3.80 E-03			3.80 E-03	0.87 %
AXFRAW	1.679 E-01	millivolts	ACH18	10 mv	3.80 E-03			3.80 E-03	2.26 %
SF1RAW	-3.495 E-01	millivolts	ACH20	10 mv	3.84 E-03			3.84 E-03	1.10 %
SF2RAW	-7.465 E-01	millivolts	ACH21	10 mv	3.83 E-03			3.83 E-03	0.51 %
RLMRAW	1.608 E+00	millivolts	ACH13	5 mv	3.65 E-03			3.65 E-03	0.23 %
PT100V	6.322 E+00	volts	ACH179	10 v	1.39 E-03	1.30 E-03		1.90 E-03	0.03 %
PS50V	8.275 E+00	volts	ACH185	10 v	2.05 E-03	1.60 E-03		2.60 E-03	0.03 %
ELEVA	-1.121 E-02	volts	DCH3				4.30 E-06	4.30 E-06	0.04 %
AOA1S	2.702 E-01	volts/g					1.59 E-03	1.59 E-03	0.59 %
AOA1B	2.015 E-04	volts					8.59 E-05	8.59 E-05	42.63 %
AOA1Z	4.727 E+01	deg					3.73 E+00	3.73 E+00	7.89 %
AOA1M	3.211 E-01	deg					1.51 E-02	1.51 E-02	4.70 %
WNF1	2.451 E+02	lb					1.00 E-01	1.00 E-01	0.04 %
WAF1	2.450 E+02	lb					1.00 E-01	1.00 E-01	0.04 %
RO	1.001 E+03	ohms				1.64 E-01		1.64 E-01	0.02 %
alpha	3.920 E-03					3.40 E-06		3.40 E-06	0.09 %
beta	1.159 E-01					1.90 E-02		1.90 E-02	16.39 %
lambda	1.496 E+00					3.62 E-02		3.62 E-02	2.42 %

Table 4. Parameter Bias Error Estimates - Test Point B

Parameter	Bias Factor Mach Number
PS50V	1.55 E-07
PT100V	1.39 E-07
beta	9.40 E-08
lambda	1.31 E-09

Table 5. Prioritized Bias Factors, Mach Number, Test Point A

Parameter	Bias Factor Reynolds Number
beta	6.02 E-06
lambda	3.03 E-06
alpha	2.66 E-06
PT100V	2.56 E-07
PS50V	4.84 E-08
RO	3.08 E-08

Table 6. Prioritized Bias Factors, Reynolds Number, Test Point A

Parameter	Bias Factor Angle of Attack
AOA1B	3.94 E-04
AOA1Z	2.34 E-04
AOA1M	1.45 E-04
AOA1S	1.88 E-05
ELEVA	9.80 E-07

Table 7. Prioritized Bias Factors, Angle of Attack, Test Point A

Parameter	Bias Factor Drag Coefficient
S1 - AF	1.25 E-04
AXFRAW	2.34 E-05
S3 - NF	5.30 E-06
AOA1Z	2.64 E-06
S5 - PM	1.81 E-06
AOA1M	1.61 E-06
NF1RAW	6.83 E-07
AOA1B	6.76 E-07
PT100V	5.40 E-07
PS50V	2.42 E-07

Table 8. Prioritized Bias Factors, Drag Coefficient, Test Point A

Parameter	Bias Factor Lift Coefficient
S3 - NF	1.31 E-03
NF1RAW	1.28 E-04
NF2RAW	3.70 E-05
WNF1	6.04 E-07
S5 - PM	5.98 E-07
PT100V	5.35 E-07
BALPOW	2.65 E-07
PS50V	2.35 E-07
beta	1.76 E-07

Table 9. Prioritized Bias Factors, Lift Coefficient, Test Point A

Parameter	Bias Factor Mach Number
PS50V	1.56 E-07
PT100V	1.41 E-07
lambda	3.31 E-10
alpha	5.95 E-11

Table 10. Prioritized Bias Factors, Mach Number, Test Point B

Parameter	Bias Factor Reynolds Number
beta	4.56 E-06
lambda	2.94 E-06
alpha	2.65 E-06
PT100V	2.59 E-07
PS50V	4.92 E-08
RO	3.09 E-08

Table 11. Prioritized Bias Factors, Reynolds Number, Test Point B

Parameter	Bias Factor Angle of Attack
AOA1B	6.72 E-05
AOA1Z	4.18 E-05
AOA1S	4.17 E-05
AOA1M	2.58 E-05
ELEVA	1.74 E-07

Table 12. Prioritized Bias Factors, Angle of Attack, Test Point B

Parameter	Bias Factor Drag Coefficient
S3 - NF	7.83 E-05
AXFRAW	7.30 E-05
S1 - AF	5.75 E-05
AOA1B	3.38 E-05
AOA1Z	2.78 E-05
AOA1S	2.44 E-05
AOA1M	1.72 E-05
NF2RAW	4.32 E-06
PT100V	5.47 E-07
S5 - PM	3.37 E-07
NF1RAW	2.69 E-07
PS50V	2.45 E-07
ELEVA	1.02 E-07

Table 13. Prioritized Bias Factors, Drag Coefficient, Test Point B

Parameter	Bias Factor Lift Coefficient
S3 - NF	1.94 E-04
NF2RAW	8.23 E-06
NF1RAW	8.99 E-07
PT100V	5.43 E-07
PS50V	2.38 E-07
BALPOW	4.29 E-08
beta	1.49 E-08

Table 14. Prioritized Bias Factors, Lift Coefficient, Test Point B

Parameter	Nominal Parameter Value	Bias Limit Estimate
Mach Number	0.801	± 0.0005
Reynolds Number	40.05×10^6	$\pm 0.14 \times 10^6$
Angle of Attack	-0.92 °	± .03 °
Drag Coefficient	0.0156	± .0002
Lift Coefficient	0.0351	± .0013

Table 15. Bias Limit Estimates for Results - Test Point A

Parameter	Nominal Parameter Value	Bias Limit Estimate
Mach Number	0.798	± 0.0004
Reynolds Number	39.91×10^6	$\pm 0.13 \times 10^6$
Angle of Attack	2.18 °	± .03 °
Drag Coefficient	0.0220	± .0004
Lift Coefficient	0.404	± .0067

Table 16. Bias Limit Estimates for Results - Test Point B

Parameter	Nominal Parameter Value	Units	Precision index	Precision Index of the Mean	Degrees of Freedom	t Factor	Precision Limit of Mean
BALPOW	4.998 E+00	volts	3.110 E-04	9.835 E-05	9	2.26	2.223 E-04
NF1RAW	2.581 E+00	millivolts	3.740 E-03	1.183 E-03	9	2.26	2.673 E-03
NF2RAW	-3.111 E+00	millivolts	6.260 E-03	1.980 E-03	9	2.26	4.474 E-03
AXFRAW	1.116 E+00	millivolts	2.500 E-03	7.906 E-04	9	2.26	1.787 E-03
SF1RAW	-3.282 E-01	millivolts	1.190 E-02	3.763 E-03	9	2.26	8.505 E-03
SF2RAW	-7.665 E-01	millivolts	1.250 E-02	3.953 E-03	9	2.26	8.933 E-03
RLMRAW	1.622 E+00	millivolts	3.440 E-03	1.088 E-03	9	2.26	2.458 E-03
PT100V	6.322 E+00	volts	7.380 E-04	2.334 E-04	9	2.26	5.274 E-04
PS50V	8.248 E+00	volts	1.990 E-03	6.293 E-04	9	2.26	1.422 E-03
ELEVA	3.431 E-03	volts	2.380 E-05	7.526 E-06	9	2.26	1.701 E-05

Table 17. Precision Limits, Measured Parameters, Test Point A

Parameter	Precision Factor Drag Coefficient
AXFRAW	3.47 E-06
NF1RAW	3.53 E-07
NF2RAW	1.49 E-07
PS50V	7.23 E-08
ELEVA	5.12 E-08
PT100V	4.15 E-08
BALPOW	1.43 E-09

Table 18. Prioritized Precision Factors, Drag Coefficient, Test Point A

Parameter	Precision Factor Lift Coefficient
NF1RAW	6.63 E-05
NF2RAW	5.13 E-05
PS50V	7.01 E-08
PT100V	4.11 E-08
BALPOW	1.63 E-08

Table 19. Prioritized Precision Factors, Lift Coefficient, Test Point A

Parameter	Nominal Parameter Value	Precision Limit Estimate
Mach Number	0.8015	± 0.0002
Reynolds Number	40.056×10^6	$\pm 0.007 \times 10^6$
Angle of Attack	-0.921 °	± 0.004 °
Drag Coefficient	0.01554	± 0.00003
Lift Coefficient	0.0351	± 0.0004

Table 20. Precision Limit Estimates for a Single Result - Test Point A

Parameter	Nominal Parameter Value	Precision Limit Estimate
Mach Number	0.7982	± 0.00015
Reynolds Number	39.913×10^6	$\pm 0.005 \times 10^6$
Angle of Attack	2.184 °	± 0.004 °
Drag Coefficient	0.022198	± 0.00015
Lift Coefficient	0.404	± 0.002

Table 21. Precision Limit Estimates for a Single Result - Test Point B

Test Point	Mach Number	Reynolds No.	Angle of Attack (deg)	Drag Coefficient	Lift Coefficient
		x e6			
C	0.799	40.15	1.6488	0.01941	0.3564
D	0.798	40.17	1.6509	0.01940	0.3555
E	0.797	40.10	1.6316	0.01927	0.3549
F	0.799	40.11	1.6382	0.01929	0.3565
G	0.800	40.10	1.6433	0.01937	0.3570
H	0.800	40.03	1.6323	0.01930	0.3570
I	0.801	40.10	1.6516	0.01944	0.3575
J	0.800	40.05	1.6365	0.01931	0.3570
K	0.800	40.10	1.6425	0.01932	0.3571
L	0.800	40.12	1.6455	0.01939	0.3568
Average	0.799	40.103	1.6421	0.01935	0.3566
Precision Index	1.17E-03	4.11E-02	7.29E-03	5.89E-05	7.97E-04
t factor (DOF=9)	2.26	2.26	2.26	2.26	2.26
Precsion limit	0.0027	0.093	0.016	0.00013	0.0018

Table 22. Precision Limit Estimates, Multiple Test Results, Test Points C - L

Parameter	Mach No.	Reynolds No.	Alpha (deg)	C_D	C_L
Nominal Parameter Value	0.801	4.01E+07	-0.92	0.0156	0.0351
Bias Limit	0.0005	1.40E+05	0.03	0.0002	0.0013
Precision Limit	0.0002	7.00E+03	0.004	0.000032	0.00038
Uncertainty	± 0.0005	± 1.40E+05	± 0.03	± 0.0002	± 0.0014
Confidence Level	95%	95%	95%	95%	95%

Table 23. Uncertainty Estimates, Single Measurement Method, Test Point A

Parameter	Mach No.	Reynolds No.	Alpha (deg)	C_D	C_L
Nominal Parameter Value	0.798	3.99 E+07	2.18	0.0220	0.404
Bias Limit	0.0004	1.3 E+05	0.03	0.0004	0.007
Precision Limit	0.00015	5.0 E+03	0.004	0.00015	0.002
Uncertainty	± 0.0004	± 1.3 E+05	± 0.030	± 0.0004	± 0.007
Confidence Level	95%	95%	95%	95%	95%

Table 24. Uncertainty Estimates, Single Measurement Method, Test Point B

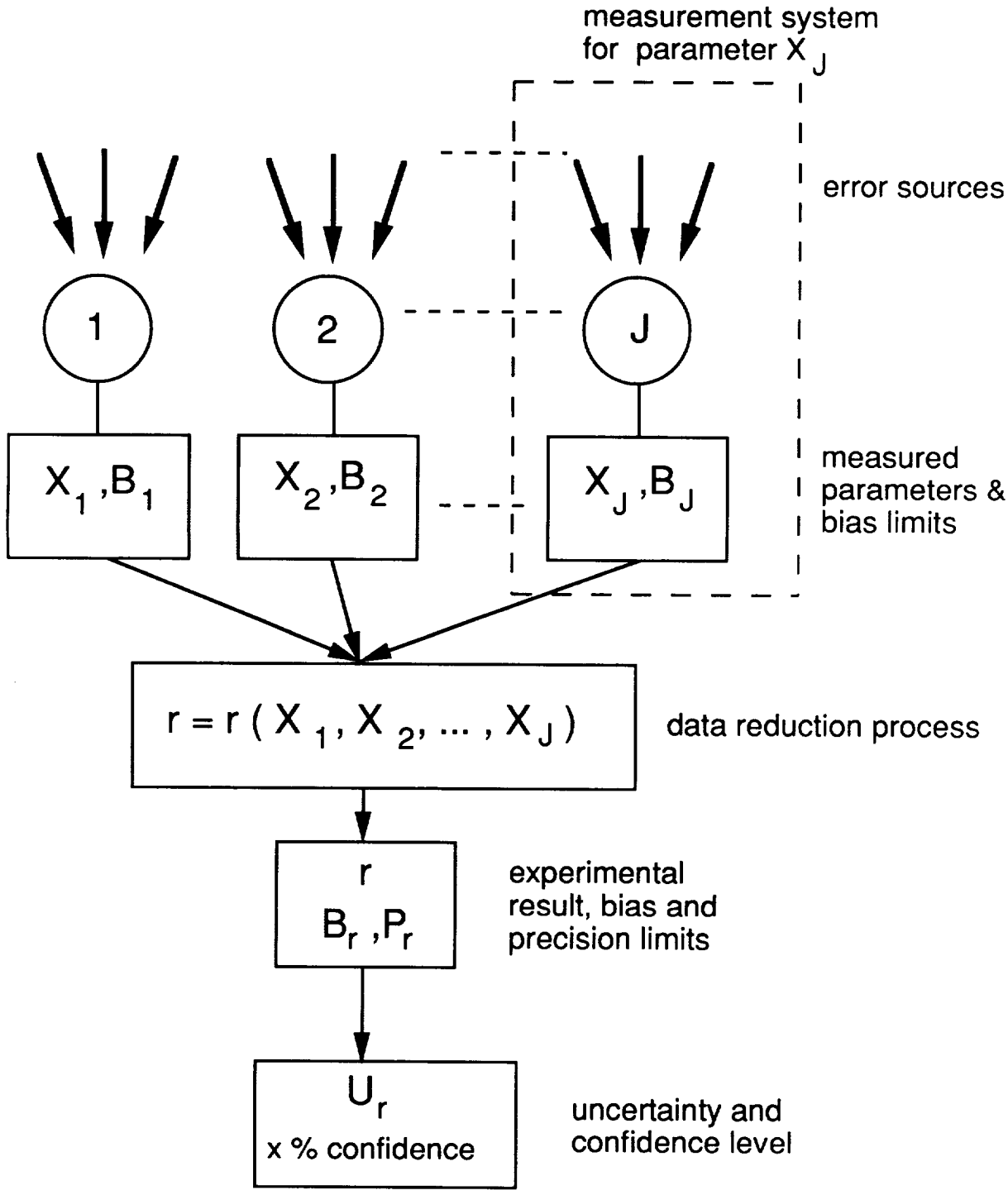

Figure 1. Schematic of Uncertainty Analysis Methodology

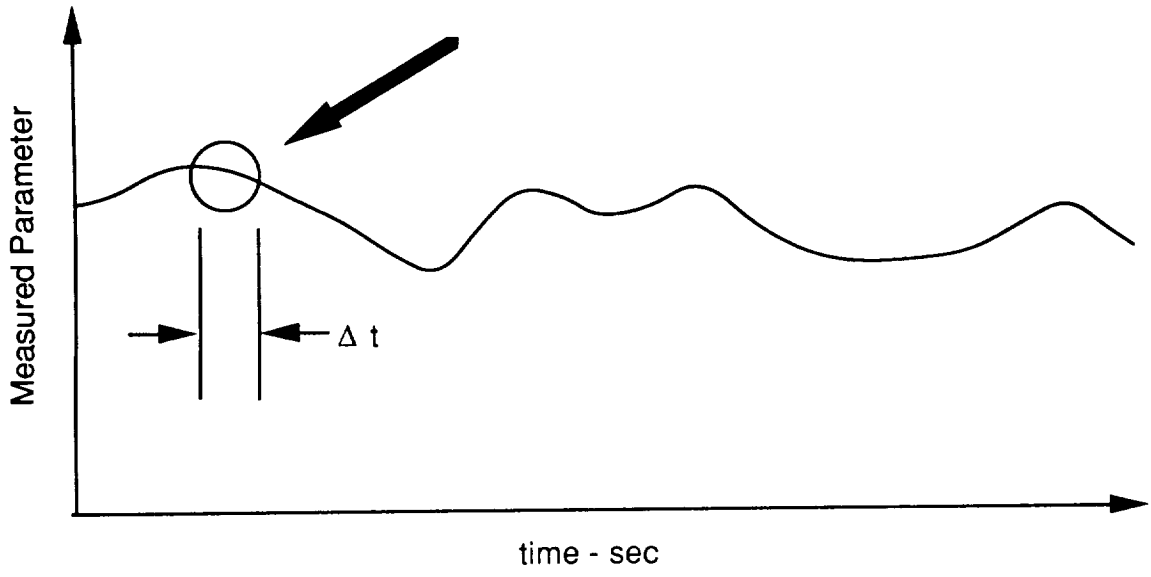

a. "Long" Time Interval

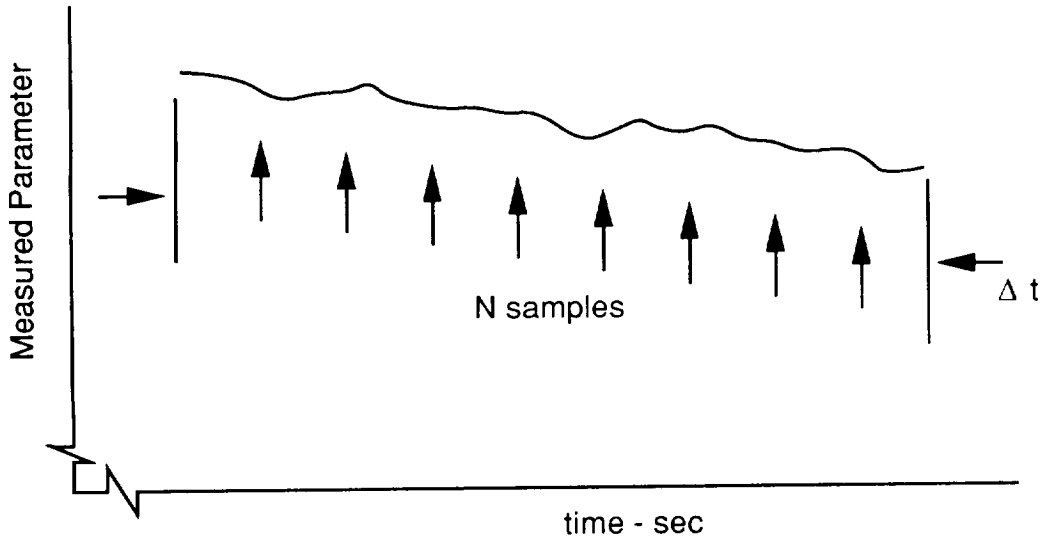

b. "Short" Sample Inverval

Figure 2. Time History of Random Data Sample

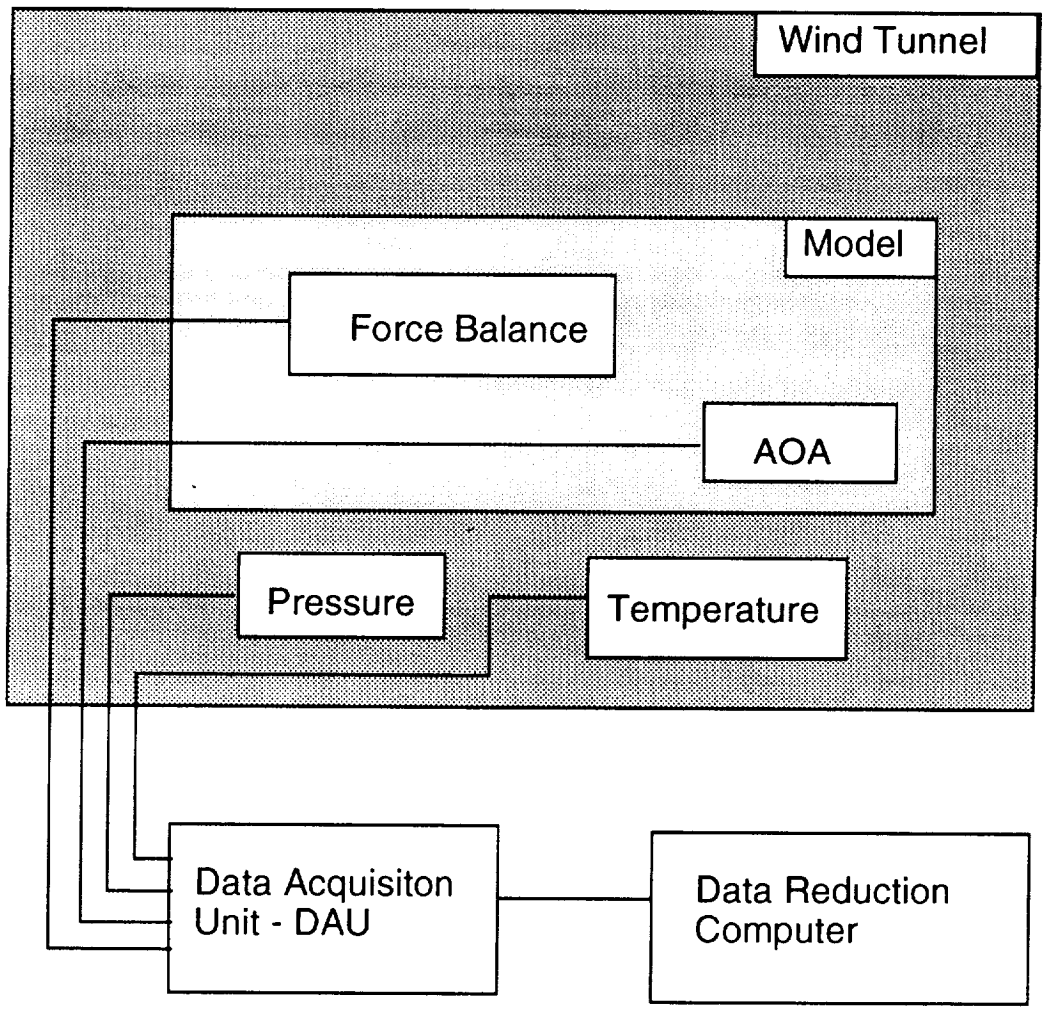

Figure 3. Basic Measurement System Schematic

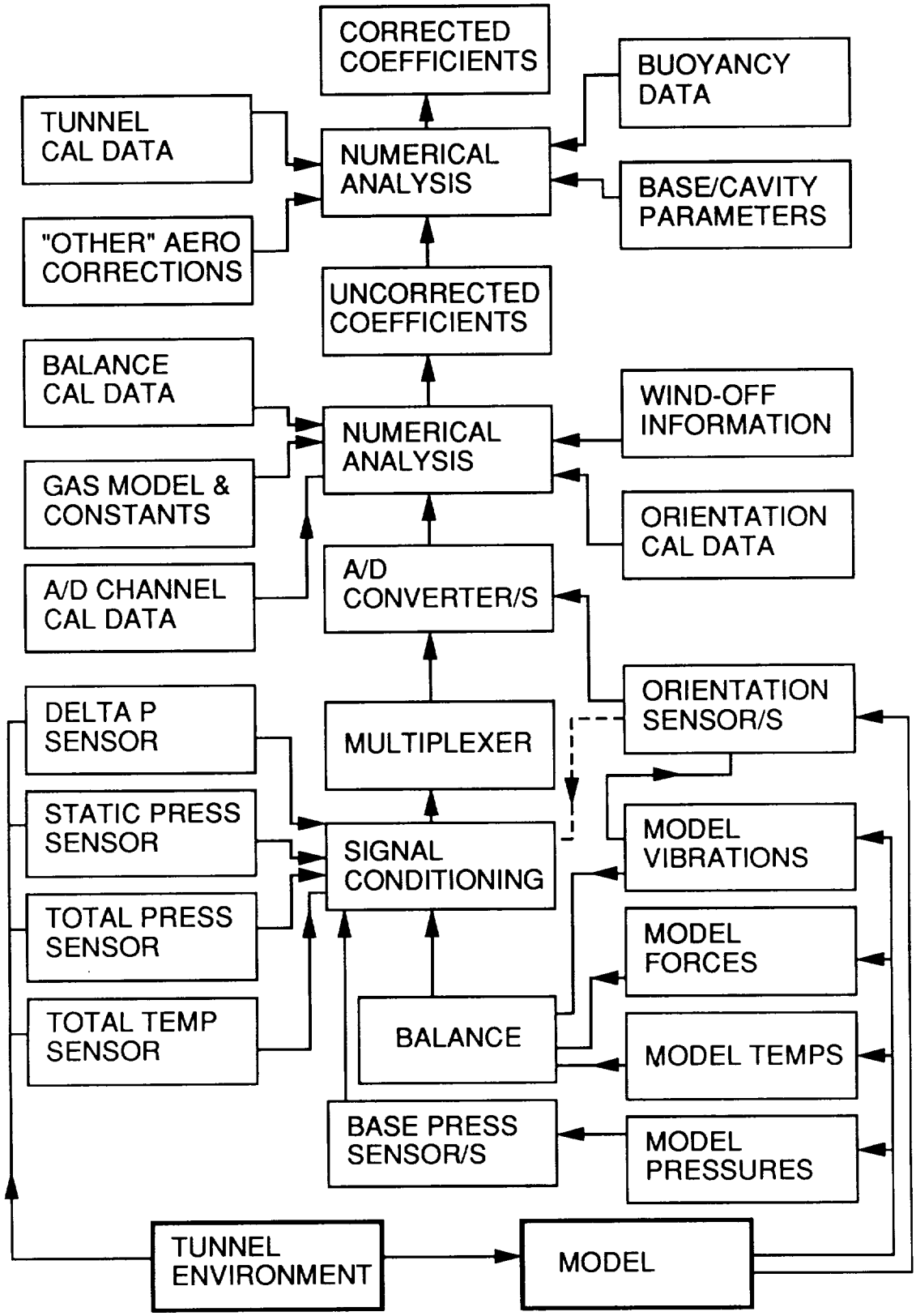

Figure 4. NTF Information Flow Schematic

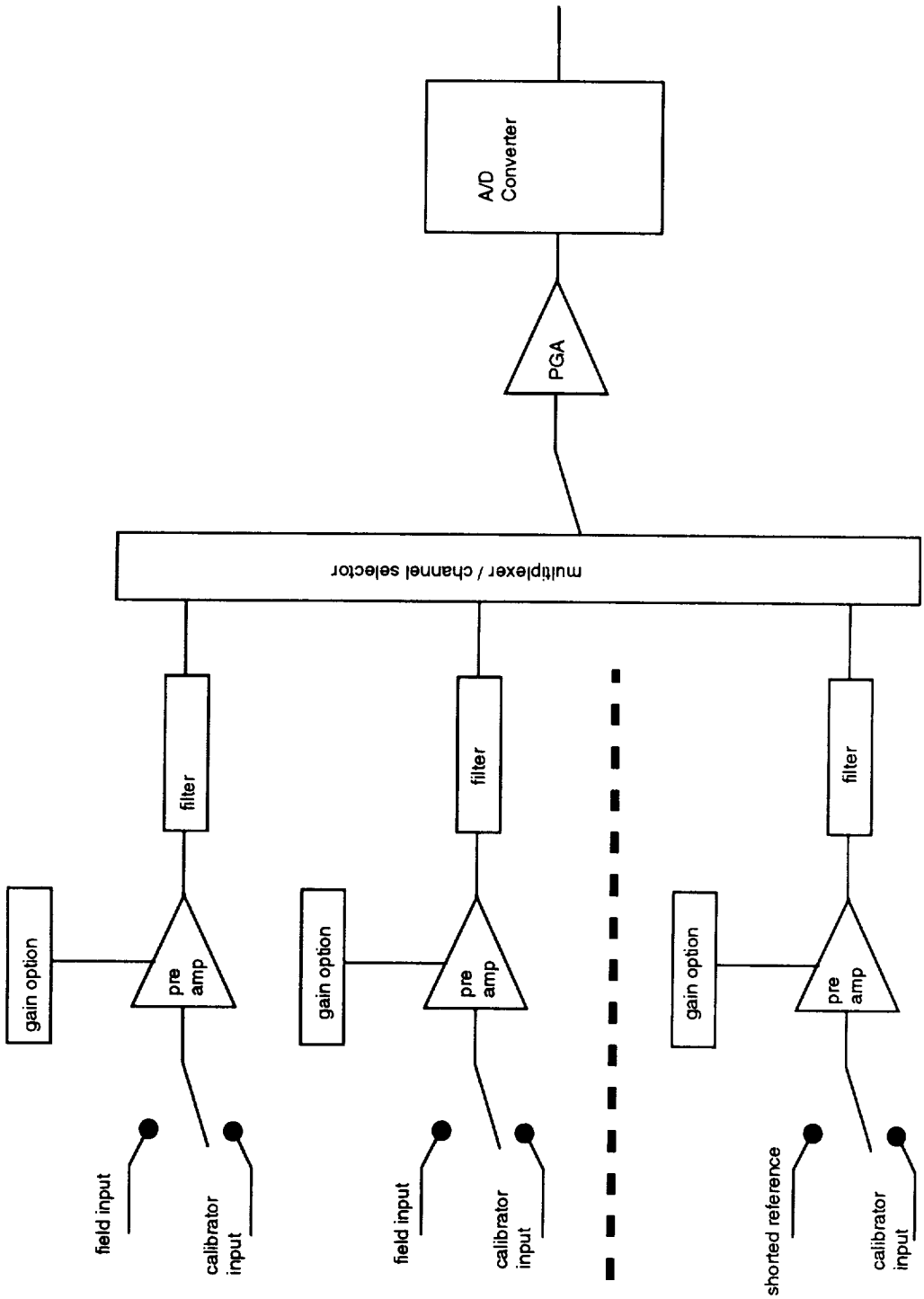

Figure 5. NTF DAU Schematic

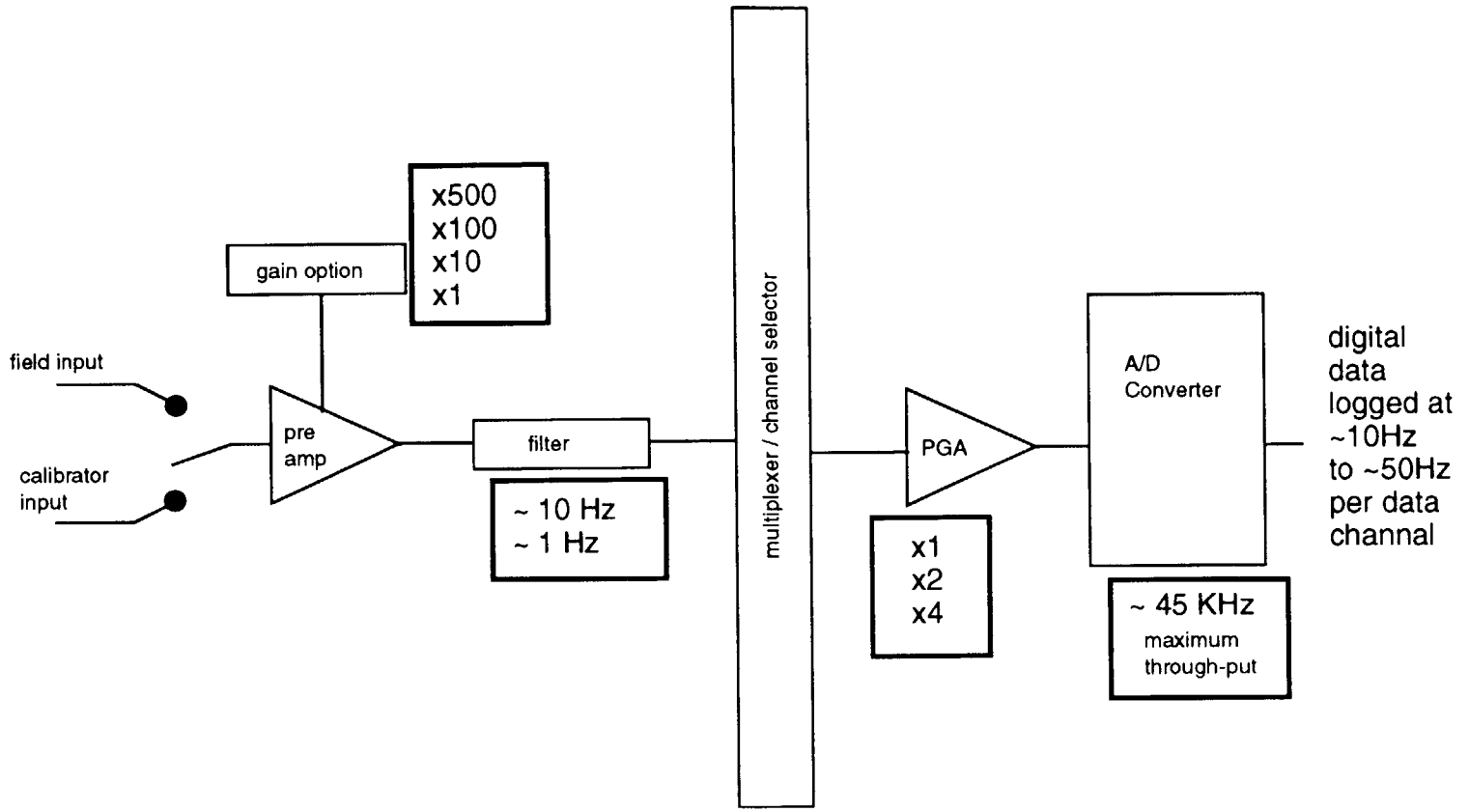

Figure 6. NTF DAU Details

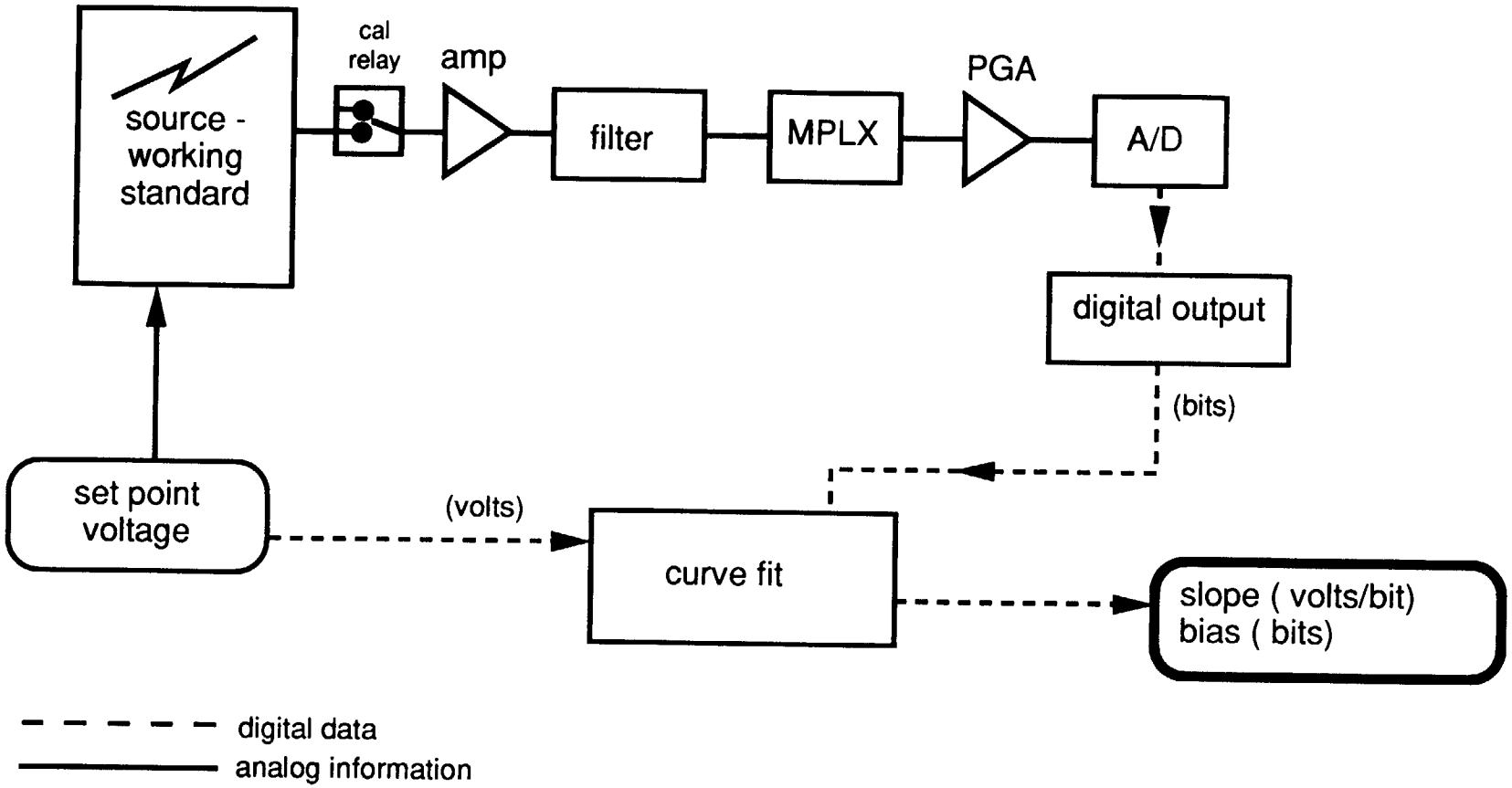

Figure 7. DAU Calibration, In- Tunnel

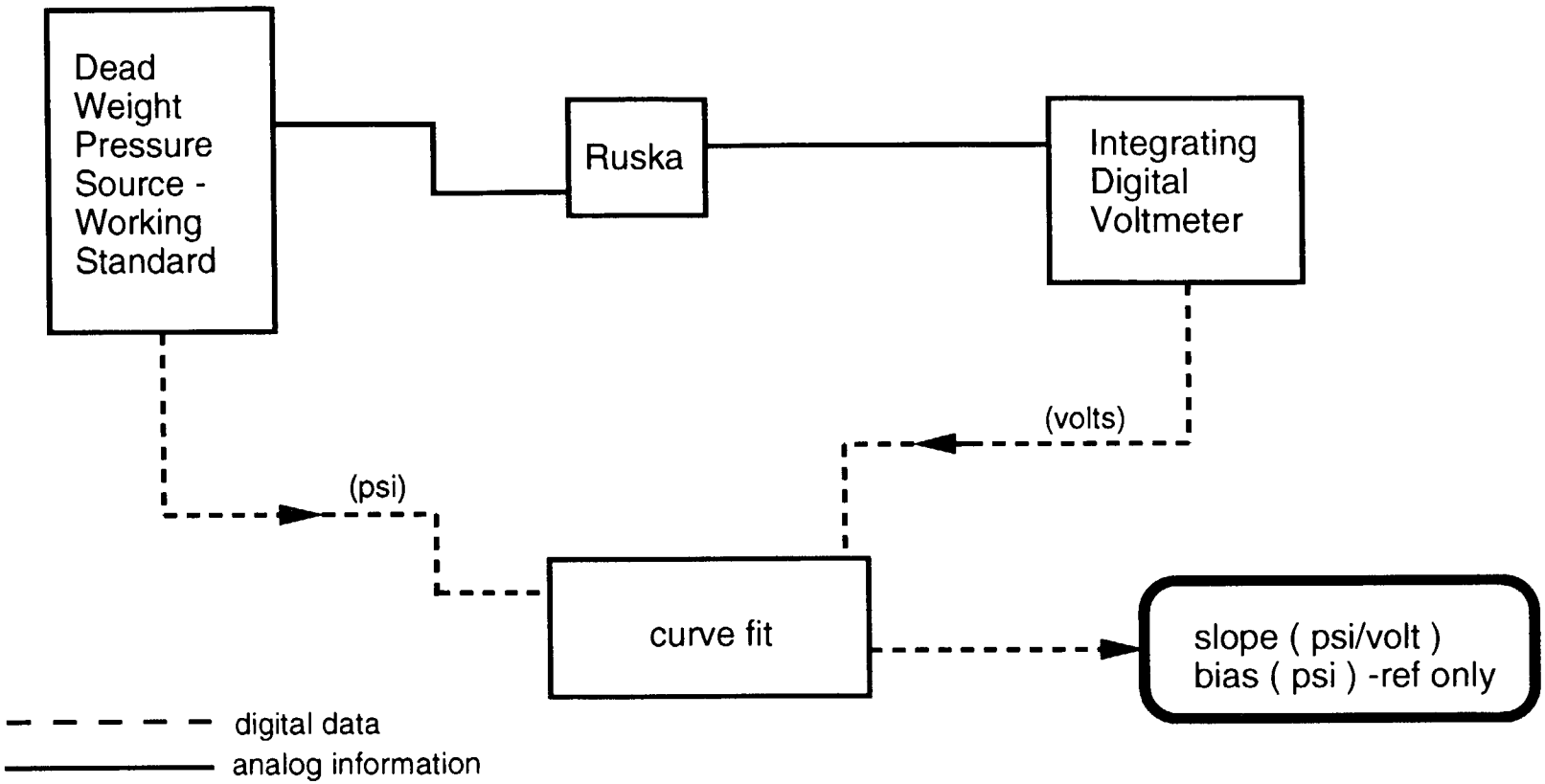

Figure 8. Ruska Calibration, Calibration Laboratory

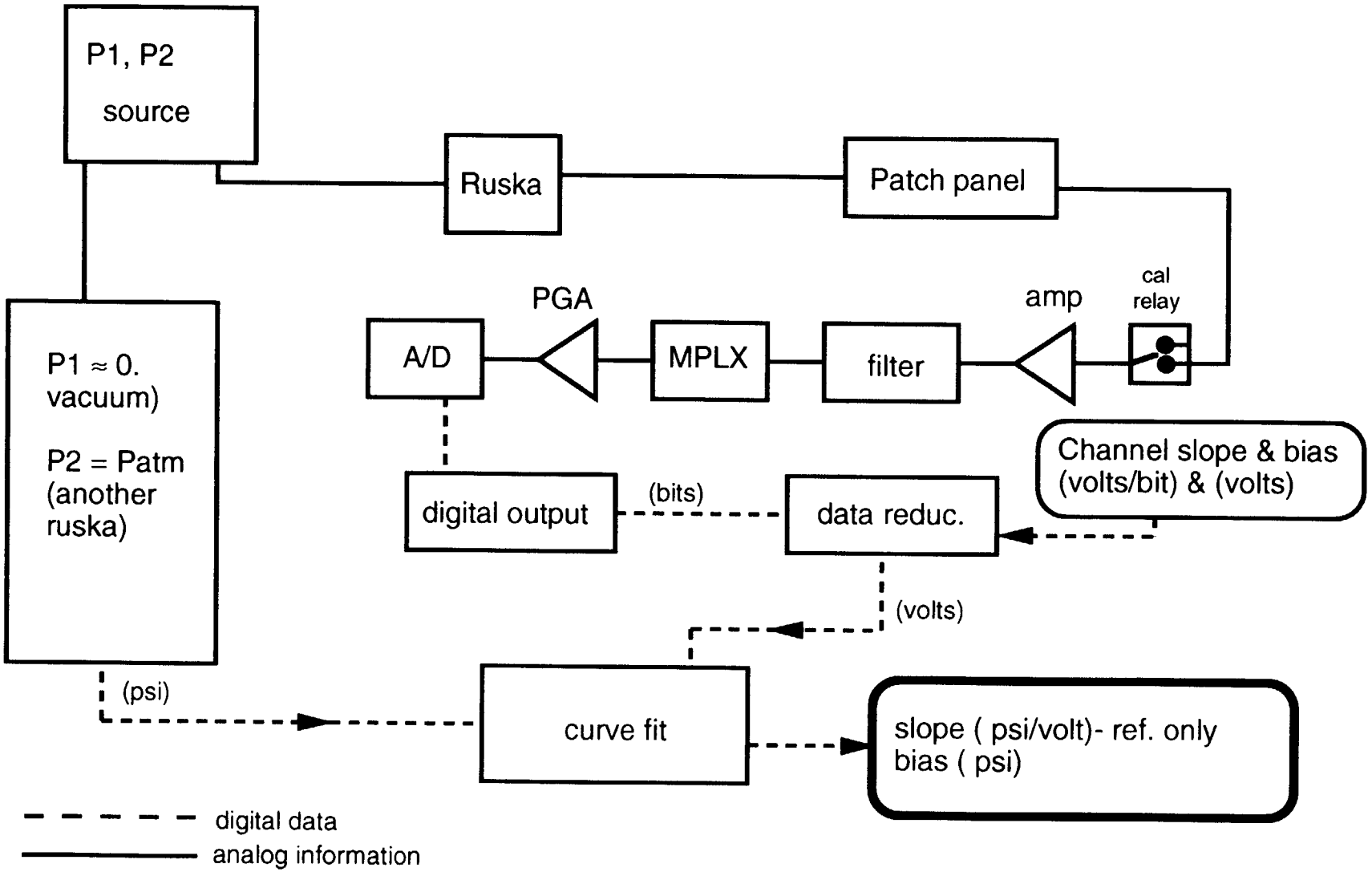

Figure 9. Ruska Two-point Calibration, In-Tunnel

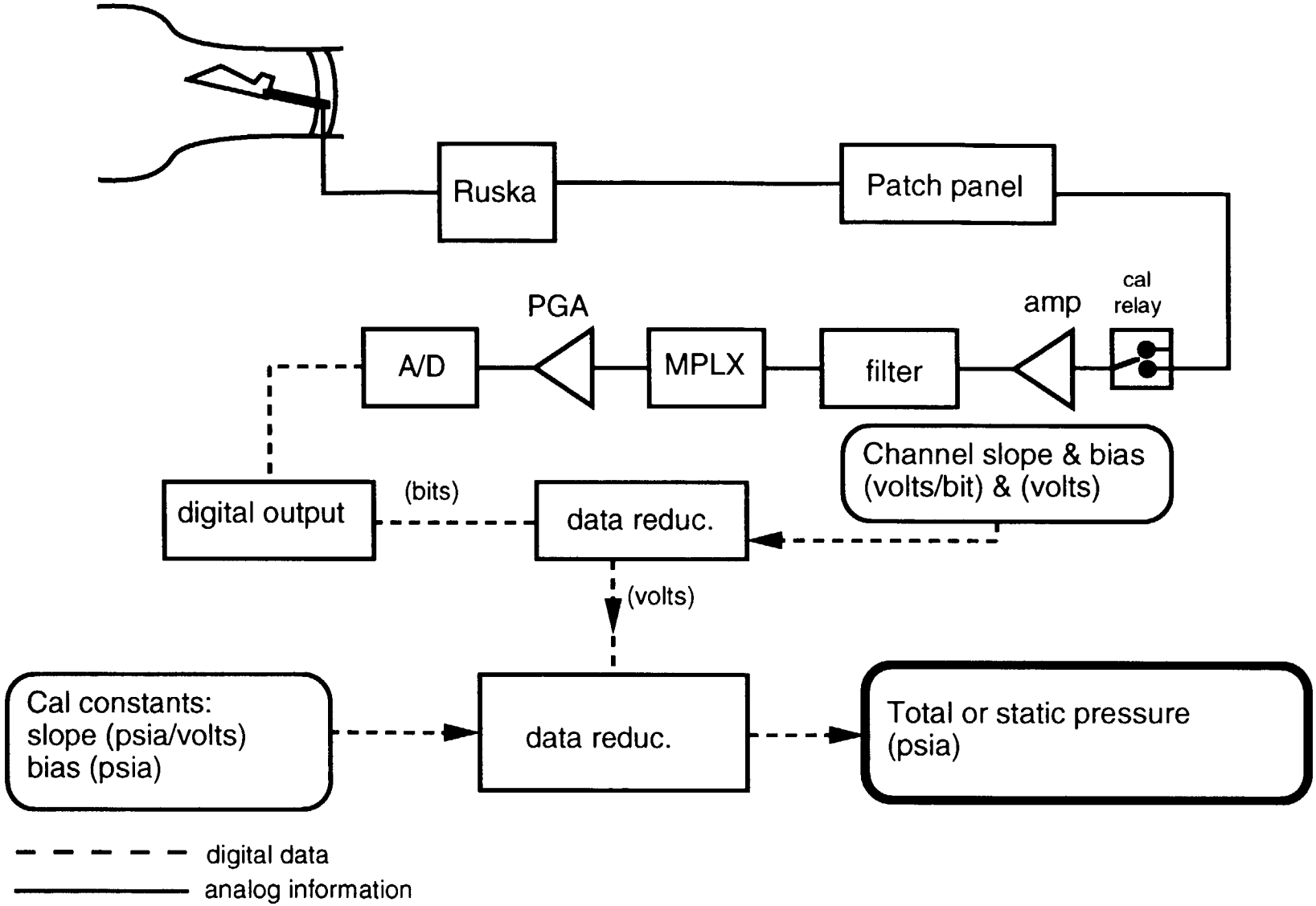

Figure 10. Ruska Pressure Measurement

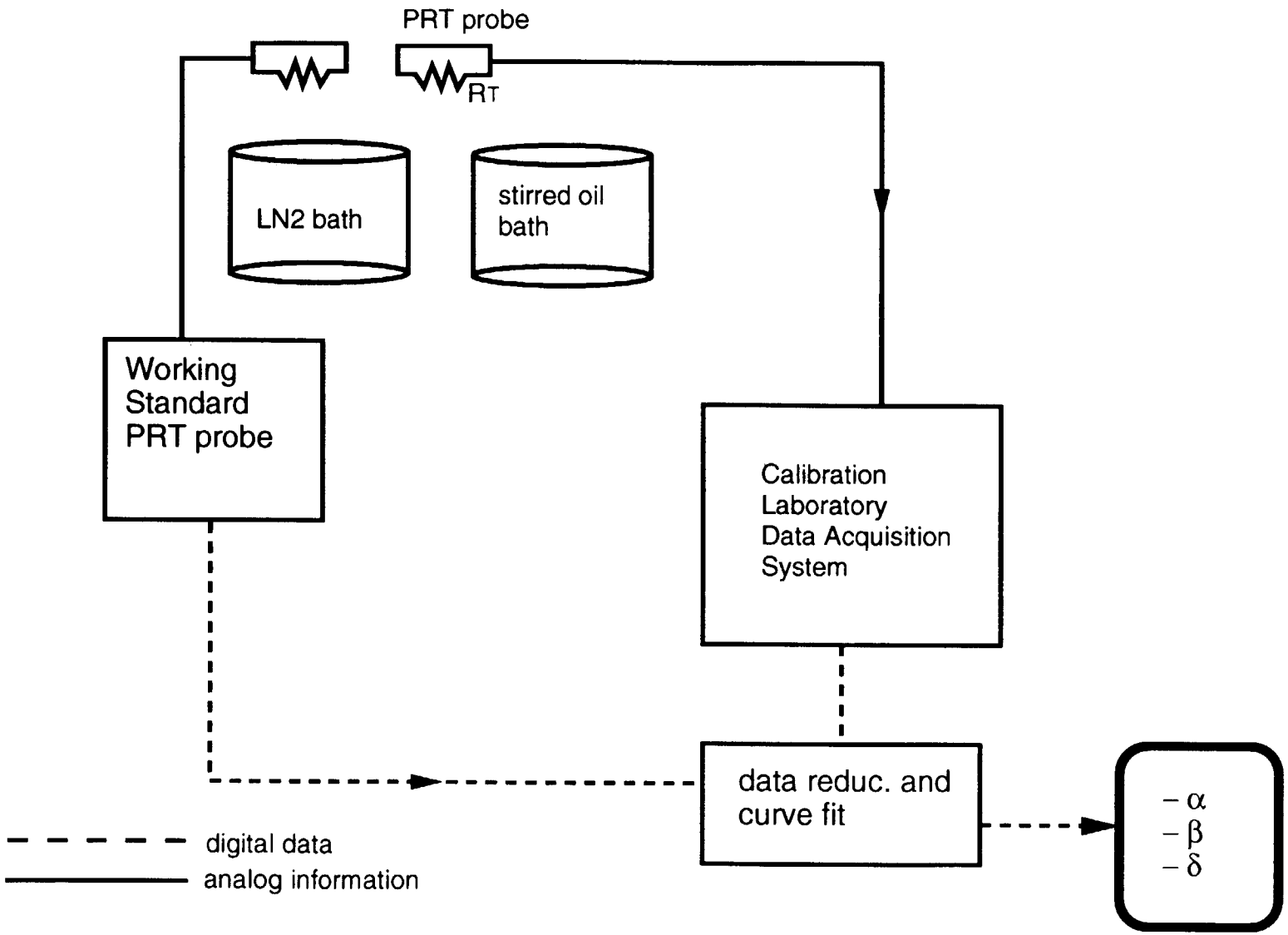

Figure 11. PRT - Calibration Laboratory

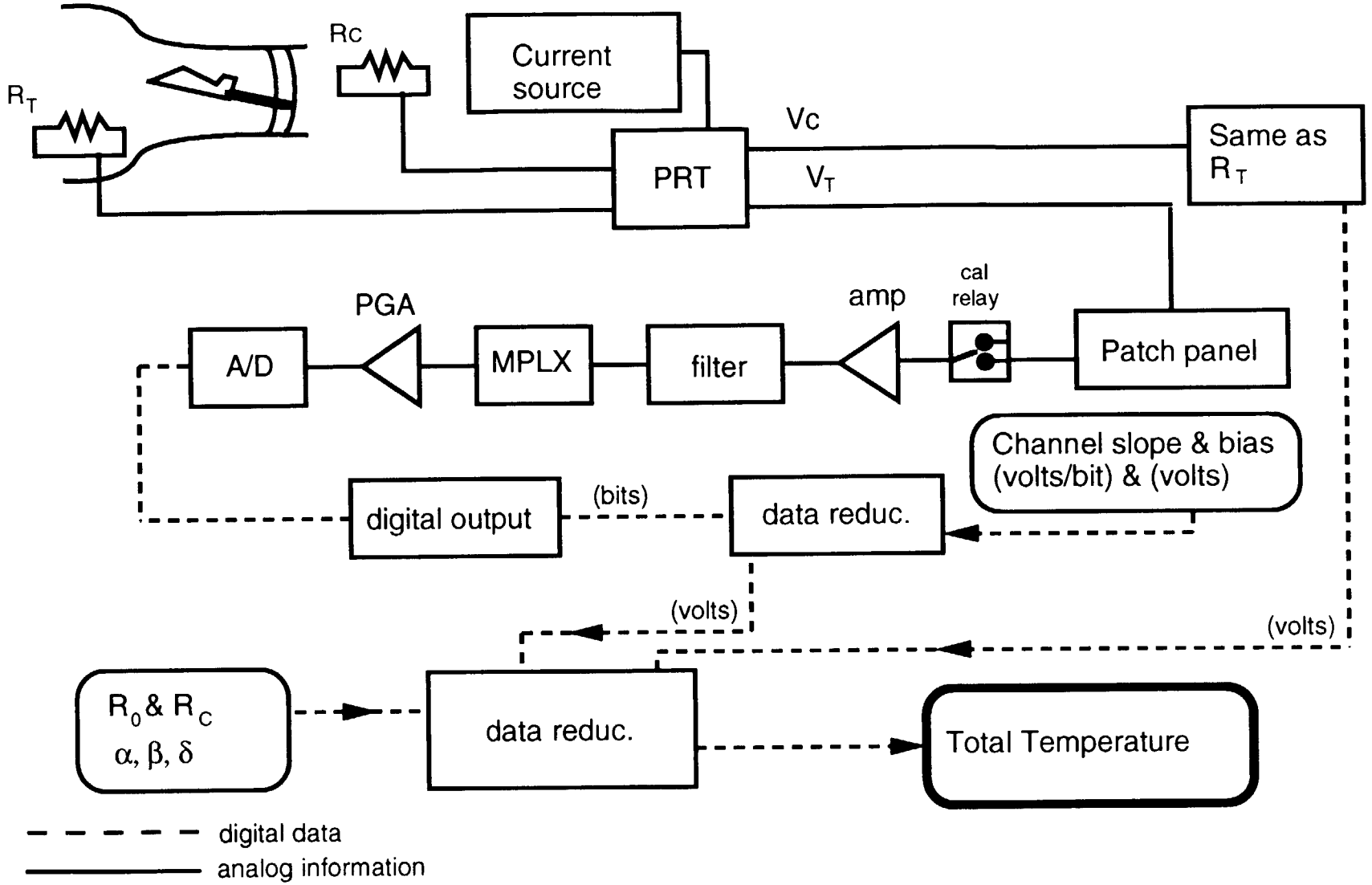

Figure 12. PRT Total Temperature Measurement

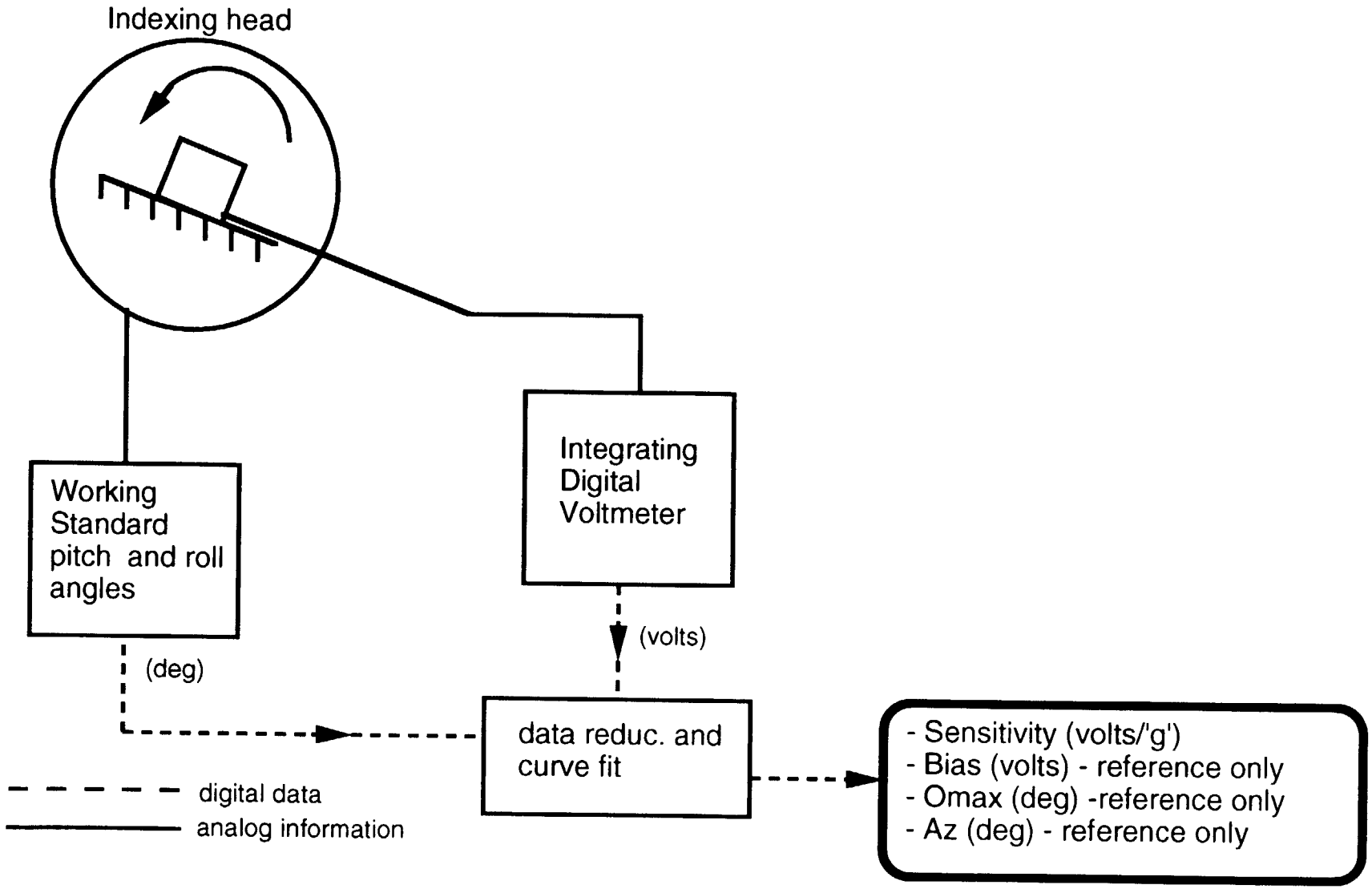

Figure 13. Single Axis AOA, Calibration Laboratory

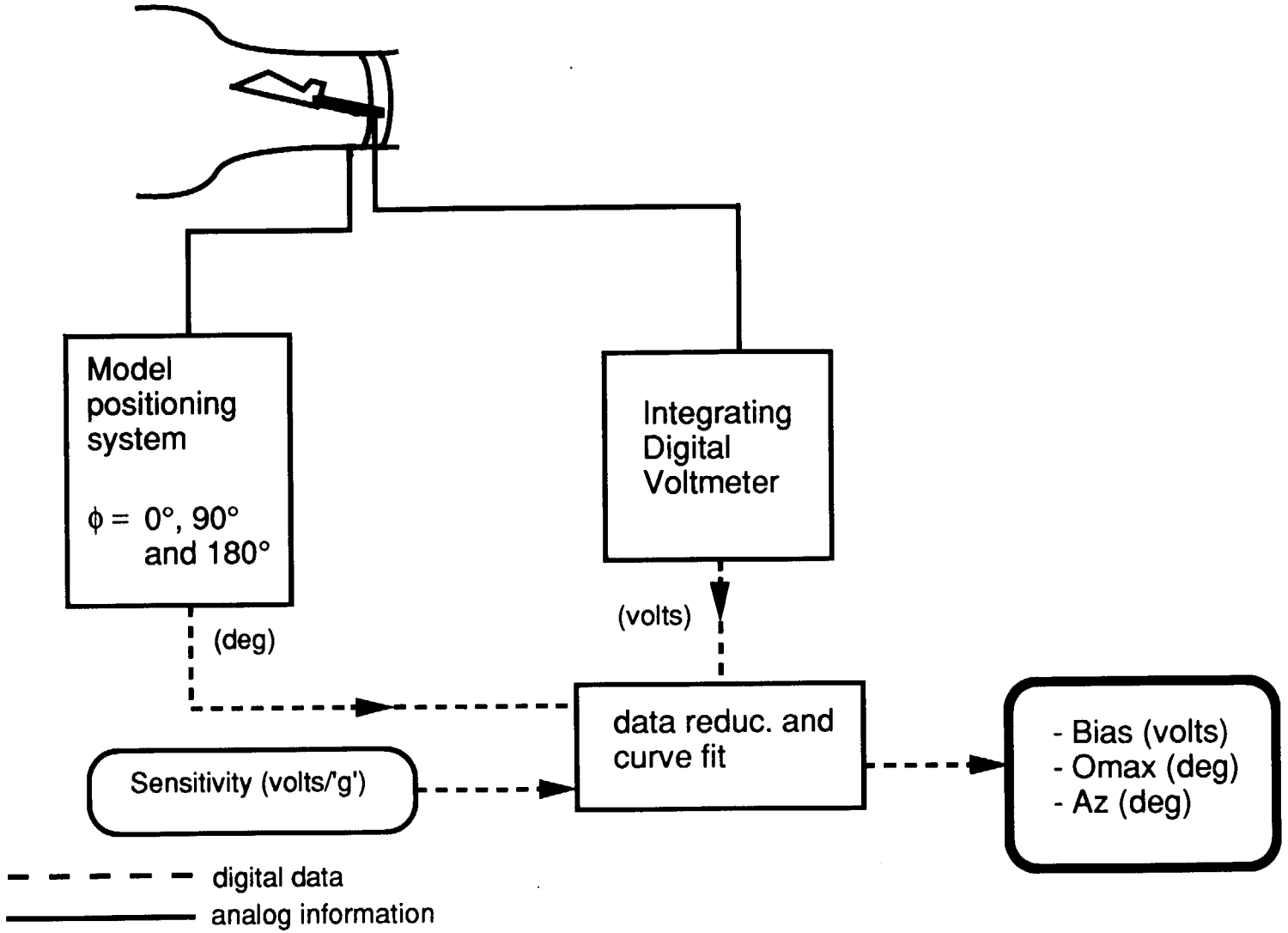

Figure 14. Single Axis AOA, In-Tunnel Calibration

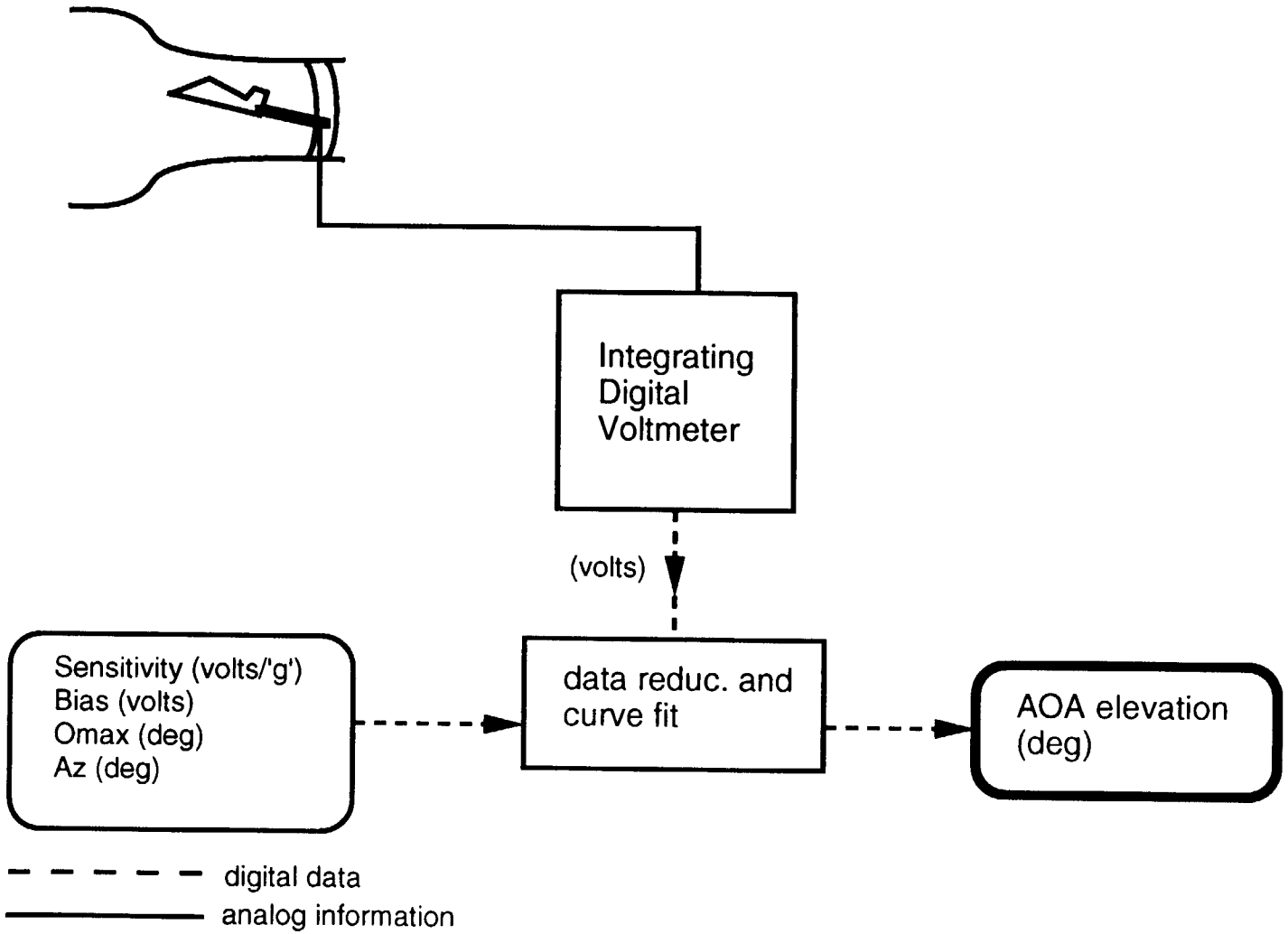

Figure 15. Single Axis AOA, Orientation Measurement

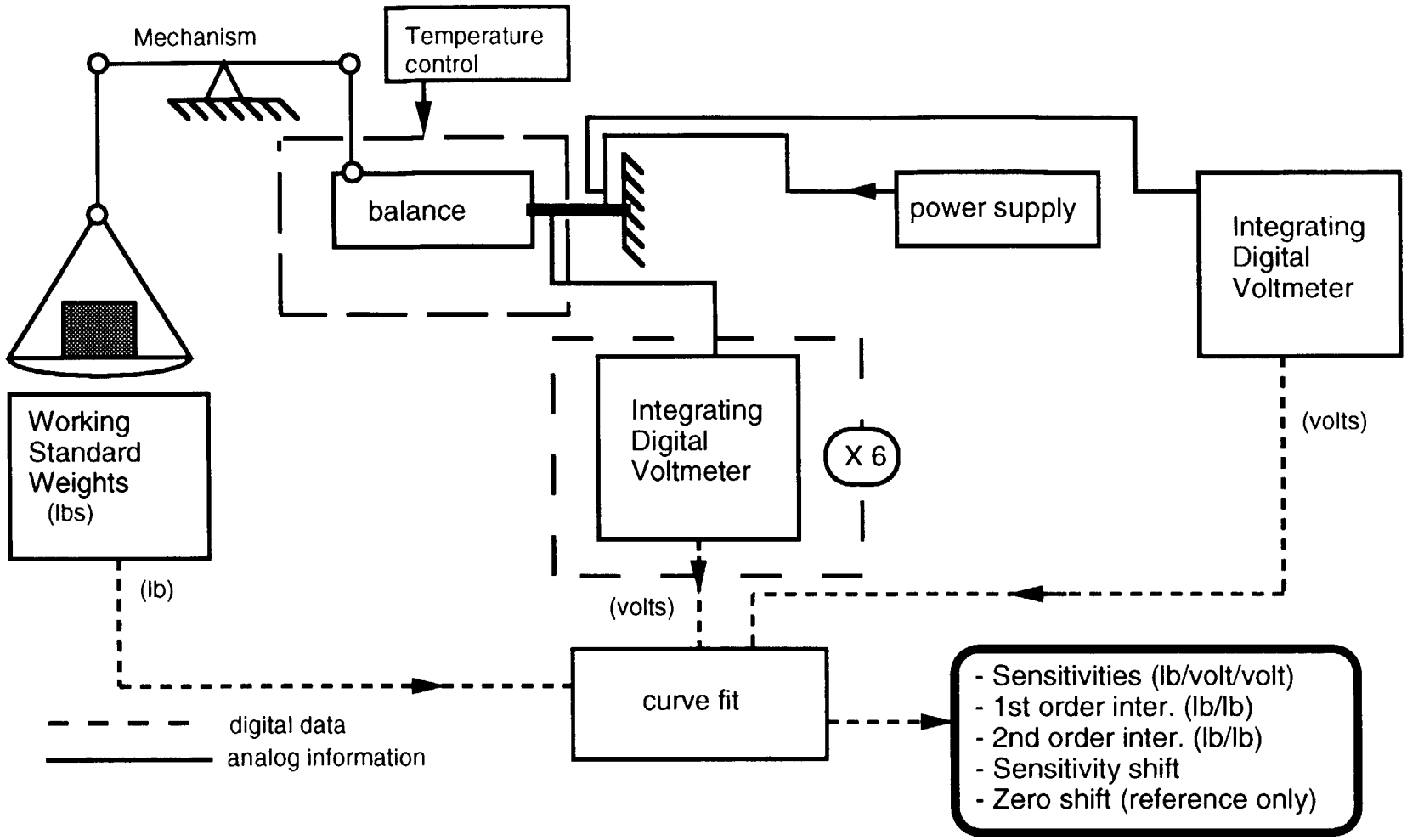

Figure 16. Force Balace, Calibration Laboratory

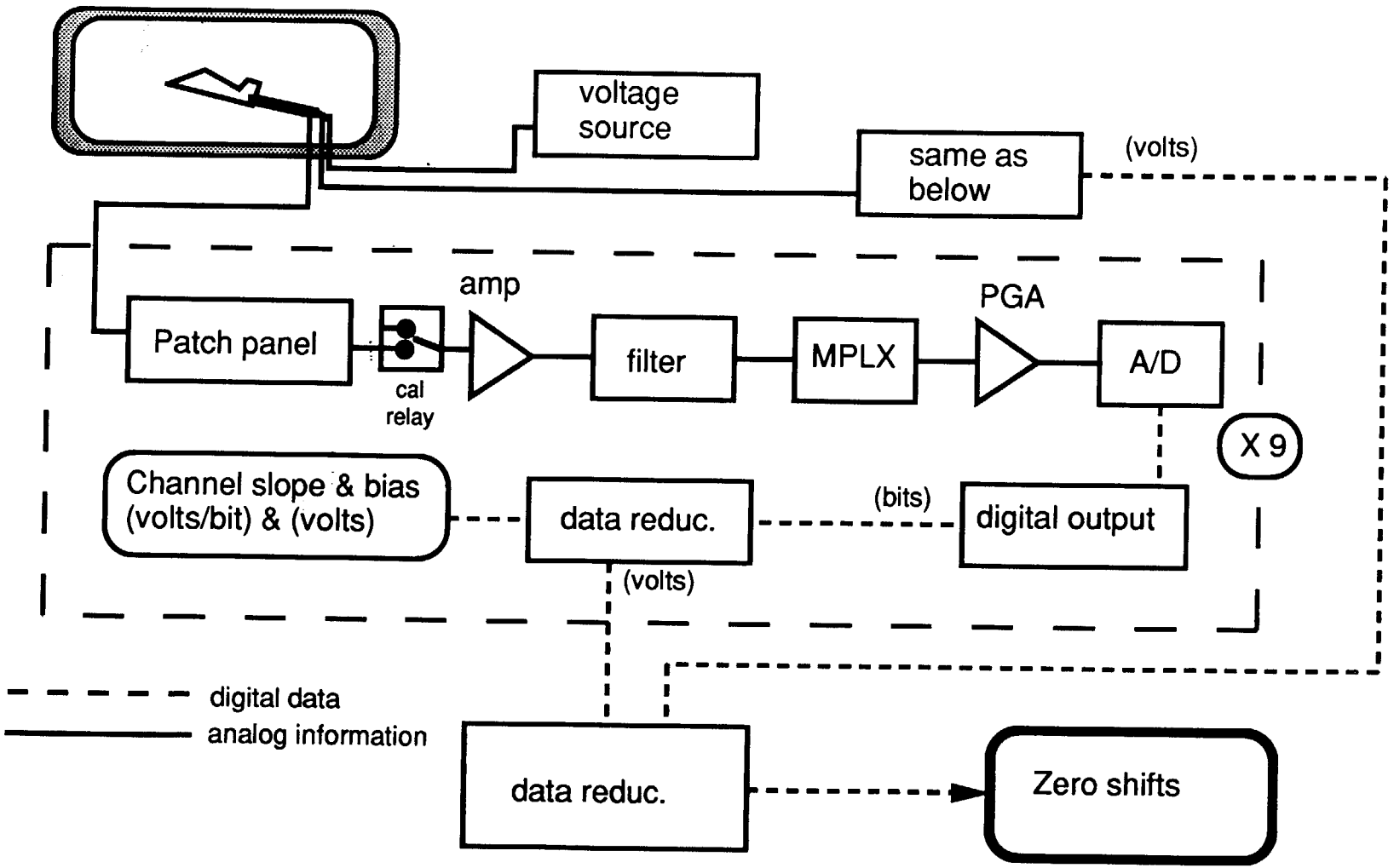

Figure 17. Force Balance Calibration in Model Preparation Area

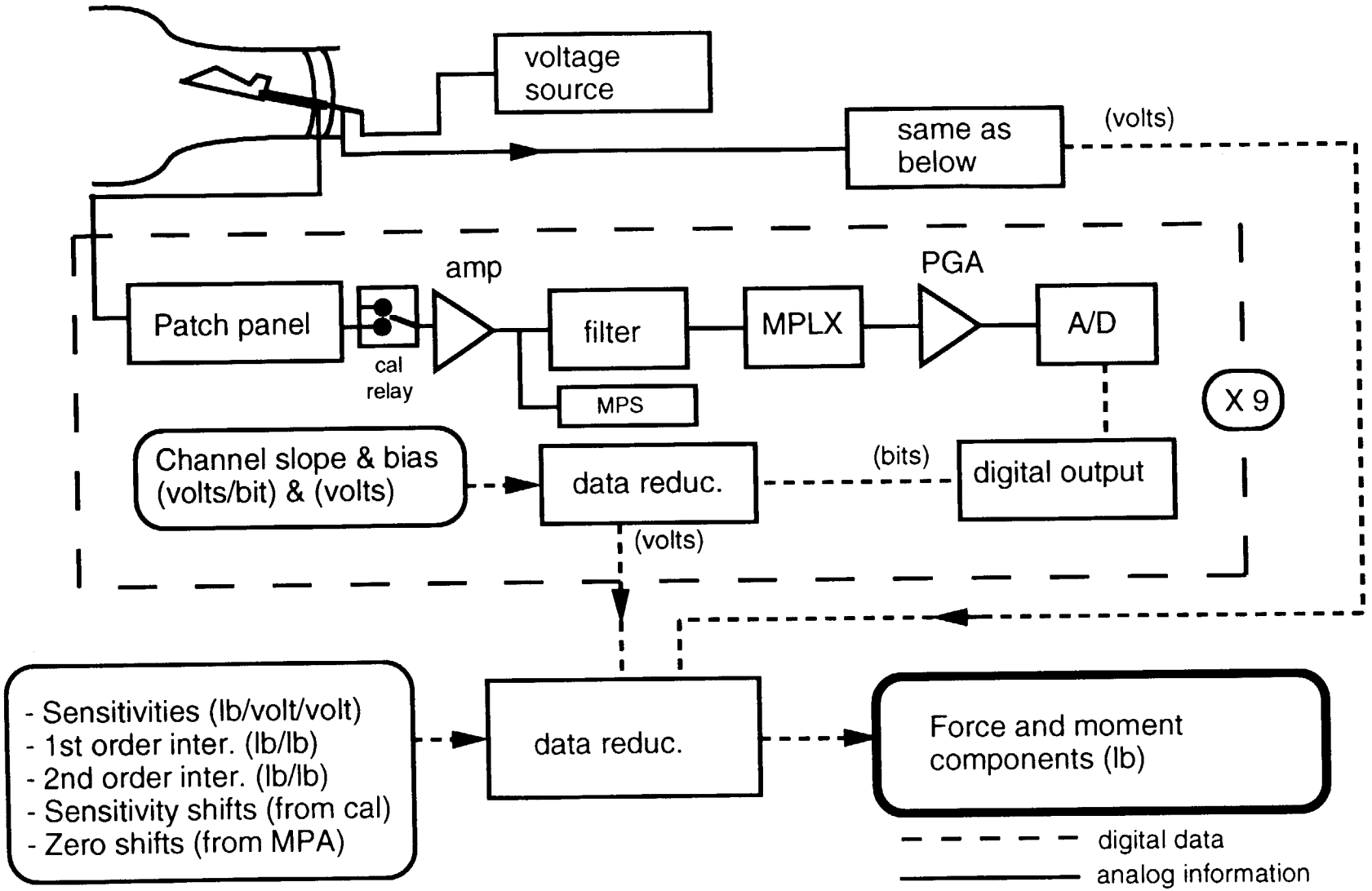

Figure 18 . Force Balance, In-Tunnel Force and Temperature Measurement

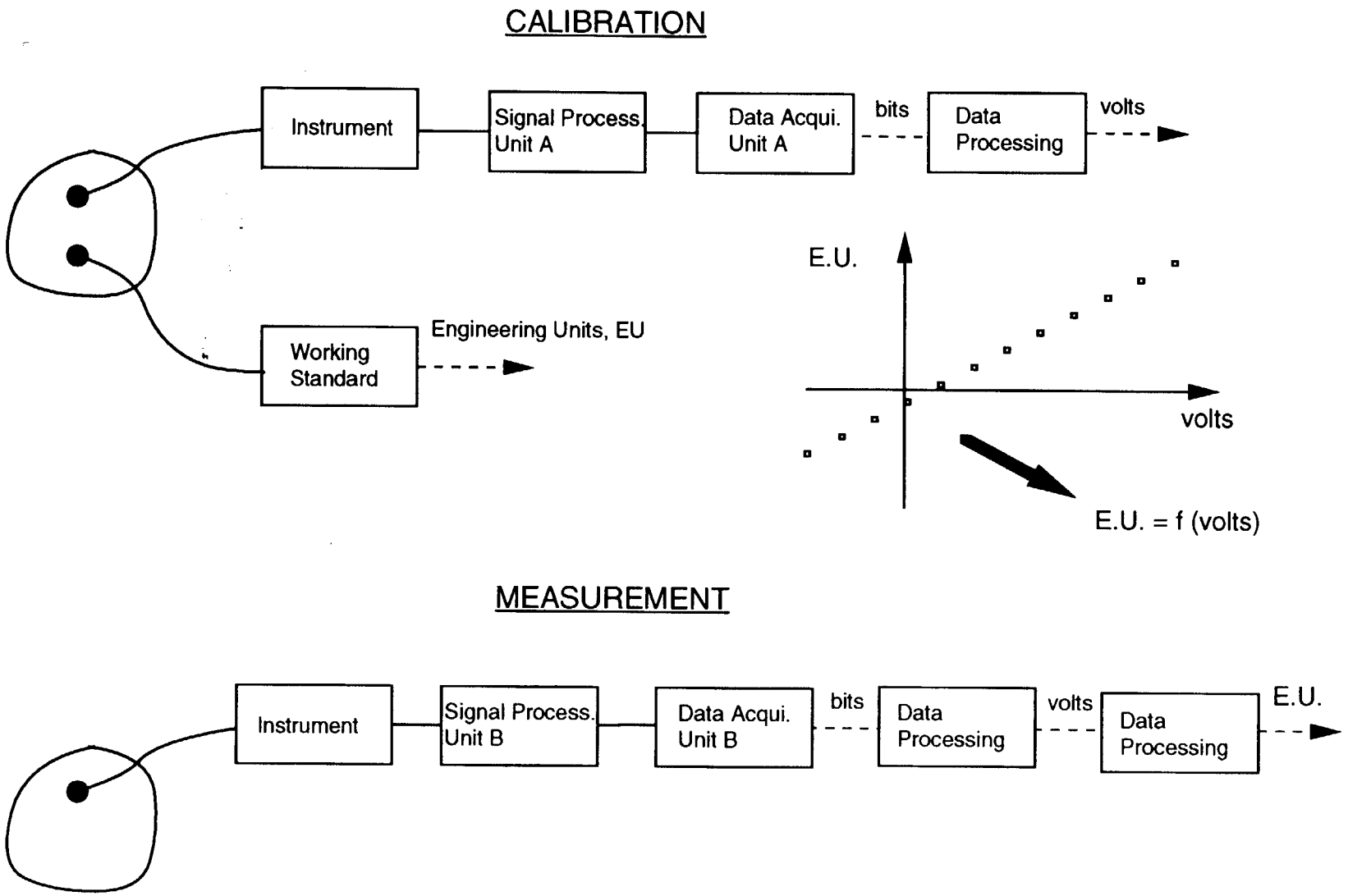

Figure 19. Calibration Experiment and Measurement Schematic

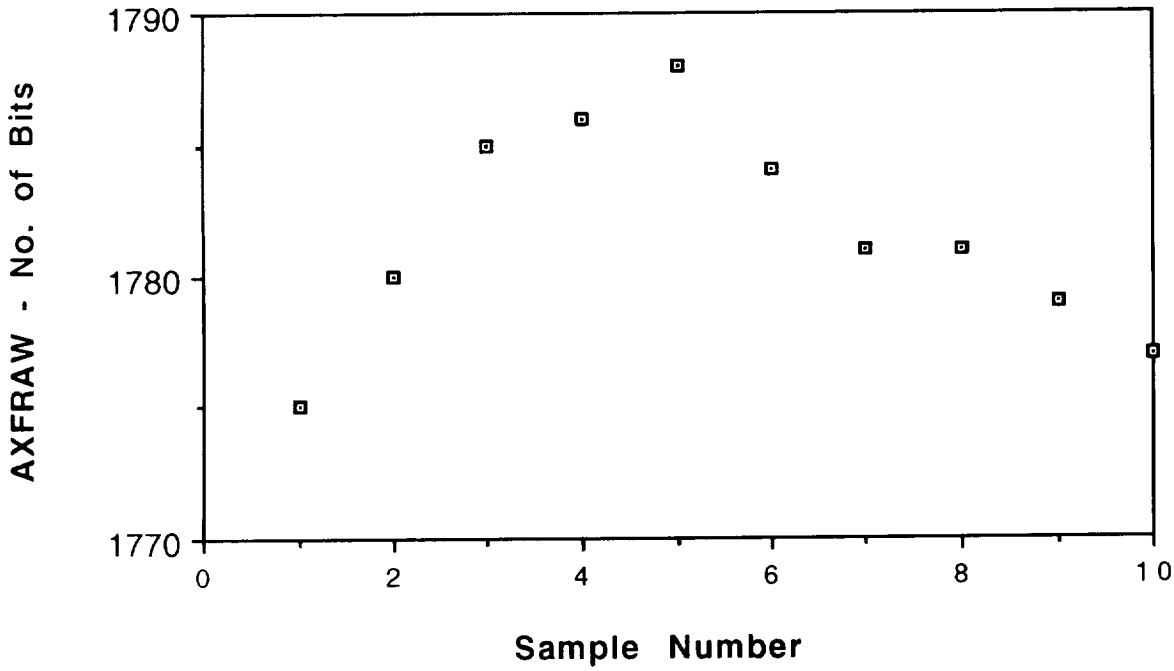

Figure 20. Test Point A, Sample Time History, AXFRAW

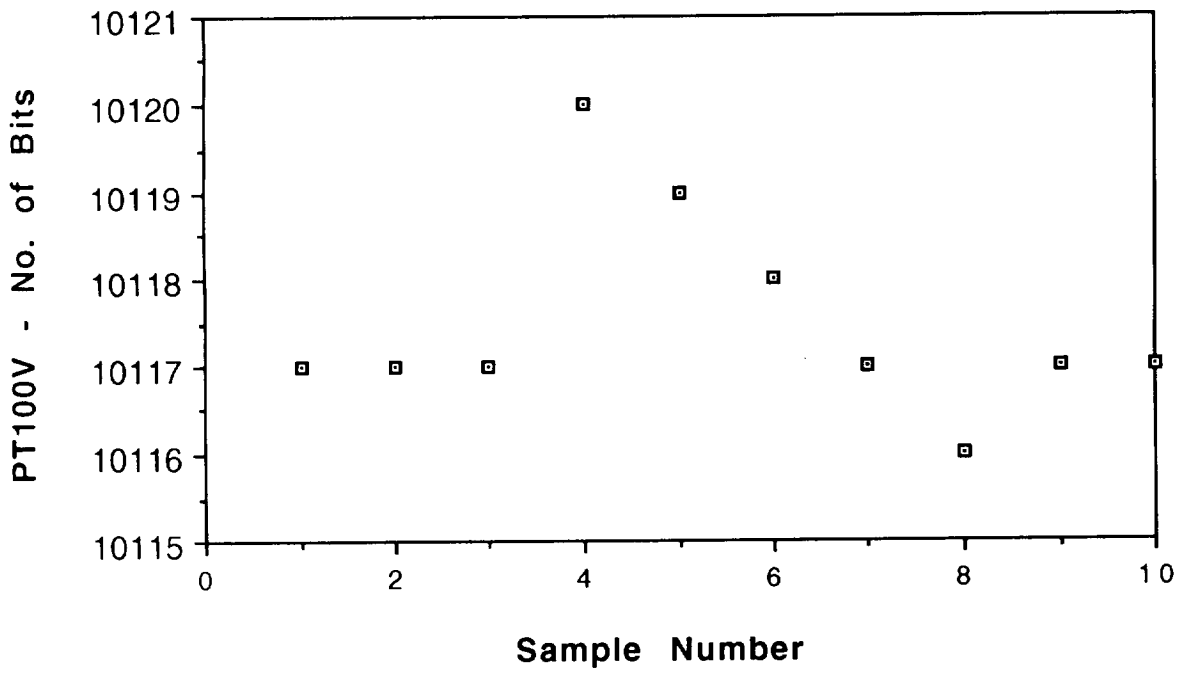

Figure 21. Test Point A, Sample Time History, PTV100

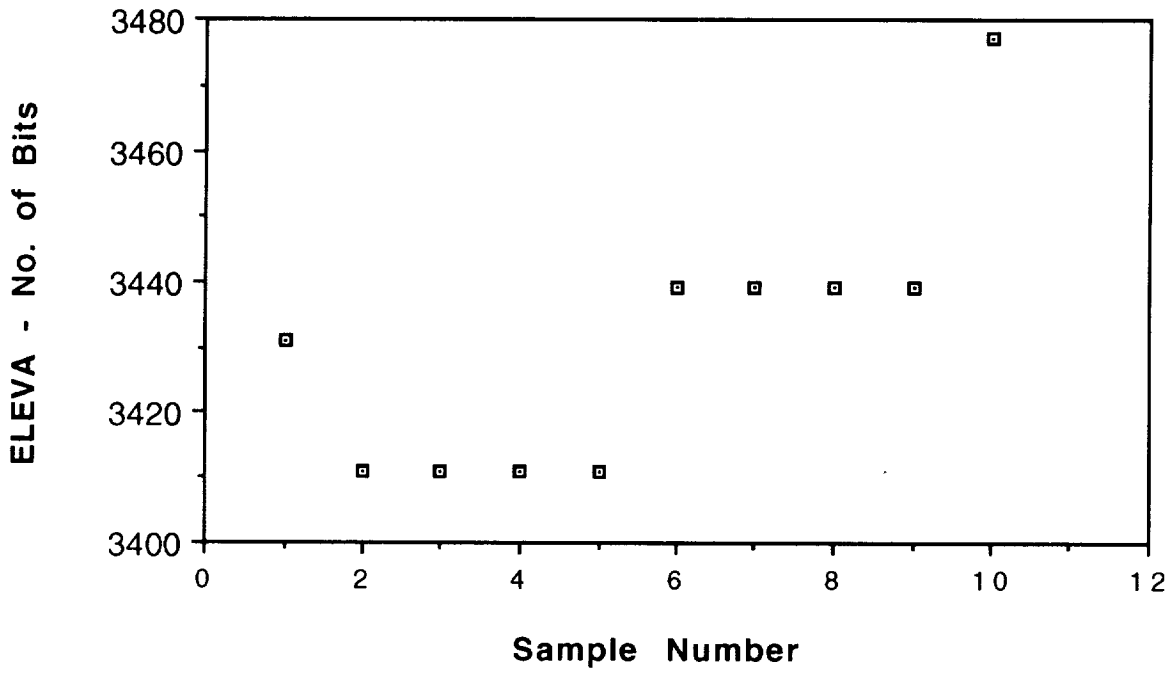

Figure 22. Test Point A, Sample Time History, ELEVA

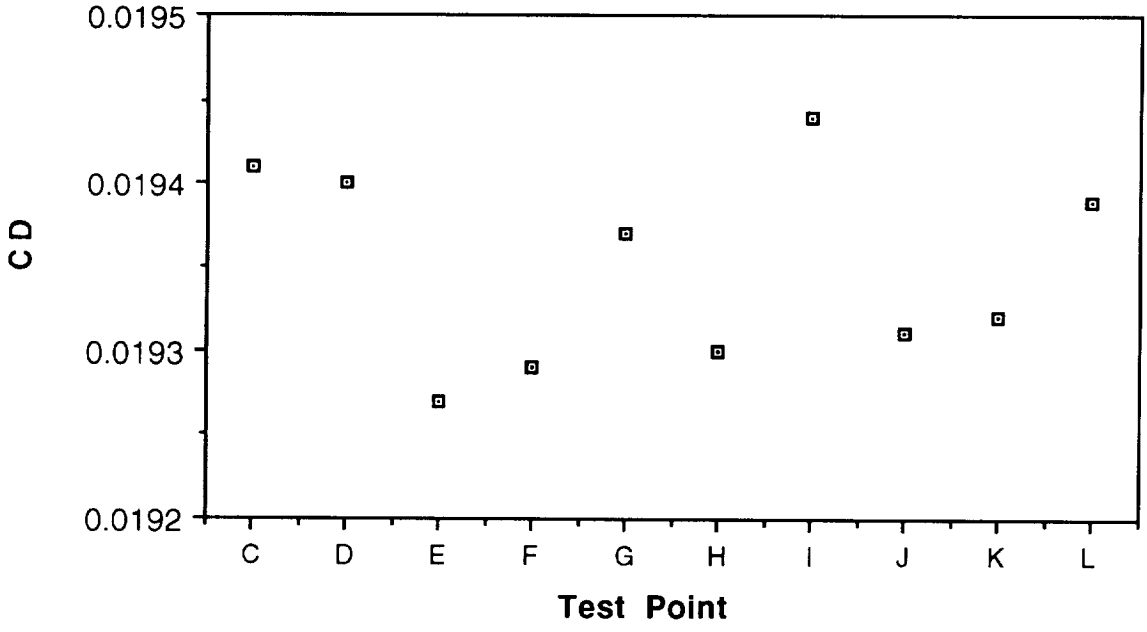

Figure 23. Drag Coefficient, Test Points C - L

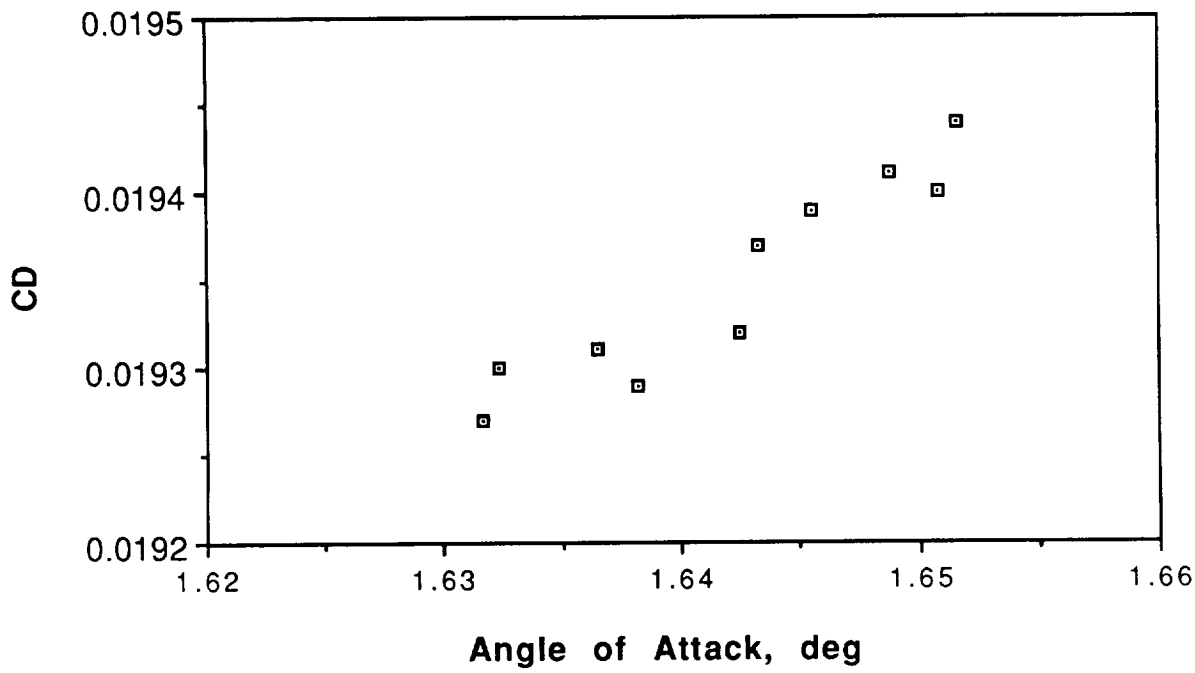

Figure 24. Drag Coefficient vs. Angle of Attack, Test Points C - L

REPORT DOCUMENTATION PAGE

Form Approved
OMB No. 0704-0188

1. AGENCY USE ONLY *(Leave blank)*	2. REPORT DATE	3. REPORT TYPE AND DATES COVERED
	June 1994	Contractor Report

4. TITLE AND SUBTITLE
Experimental Uncertainty and Drag Measurements in the National Transonic Facility

5. FUNDING NUMBERS
NCC1-177

WU 505-59-54-01

6. AUTHOR(S)
Stephen M. Batill

7. PERFORMING ORGANIZATION NAME(S) AND ADDRESS(ES)
University of Notre Dame
Hessert Center for Aerospace Research
Department of Aerospace and Mechanical Engineering
Notre Dame, IN 56556

8. PERFORMING ORGANIZATION REPORT NUMBER

9. SPONSORING / MONITORING AGENCY NAME(S) AND ADDRESS(ES)
National Aeronautics and Space Administration
Langley Research Center
Hampton, VA 23681-0001

10. SPONSORING / MONITORING AGENCY REPORT NUMBER
NASA CR-4600

11. SUPPLEMENTARY NOTES
Langley Technical Monitor: Lawrence E. Putnam
Final Report

12a. DISTRIBUTION / AVAILABILITY STATEMENT
Unclassified-Unlimited

Subject Category 09

12b. DISTRIBUTION CODE

13. ABSTRACT ***(Maximum 200 words)***

This report documents the results of a study which was conducted in order to establish a framework for the quantitative description of the uncertainty in measurements conducted in the National Transonic Facility (NTF). The importance of uncertainty analysis in both experiment planning and reporting results has grown significantly in the past few years. Various methodologies have been proposed and the engineering community appears to be "converging" on certain accepted practices. The practical application of these methods to the complex wind tunnel testing environment at the NASA Langley Research Center was based upon terminology and methods established in the American National Standard Institute (ANSI) and the American Society of Mechanical Engineers (ASME) standards. The report overviews this methodology.

14. SUBJECT TERMS
National Transonic Facility (NTF) uncertainty analysis
wind tunnel measurements
data accuracy

15. NUMBER OF PAGES
128

16. PRICE CODE
A07

17. SECURITY CLASSIFICATION OF REPORT	18. SECURITY CLASSIFICATION OF THIS PAGE	19. SECURITY CLASSIFICATION OF ABSTRACT	20. LIMITATION OF ABSTRACT
Unclassified	Unclassified	Unclassified	